PROTEIN REQUIREMENTS FOR THE INITIATION OF POLIOVIRUS NEGATIVE-STRAND RNA SYNTHESIS

By

ALLYN R. SPEAR

A DISSERTATION PRESENTED TO THE GRADUATE SCHOOL
OF THE UNIVERSITY OF FLORIDA IN PARTIAL FULFILLMENT
OF THE REQUIREMENTS FOR THE DEGREE OF
DOCTOR OF PHILOSOPHY

UNIVERSITY OF FLORIDA

2009

To my loving and supportive parents,
who have always taught me to never stop working towards my dreams

ACKNOWLEDGMENTS

I would like to thank Dr. J. Bert Flanegan for the many opportunities he has provided as well as the extensive scientific freedom he has granted me to pursue many varied avenues of research. I would like to thank the members of the Flanegan lab for their advice, support, assistance, and guidance. Brian O'Donnell, Joan Morasco, Nidhi Sharma, Sushma Ogram, and Jessica Parilla have all contributed in innumerable ways to my scientific development and have been and always will be my friends. And for the many insightful discussions and suggestions, I would like to thank all of the members of my committee, Dr. Rich Condit, Dr. David Bloom, Dr. Linda Bloom, and Dr. Jorg Bungert. I would also like to thank Dr. Rob McKenna for always being available and willing to listen; you have been like a second mentor to me.

I would like to sincerely thank my parents for their undying support for *almost* every crazy thing I have wanted to try in my life, including crossing the country for graduate school.

I would also like to thank my first scientific mentor, Dr. Michael Hoffman. His patience with me as a young scientist and his extensive mentoring provided me with the foundations of my scientific training. Dr. Hoffman's commitment to balancing his professional and personal life, and his dedication to scientific education, continues to be an inspiration to me to this day.

Particularly for her exceptional patience and support during the writing of my thesis, I would like to thank Zenia Torres. She has given me a brighter outlook on my future than I ever could have dreamed and I can't imagine my life without her.

Last, but certainly not least, I would like to more directly thank Sushma Ogram for her camaraderie and support throughout my graduate career. Selfless, caring, and a friend without condition, Sushma always helped bring me up during the worst of times. I know that I would not have made it through graduate school without her, and for that I offer my sincerest thanks.

TABLE OF CONTENTS

page

LIST OF FIGURES

LIST OF ABBREVIATIONS

ATP	Adenosine 5’ triphosphate
cDNA	Complimentary DNA
CTP	Cytidine 5’ triphosphate
DNA	Deoxyribonucleic Acid
GTP	Guanosine 5’ triphosphate
GuHCl	Guanidine Hydrochloride
HeLa	Human cervical carcinoma cell line
IF	Initiation factors (Ribosomal salt wash protein preparation)
IRES	Internal ribosomal entry site
kDa	Kilodalton
NTP	Nucleoside 5’ triphosphate
NTR	Non-translated region
PABP	Poly(A) binding protein
PCBP	Poly(C) binding protein
PIRC	Pre-initiation replication complex
pol	Polymerase
poly(A)	Polyadenosine 5’ triphosphate
pro	Protease
RNA	Ribonucleic Acid
S10	Supernatant from a 12,000 x g centrifugation
UTP	Uridine 5’ triphosphate
vRNA	Virion RNA
wt	Wild type

Abstract of Dissertation Presented to the Graduate School
of the University of Florida in Partial Fulfillment of the
Requirements for the Degree of Doctor of Philosophy

PROTEIN REQUIREMENTS FOR THE INITIATION OF POLIOVIRUS NEGATIVE-STRAND RNA SYNTHESIS

By

Allyn R. Spear

August 2009

Chair: James Bert Flanegan
Major: Medical Sciences - Biochemistry and Molecular Biology

During infection, poliovirus genomic RNA acts first as a messenger RNA and subsequently serves as a template for RNA replication. Because these processes require exclusive use of the genome, the mechanism by which this transition occurs must be carefully orchestrated. The first step in RNA replication is initiation of negative-strand RNA synthesis, however, prior to this initiation a membrane associated viral replication complex must form, requiring key viral and cellular proteins. Using a cell-free system, experiments were performed to investigate specific cellular and viral protein requirements for replication complex formation and subsequent initiation of negative-strand RNA synthesis.

A protein-RNA tethering system was developed to study the involvement of cellular poly(C) binding protein (PCBP) in the initiation of poliovirus negative-strand RNA synthesis. The results of these studies showed that PCBP is essential for initiation of negative-strand synthesis, and did not require direct RNA binding or multimerization. The critical domain of PCBP was identified and it was shown that multiple PCBP isoforms share this activity.

To investigate the viral proteins required for efficient initiation of negative-strand synthesis, a series of *trans* replication reactions were performed. The results of these studies implicate 2BC-P3 as the critical cis-acting viral protein precursor, essential for

membrane-associated replication complex formation. This precursor would be severely trans-restricted by its association with membranes and its rapid processing, accounting for the dramatic increase in RNA replication efficiency of RNAs which generate the 2BC-P3 precursor in cis.

Another viral protein precursor, $3CD^{pro}$, is also critical for many aspects of viral replication. It has multiple functions, including polyprotein processing, RNA binding, and as the precursor for the polymerase ($3D^{pol}$). To investigate the function(s) of $3CD^{pro}$ involved in the initiation of negative-strand RNA synthesis, poliovirus RNAs containing distinct functional mutations within the 3CD coding region were assayed for their ability to be complemented by either wild type or mutant 3CD proteins. The results of these studies indicate the presence of two or more molecules of $3CD^{pro}$ in the replication complex, and also clearly show that active polymerase must be delivered to this complex in the form of $3CD^{pro}$ or a larger precursor.

CHAPTER 1
BACKGROUND AND SIGNIFICANCE

Poliovirus Pathogenesis and Epidemiology

Poliovirus (PV), the causative agent of poliomyelitis, is a member of the family *Picornaviridae*, in the genus *enterovirus*. The viruses of the family *Picornaviridae* are small (25-30 nm diameter), non-enveloped, icosahedral (T=3), positive-sense ssRNA viruses, and can cause a variety of human diseases, including meningitis, encephalitis, poliomyelitis, pancreatitis, myocarditis, rhinitis, and hepatitis. PV is spread via the fecal-oral route, typically by ingestion of contaminated food or water. The primary site of replication is in the mucosal lining of the oropharyngeal and intestinal tract, either in epithelial or lymphoid cells, and during acute infection, virus is shed at high levels in the feces of infected individuals (171). Infectious virus is very stable in the environment, persisting in contaminated groundwater for 3-6 weeks or more (81). After primary infection in the alimentary tract, PV may enter the central nervous system by one of two routes, either by infection of a peripheral nerve and subsequent retrograde intraaxonal transport or by crossing the blood-brain barrier following viremia (171). Paralytic poliomyelitis occurs in 0.5-1% of infected individuals and is a direct result of the death of motor neurons in the spinal cord and/or motor cortex caused by infection and lysis from PV infection. Due, in part, to its extensive study following the poliomyelitis epidemics in the mid 20th century, PV has become the prototypical member of the *Picornaviridae* for studying the molecular mechanisms of viral replication.

Although paralytic polio has probably affected mankind throughout much of recorded history, the epidemics of infantile paralysis in the early to mid 20th century are what most people associate with the concept of poliomyelitis. It was the widespread, devastating nature of this disease that spurred scientists around the world to further characterize the infectious agent and

develop effective vaccines. The success of the vaccination campaign, and the lack of an animal reservoir, led the World Health Organization (WHO) to attempt global eradication set to be completed by the early 21st century. In the course of the 20 year campaign, the cost of the Global Polio Eradication Initiative (GPEI) has exceeded six billion dollars, and despite tremendous progress, poliomyelitis has recently been on the rise in areas in which poliovirus remains endemic (3, 4, 177). The Americas were the first region certified polio-free by the WHO in 1994, followed by the Western Pacific in 2000, and Europe in 2002 (69). Unfortunately, a few regions in Africa and Asia have resisted the best efforts by the GPEI, specifically Nigeria, Afghanistan, Pakistan, and India, and all cases of wild poliovirus transmission since 2006 can be traced back to virus export from one of these four countries (3). The lack of success in these regions can be attributed to multiple factors, not the least of which are inhospitable socio-political climates, adverse geography, and an as yet unexplained variance in the host immune response to vaccination (69). In Nigeria, as a result of rumors of vaccine-induced infertility, vaccination coverage dropped dramatically in 2002-03, leaving an even larger proportion of the population susceptible. Additionally, due to apparent success in northern India, aggressive vaccination campaigns were scaled back beginning in 2002. By 2006, 20 countries that had previously been polio-free reported importation of Nigerian polioviruses, 3 polio-free countries reported cases of Indian poliovirus, and worldwide cases had risen to over 2000 (1-3, 174). This number has not changed significantly since 2006 and worldwide incidence of poliovirus remains between 1000 and 2000 cases per year, with exportation of poliovirus from endemic countries remaining a serious concern. The WHO and GPEI has recently recommitted itself to the campaign, setting new deadlines for polio eradication: India, Afghanistan, and Pakistan by 2010, Nigeria by 2011 (177). The prospect of nearing eradication presents new

challenges and generates some interesting scientific questions: Since the use of oral polio vaccine (OPV) has an associated risk of causing vaccine derived poliomyelitis, how will the OPV be phased out and the inactivated polio vaccine (IPV) be phased in? Will the immune responses and vaccine coverage attainable using the IPV be sufficient to protect the world's population? Will we ever be able to stop vaccination for poliovirus? In the process of discussing these issues, the field has determined that the development of anti-polioviral drugs would be a significant benefit to public health, particularly during the transition into a "polio-free world" (reviewed in 59). To date, there have been no such drugs that have shown any clinically promising results, indicative of a need for a better understanding of the molecular biology of poliovirus replication and the identification of new potential drug targets.

Poliovirus Molecular Biology

The PV RNA genome (Figure 1-1A) is ~7.5 kilobases long, uncapped, and covalently linked to a 22 amino acid viral protein $3B^{VPg}$ (viral protein genome-linked; VPg) via a phosphodiester linkage between O^4 on tyrosine 3 of VPg and the 5' phosphate on the genome terminal uridine (10, 120, 179). This VPg moiety is quickly removed by a cellular unlinking activity (11) and is not required for viral translation (166). Bases 1-89 of the 5' non-translated region (NTR) of PV genomic RNA form a *cis*-acting structure known as the 5' cloverleaf (5'CL) which is required for genomic replication (13, 26, 93, 126, 196), RNA stability (144), and optimal translation (78, 158, 187; Ogram *et al.*, unpublished results). More recently, a conserved cytidine-rich sequence (poly(C) tract) in the 12 nucleotides adjacent to the 5'CL was identified and shown to be required for RNA replication (205). The remainder of the 5'NTR contains a highly structured region which functions as a type-1 internal ribosomal entry site (IRES), driving cap-independent initiation of translation (97, 164). Downstream of the IRES is a single open reading frame encoding viral capsid and non-structural proteins as a single large polyprotein

which is processed by viral proteases (Figure 1-1B) (113). The 3' NTR of PV genomic RNA contains additional *cis*-acting structures which, while not absolutely essential (201), are required for efficient RNA replication (100, 138, 168). Finally, the genomic RNA terminates in a poly(A) tail of heterogeneous length (~90 nts) (218) which enhances IRES translation (32, 136, 192, 193) and is required for PV RNA infectivity (190).

Attachment and Entry

The PV lifecycle initiates with the attachment of virions to the Ig-like cell surface receptor CD155/Pvr (Figure 1-2, Step 1)(111, 134)via surface residues on the PV capsid in a region known as the "canyon" which surrounds a vertex on the icosahedral particle (87). The capsid then undergoes conformational changes whereby the myristoylated N-terminus of VP4 and the hydrophobic N-terminus of VP1 insert into the cell-membrane, forming a pore structure and a membrane anchor (41, 42, 75). Recent work by Brandenburg *et al*. showed that PV internalization into HeLa cells by endocytosis utilizes a clathrin-, calveolin-, and flotillin-independent pathway, and that subsequent uncoating and genome release occurs just inside the plasma membrane at the cell periphery (39). The study further showed that PV entry and uncoating required ATP, the actin cytoskeleton, and tyrosine-kinase activity. Work by Coyne *et al.* showed that PV entry into polarized brain vascular endothelial cells did require calveolin and dynamin, indicating different mechanisms of entry into different cell types (63). More interestingly, Coyne *et al*. also showed that the interaction of PV with CD155 triggered a signaling cascade involving tyrosine phosphorylation and dramatic rearrangements in the actin cytoskeleton which were also essential for viral entry and uncoating. Together, these studies indicate that receptor binding by PV serves a purpose beyond attachment, in the induction of cellular signaling cascades critical to establishing a cellular environment conducive to infection.

Viral Translation and Polyprotein Processing

Cap-independent translation of the genomic RNA is the first intracellular step in the viral life cycle (Figure 1-2, Step 2). Because viron RNA (vRNA) does not contain a 5' 7^{m}G cap structure, it cannot undergo canonical cap-dependent ribosomal scanning and translation as would a typical eukaryotic mRNA. Instead, picornaviruses utilize a complex series of RNA secondary structures in their 5'NTR called an IRES to recruit and position ribosomes in a cap-independent manner (97, 164). The PV IRES is sub-classified as a type-1 IRES based on structural characteristics, and shares homology with the IRESes of other entero- and rhinoviruses (99). Like other type-1 IRESes, the PV IRES binds a set of host cell proteins to assist in RNA folding and ribosome recruitment, including the La autoantigen, poly(C) binding protein 2 (PCBP2), SRp20, polypyrimidine tract binding protein (PTB), upstream-of-N-ras protein (*unr*), and eIF4G (90, 131). In addition to these co-factors, certain RNA elements within the IRES presumably act as a scaffold for the assembly of ribosomal subunits to facilitate efficient translation initiation.

Eukaryotic cells have evolved a mechanism to further optimize the cap-dependent translation of their own mRNA by inducing a 5'-3' circularization via interactions between cap binding protein (eIF4G) and poly(A) binding protein (PABP) bound to the 3' poly(A) tail (212). In turn, there is a growing body of evidence (reviewed by (131)), as well as a significant amount of unpublished data from our lab, that indicates a similar enhancement strategy in use by PV (Ogram *et al*., unpublished results). Because the PV genome has VPg linked to its 5' end rather than a 5' 7^{m}G cap structure, it is likely that an alternative protein bridge mediates the 5'-3' circularization of PV genomic RNA (Figure 1-3). This presumably involves interactions between PCBP bound to the 5'CL and PABP bound to the 3' poly(A) tail, although additional

and/or alternative interactions have been proposed, including as yet unidentified cellular proteins (131).

Downstream of the IRES is the single open reading frame which encodes the approximately 2200 amino acid viral polyprotein. This large protein product is processed by the viral proteases 2A ($2A^{pro}$) and 3C/3CD ($3C^{pro}$/$3CD^{pro}$) and the resultant polyprotein cleavage cascade is depicted in Figure 1-1B (119, 155, 156). Initial polyprotein processing occurs co-translationally at the boundary between the structural and non-structural proteins by $2A^{pro}$ (206), and all subsequent cleavage events (except at the capsid protein VP4-VP2 junction) are mediated by the other viral protease or its immediate precursor, $3C^{pro}$/$3CD^{pro}$ (113, 155). The cleavage at the VP4-VP2 junction is catalyzed by amino acids in VP0 and is induced upon RNA packaging following final capsid assembly (15, 27, 155). Processing of the non-structural replication proteins occurs by two distinct pathways determined by the site of primary cleavage by $3C^{pro}$/$3CD^{pro}$ (119). If the primary cleavage occurs at the 2C-3A junction, processing of the resultant P2 and P3 precursors proceeds in the soluble phase, and proceeds very slowly. However, with 3-fold higher frequency, the primary cleavage occurs at the 2A-2B junction, shunting the resultant 2BC-P3 precursor into the rapid processing membrane associated pathway. This is of particular importance given that PV infection induces dramatic membrane rearrangements which are essential for PV replication (44, 45).

Virus-Induced Alteration of Host Cell Environment

The remarkable rearrangement of intracellular membranes observed during PV infection is dependent on PV translation and results in the formation of rosette-like vesicles to which PV replication complexes localize (44, 45, 70). It has been shown that viral protein precursor 2BC and viral protein $2C^{ATPase}$ are responsible for these rearrangements (9, 20, 50). In addition, 2BC and $2C^{ATPase}$, as well as 3AB, have been shown to affect membrane permeability and

nucleo-cytoplasmic trafficking (8, 30, 31, 84, 117). The collective effect of these activities increases the cytoplasmic availability of nuclear factors utilized in PV replication and also generates the ideal membrane microenvironment which is essential for replication complex assembly and RNA replication.

In addition to the alteration of host cell membranes, PV also induces a global down-regulation of host-cell translation and transcription. Beyond their role in PV polyprotein processing, $2A^{pro}$ and $3CD^{pro}/3C^{pro}$ are also responsible for the comprehensive proteolytic attack on critical cellular proteins and processes that causes this host shut-off. The host cell translational machinery is primarily disabled by $2A^{pro}$ cleavage of eIF4GI/II, an essential component of the cap binding complex eIF4F (72, 82, 125). In addition, both $2A^{pro}$ and $3CD^{pro}/3C^{pro}$ cleave poly(A) binding protein (PABP), another cellular protein involved in stimulating cap-dependent translation (101, 116). Transcriptional machinery is also proteolytically inactivated by $2A^{pro}$ cleavage of TATA-binding protein (TBP) (214), as well as $3CD^{pro}/3C^{pro}$ cleavage of TBP (55), cAMP responsive element binding protein (CREB) (215), Oct-1 (216), and multiple other transcription factors specific for RNA polymerase II (181), and RNA polymerase III (54, 184). The net effect of these cleavage events is a shut-off of over 95% of host cell gene expression by three hours post-infection (102).

Host Protein Involvement in RNA Replication

Both PCBP and PABP, discussed above relative to PV translation, have also been shown to be involved in other aspects of PV replication. As previously discussed, the PV genome contains an essential RNA structure at the 5' end, so-termed the 5' cloverleaf (5'CL). PCBP binding to a stem-loop within this structure has been shown to be involved in RNA replication (12, 13, 158, 209), as well as in stabilizing PV RNA (144). In addition to its association with the

5'CL, PCBP also binds to a conserved cytidine-rich sequence adjacent to the 5'CL and this interaction was also shown to be required for RNA replication (205).

At the opposite end of the PV genome, the 3' poly(A) tail is of sufficient length to bind cellular PABP. It has been established that the poly(A) tail plays a role in stability, translation, and RNA replication, most likely as a result of its interaction with PABP (93, 182, 190; Ogram *et al.*, unpublished results) Moreover, Silvestri *et al*. showed that the PABP/poly(A) requirement was specific for the initiation of negative-strand RNA synthesis (186).

Negative-Strand RNA Synthesis

The transition from PV translation to genomic RNA replication, as with all positive-strand RNA viruses, must initiate with the synthesis of anti-genomic negative-strand RNA (Figure 1-2, Step 3. As discussed previously, membrane vesicles are essential for RNA replication since the cytoplasmic surface of these membranes is the site of replication complex assembly (34, 51). In addition to membrane vesicles, RNA replication requires viral proteins as well as some forms of their precursors. Of all the viral proteins and precursors described to date, it has been shown that 2B, $2C^{ATPase}$, 3AB, VPg(3B), $3C^{pro}$/$3CD^{pro}$, and $3D^{pol}$ are essential for RNA replication (12, 175, 213). Additional data generated from complementation analysis has indicated that optimal replication may require larger precursor forms of one or more of these essential proteins (104, 124, 204). The precise functions of 2B and $2C^{ATPase}$ in RNA replication are unknown, however, negative-strand initiation is blocked by millimolar concentrations of guanidine HCl (GuHCl) and GuHCl resistance mutations map to $2C^{ATPase}$ (23, 170). The requirement for 3AB may arise from a need to provide the essential VPg protein primer to the replication complex in a membrane associated precursor form (46). Data from our lab has suggested that the RNA dependent-RNA polymerase ($3D^{pol}$) must also be delivered to the replication complex in the form of its precursor $3CD^{pro}$, prior to processing and negative-strand initiation (25).

The polymerase initiates negative-strand synthesis at the extreme 3' end of the viral RNA, using the poly(A) tail as a template and VPg as a protein primer. In addition to the presence of the PABP-poly(A) RNP complex, additional interactions occur on the adjacent 3'NTR, including recruitment of $3CD^{pro}/3D^{pol}$ and 3AB/VPg to provide the active polymerase and protein primer, respectively (89). Interestingly, despite its location at the opposite side of the genome, an RNP complex formed on the 5'CL has also been shown to be essential for RNA replication (12, 13). This complex consists of both cellular PCBP as well as the viral $3CD^{pro}$ (12, 158, 209). The involvement of both distal and proximal RNA elements in negative-strand initiation lead our lab and others to propose the formation of a 5'-3' circular RNP complex, driven by protein-protein interactions between RNP complexes at the 5'CL and 3'NTR/poly(A) tail (Figure 1-3) (26, 93, 126, 196). Potential bridging interactions could involve a PCBP and PABP interaction, as has been shown to occur on the 3' end of α-globin mRNA (49, 210). A $3CD^{pro}$-$3CD^{pro}$ interaction could also either drive or augment circularization, since the viral precursor has been shown to bind to both 5' and 3' ends (12, 89), and interaction surfaces were identified in the crystal structure of $3D^{pol}$ and $3CD^{pol}$ (86, 130, 153) Regardless of which is the critical interaction, the formation of the complete circular RNP complex represents the last pre-replication state of viral genomic RNA. Once the complex has formed and subsequent processing of any necessary protein precursors is complete, $3D^{pol}$ initiates RNA replication via uridylylation of VPg on the poly(A) tail. This would then be followed by elongation of negative-strand RNA, generating a full-length double-stranded replicative form (RF) RNA.

Positive-Strand RNA Synthesis

Poliovirus RNA replication is highly asymmetric, generating 10-100 molecules of VPg linked positive-strand RNA for every one negative-strand template synthesized (Figure 1-2,

Step 4) (150, 207). The requirements for the initiation of positive-strand synthesis differ significantly from those for negative-strand initiation.

First among these differences is the requirement for pre-uridylylated VPg (VPgpUpU) as a primer for positive-strand elongation (141, 143). The synthesis of VPgpUpU occurs on an RNA hairpin template in the $2C^{ATPase}$ coding region termed the *cis* replication element or *cre*(2C) hairpin, and requires VPg, UTP, $3D^{pol}$, $3CD^{pro}$, PCBP and the 5'CL (126; Sharma *et al.*, unpublished results). The uridylylation of VPg is templated by the first of three conserved adenosines in the loop of the hairpin, and addition of the second uridyl residue is accomplished via a slide-back mechanism (161, 176). Interestingly, the *cre*(2C) dependent VPg uridylylation reaction is inhibited by GuHCl (126, 141), indicating the involvement of $2C^{ATPase}$, even though positive-strand synthesis *per se* is not sensitive to GuHCl inhibition (23).

The protein requirements for positive-strand initiation are also different from those observed for negative-strand synthesis. Despite GuHCl insensitivity, $2C^{ATPase}$ has been shown to bind specifically to the 3' end of the negative-strand, indicating a possible role in positive-strand synthesis (19). Data from the Semler lab has established the specific binding of cellular protein hnRNP C to the 3' end of negative-strand RNA, and have shown it to be required for RNA replication (40, 178). Sequences at the 3' end of PV negative-strand RNA, which correspond to a potential hnRNP C binding site, have also been shown to be essential for positive-stand synthesis (183). Taken together, these data suggest a mechanism of positive-strand initiation whereby hnRNP C, $3D^{pol}$, VPgpUpU, and possibly $2C^{ATPase}$ form an RNP complex at the 3' end of the negative strand RNA (or RF RNA) to promote multiple sequential rounds of positive-strand RNA synthesis.

Packaging and Release of Progeny Virions

When sufficient PV capsid protein and genomic RNA have been synthesized, virion assembly begins (Figure 1-2, Step 5). There is no known packaging signal or sequence requirement for encapsidation of PV RNA, however through exhaustive study of defective interfering (DI) particles and induced genomic deletions, it has been determined that the capsid coding region is not required for vRNA encapsidation (52, 115, 148). Additional studies have shown that although not essential, PV IRES sequences do enhance encapsidation (103). There also appears to be a very strict discrimination in RNA polarity, since packaging of negative-sense RNA is undetectable (150). In addition to sequence requirements, all packaged RNAs must be VPg linked (149), and there also appears to be a tight coupling between active RNA replication and encapsidation of nascent vRNA (152). Once the RNA is encapsidated, VP0 undergoes processing to generate VP4 and VP2, mediated by catalytic residues in VP2 and activated by the presence of RNA, which results in formation of the final infectious virus particle (15, 27, 91, 94).

Release of viral particles from infected cells can occur by multiple mechanisms, including programmed cell death (203), cytopathic effect (CPE) induced lysis (7), and autophagosome-mediated exit without lysis (AWOL) (195). Although poliovirus infection induces pro-apoptotic programs, the programs are quickly suppressed by viral proteins (203). In fact, it is the interaction of PV with its receptor (CD155) that induces c-Jun NH_2-terminal kinase (JNK) activation, and ultimately this activation overcomes viral protein mediated suppression and triggers cell death via Bax-dependent mitochondrial dysregulation, cytochrome *c* release, and activation of the apoptotic caspase cascade (7, 16). Alternatively, in the presence of inhibitors of apoptosis, Agol *et al*. showed that the CPE caused by PV infection (e.g. membrane rearrangements, increase in nuclear permeability) were sufficient to induce lysis of the host cell

and release of viral particles (7). The release of small amounts of infectious virus has also been observed in the absence of cell lysis, and Taylor *et al.* has recently shown that this is a consequence of viral subversion of the cellular autophagy pathway resulting in the delivery of small pockets of virus-laden cytoplasm to the extracellular space (195). In all cases, these newly formed viral particles, following release or lysis of the host cell, can now either spread to infect neighboring cells, or be shed into the environment to await a new host.

Cell-Free Replication System

Shortly after the isolation and establishment of the HeLa cervical carcinoma cell line in 1951, HeLa cells were widely used to passage and study poliovirus (5, 194). A major breakthrough in PV molecular biology was the cDNA cloning and sequencing of the PV genome by Racianello and Baltimore in 1981 (172, 173). This was followed by another significant advance ten years later, when Molla, Paul and Wimmer successfully generated infectious poliovirus *de novo* using a cell-free replication system (140). Further optimization and characterization of this system by our lab and others has produced the cell-free HeLa S10 translation-replication system in use today (21, 22, 24). This system permits us to uncouple the otherwise intertwined processes of translation and replication, allowing us to finely dissect the molecular mechanisms of these events, while still accurately recapitulating *in vivo* viral replication. Recent developments involving the use of ribozyme generated authentic 5' ends on transcript RNAs have allowed us to further dissect RNA replication and examine the molecular biology and genetics of negative-strand and positive-strand synthesis separately (92, 141). Using this system, we have begun to identify the viral and cellular proteins required for the initiation of poliovirus negative-strand RNA synthesis.

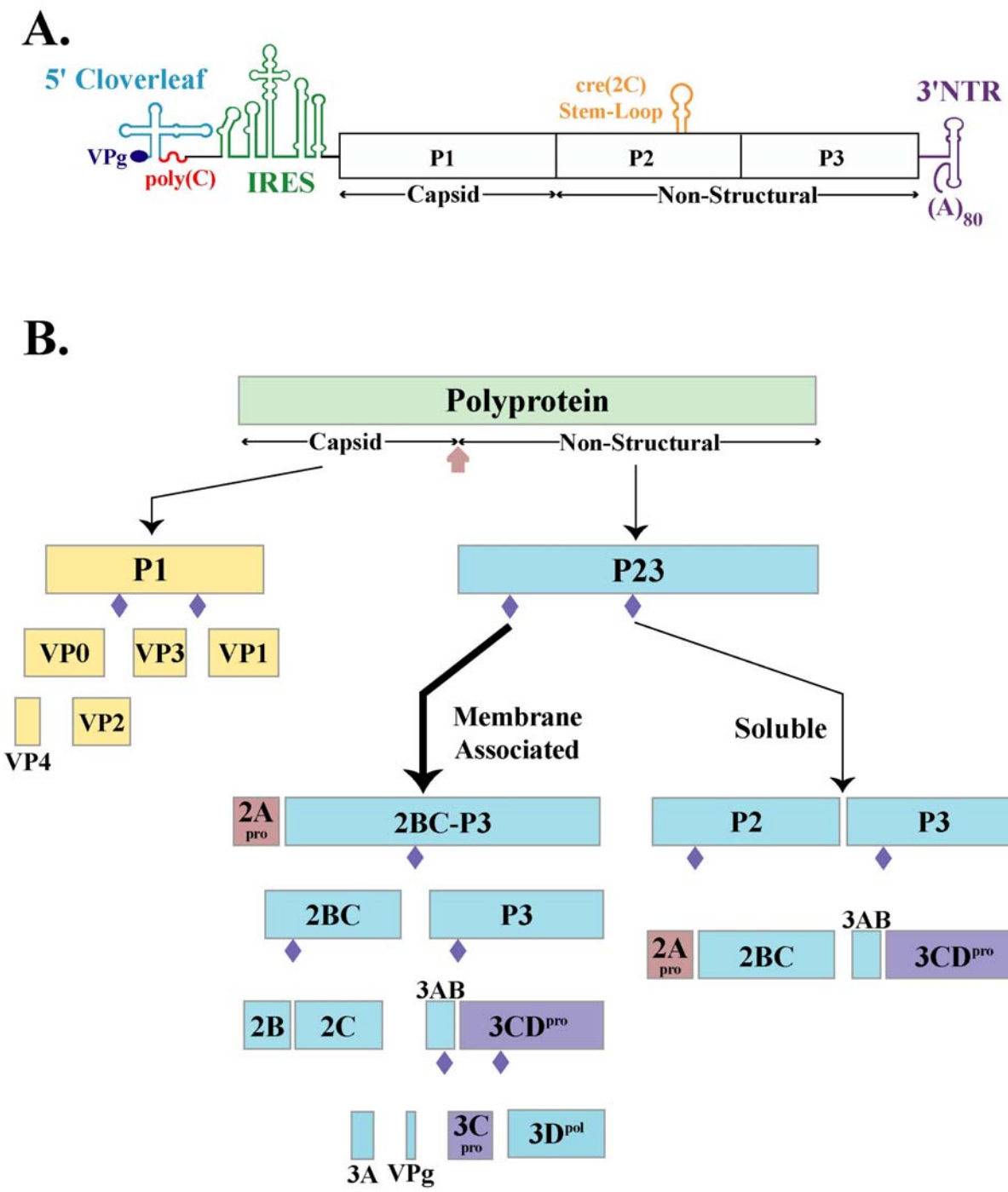

Figure 1-1. Poliovirus genome organization and polyprotein processing cascade. A) PV genomic RNA is covalently linked to VPg at its 5' end, and contains multiple cis acting RNA elements, including the 5' cloverleaf (5'CL), poly(C) tract, IRES, cre(2C) stem-loop, and 3'NTR/poly(A) tail. B) PV translates a single large polyprotein which is processed by viral proteases $2A^{pro}$ (↑) and $3C^{pro}$/$3CD^{pro}$ (◆). Primary cleavage of the P23 precursor at the 2A-2B junction occurs with 3-fold higher efficiency than cleavage at the P2-P3 junction. This initial processing event determines if the subsequent processing occurs in membrane-associated or soluble compartments.

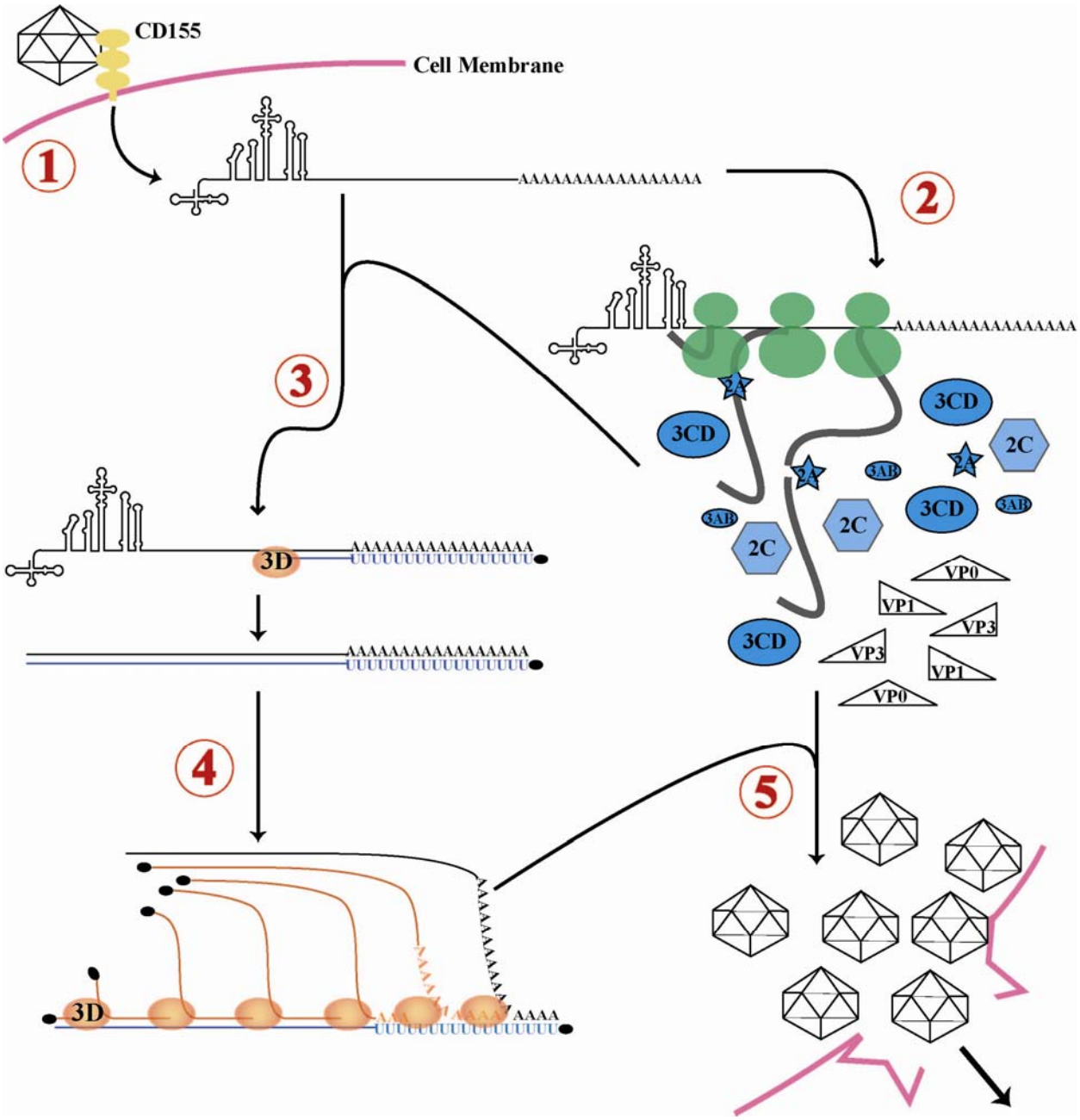

Figure 1-2. Poliovirus life-cycle. PV binds its cellular receptor CD155, undergoes internalization by endocytosis, and releases its genome into the cytoplasm at the cell periphery (Step 1). Upon release, translation factors and ribosomes assemble on the IRES and viral protein synthesis occurs (Step 2). Using these newly synthesized proteins, the viral replication complex is formed and the 3D polymerase generates a new VPg-linked negative-strand RNA (Step 3). This dsRNA intermediate is then used as a template for multiple rounds of VPg-UU primed positive-strand synthesis (Step 4). When sufficient RNA and protein synthesis has occurred, nascent positive-strand genomic RNAs are packaged by the viral capsid proteins and these progeny virions are released upon apoptosis of the host cell (Step 5).

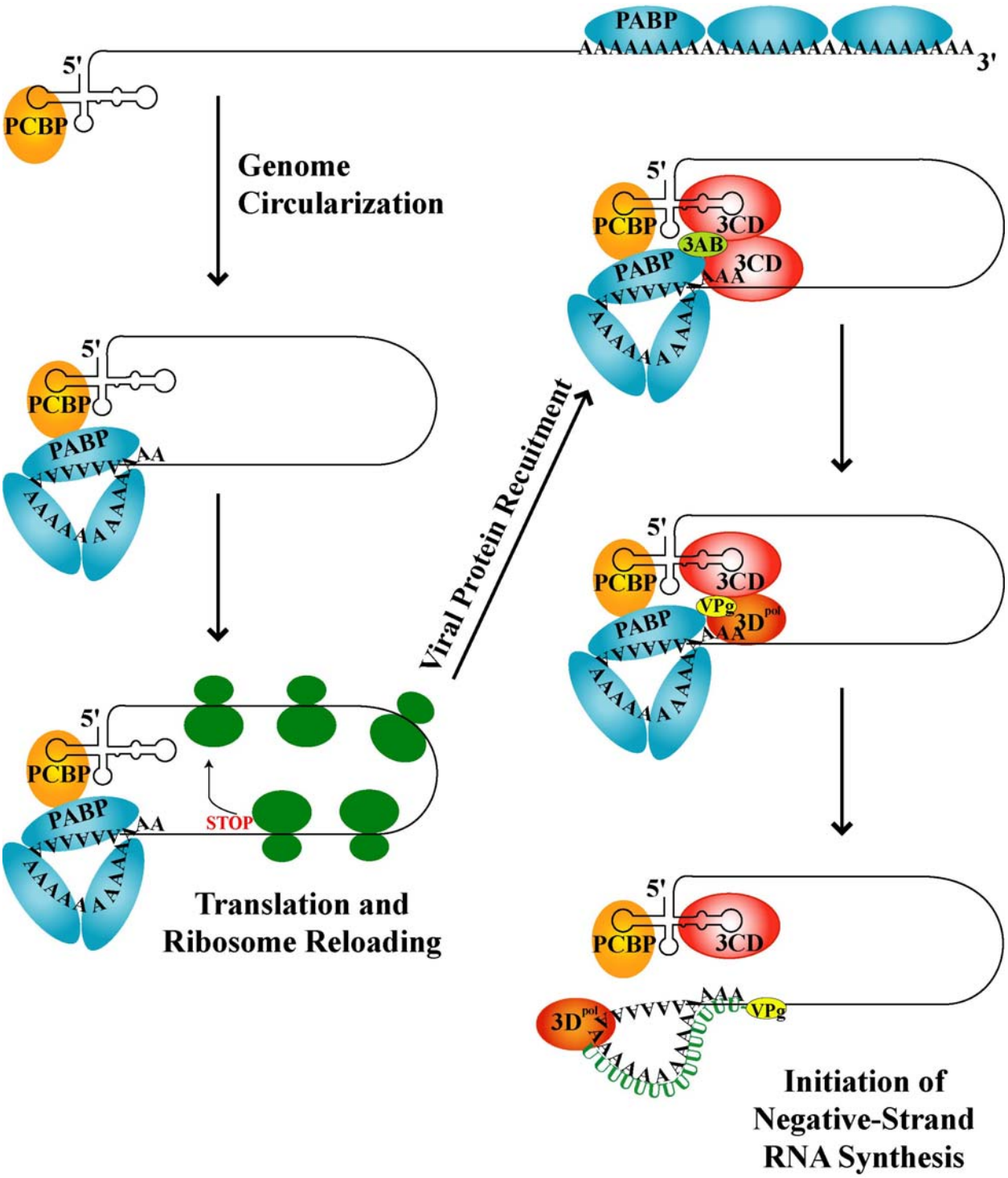

Figure 1-3. Genomic circularization models for PV translation and replication. Prior to viral protein synthesis, interactions between PCBP and PABP circularize PV genomic RNA to facilitate ribosome reloading and enhance translation. Following viral protein synthesis, replication protein precursors $3CD^{pro}$ and 3AB would be recruited to the 5'CL and 3'NTR, undergo processing, and initiate VPg-primed negative-strand RNA synthesis.

CHAPTER 2
MATERIALS AND METHODS

DNA Manipulation and Cloning Techniques

All restriction enzymes, as well as the Klenow fragment of T4 DNA polymerase, used in these studies were obtained from New England Biolabs unless otherwise noted. Restriction digests were performed according to manufacturer's protocols, and when double digests were required they were performed sequentially unless optimal conditions were available for simultaneous digests. Standard PCR reactions were carried out according to the manufacturer's suggested protocols using either TrueFidelity DNA polymerase (Continental Lab Products), PfuUltra Fusion II DNA polymerase (Stratagene), Accuprime Pfx DNA polymerase (Invitrogen), or Phusion DNA polymerase (New England Biolabs). Rapid purification of PCR products for direct restriction digest was performed using QiaQuick PCR Cleanup kit from Qiagen. Gel purification of PCR fragments or restriction enzyme digested DNA was performed using the GeneClean II Spin Kit from Bio101. For gel purification, DNA fragments were resolved on SeaKem GTG agarose (formulated for gel purification) from Cambrex, visualized by ethidium bromide staining on a low intensity UV transilluminator, and appropriate bands were excised using a scalpel. All vector DNAs, where required, were dephosphorylated using Shrimp Alkaline Phosphatase (SAP) from Roche Applied Science. It is critical that dephosphorylation be performed <u>after</u> gel purification, as this will reduce vector background to near zero. Dephosphorylation reactions were performed by adding SAP to 10% of the total reaction volume and using the provided 10X dephosphorylation buffer [500 mM TrisHCl (pH=8.5), 50 mM $MgCl_2$,]. Following a 1 h incubation at 37°C, the SAP was inactivated by incubation at 65°C for 15 min. Vector and insert DNA fragments were quantitated by agarose gel electrophoresis and ethidium bromide visualization of each fragment versus the 1 kb or 100 bp DNA ladder (New

England Biolabs). Ligations were performed using T4 DNA ligase obtained from Promega. All ligations utilized the provided 10X ligase buffer [300 mM TrisHCl (pH=7.8), 100 mM $MgCl_2$, 100 mM DTT, 10 mM ATP] and contained 1 Unit/µL T4 DNA ligase. All reactions contained a total of 5 ng/µL DNA (vector + insert), however, for sticky-sticky and sticky-blunt ligations, a ratio of 1:3 (vector:insert) was used, whereas for blunt-blunt ligations, a ratio of 1:1 (vector:insert) was used. For sticky-sticky ligations, reactions were incubated at room temperature for 1 h or more prior to transformation, and for sticky-blunt or blunt-blunt ligations, reactions were incubated at room temperature for at least 12 h or more prior to transformation.

Site-Directed Mutagenesis

Site-directed mutagenesis was performed using a procedure based on that of the Stratagene's QuikChange site-directed mutagenesis kit. Briefly, two complementary mutagenic primers are designed which contain the desired mutations flanked on either side by 10-15 nts of non-mutagenic complementary sequence. Using these primers, the appropriate template, and PfuTurbo DNA polymerase (Stratagene), PCR reactions were performed where the elongation times were extended to allow complete transit around the circular plasmid DNA template. After 18 PCR cycles, 20 Units of *Dpn*I was added to the reaction and incubated for 1 h at 37°C to digest all methylated input DNA template. Following digestion, 1 µL of this reaction was transformed into XL-1 Blue competent cells (Stratagene). Resultant ampicillin resistant colonies were screened by DNA mini-prep and restriction digest and sequencing. Once the sequence of the mutated region was verified, a restriction fragment within the sequenced region, containing the mutation, was transferred back into the parent vector background to prevent accumulation of secondary vector mutations that could potentially arise during PCR of the entire plasmid.

Two-Step PCR

Two-step PCR was performed to induce mutations (two-step mutagenic PCR) as well as to fuse two DNA sequences (two-step semi-overlapping PCR). For mutagenic PCR, two complementary mutagenic primers were designed which contain the desired mutations flanked on either side by 15-20 nts of non-mutagenic complementary sequence. Additionally, two outside primers were designed, one 5' of the desired mutation and one 3' of the desired mutation. For convenience, these primers were each 300-1000 bases away from the position of the mutatgenic primers. It was also essential that these outside primers also encompassed unique restriction enzyme sites for reintroduction of the mutated fragment. Two first step PCRs were performed using standard PCR conditions and enzymes described above. These PCRs both utilized the same template DNA, however one contained the primer pair to generate the 5' product and the other reaction contained the primer pair to generate the 3' product. Here, both products share the entire mutagenic primer sequence (i.e. the 3' end of one product is fully complementary to the 5' end of the other). These first step PCR products were then gel purified and quantitated using methodology described above. The second step PCRs contained 10-20 ng of each first step PCR product and only the 5' and 3' outside primers. Here, the first step products are added in place of plasmid template DNA and the mutations are already present in these templates, so mutagenic primers are no longer necessary. All second step PCRs used only PfuUltra Fusion DNA polymerase (Stratagene) or Phusion DNA polymerase (New England Biolabs) as these were empirically determined to generate the highest product yield with the lowest extraneous background amplification. The second step PCR product was a result of priming of one first step PCR product on the other, followed by amplification of this combined product by the outside primer pair. The second step PCR product was purified using the QiaQuick PCR purification kit and the resultant DNA was digested using the restriction enzymes

whose sites flanked the induced mutation. The restriction fragment of the second step PCR product, which contained the desired mutation, was then cloned into the corresponding sites of the parent plasmid DNA.

In cases where two DNA sequences needed to be fused, two-step semi-overlapping PCR was used. To do this, a sequence map of the final desired (fused) sequence was generated. Two complementary primers were then designed such that the primer pair equally spanned the junction between the two fused sequences. This resulted in the generation of two primers which each contained equal halves of two distinct sequences. As with two-step mutagenic PCR described above, two additional outside primers were also required, however these primers were designed to be on the 5' and 3' sides of the fusion junction of the desired sequence. The parent plasmid DNA for the 5' sequence to be fused was chosen to be the recipient vector DNA, due to the availability of convenient unique restriction sites. Therefore, the 3' outside primer was designed to include a restriction site corresponding to a site available in the vector DNA. First and second step PCRs were performed exactly as described above for two-step mutagenic PCR, except the semi-overlapping primers (primers overlapping the fusion junction) were used in place of the mutagenic primers. Here, the second step PCR product represents a new synthetic gene fusion of the two previously distinct DNA sequences. Purified second step PCR product was digested with the appropriate restriction enzymes and cloned into the corresponding sites of the recipient vector DNA.

Construct Verification and DNA Stock Preparation

Small scale plasmid DNA of potential clones was prepared using either the Eppendorf or Qiagen Mini-Prep Spin kits. The correctness of all constructs was verified by sequencing performed either at the DNA Sequencing Core Laboratory (ICBR, University of Florida) or by the SeqWright commercial sequencing facility (SeqWright, Inc., Houston, TX). All primary

clones generated using site directed mutagenesis were subsequently recloned back into the parent vector background by excision and transfer of a sequence verified restriction fragment containing the desired mutation. Although XL-1 Blue competent cells (Stratagene) were utilized for some sub-cloning applications, all final plasmid DNAs were transformed into MAX Efficiency StBL2 competent cells (Invitrogen) for preparation of glycerol stocks as well as for large scale plasmid DNA preparation. For long term storage, 50% glycerol stocks of overnight liquid cultures were maintained at -80°C and were re-struck on LB+ampicillin agar plates as needed. For large scale plasmid DNA preparations, a single colony from a newly struck LB+ampicillin plate was inoculated into 250 mL of LB broth containing 50 mg/mL ampicillin. These inoculated broth cultures were grown overnight at 37°C with shaking, and bacterial pellets were isolated by centrifugation at 5,000 x g for 10 min. Plasmid DNA was subsequently isolated using the Qiagen Midi-Prep kit. All plasmid DNA stocks were standardized to 0.5 μg/μL and stored in TE [10 mM TrisHCl (pH=8), 1 mM EDTA] at -20°C.

cDNA Clones Used in These Studies

Poliovirus Clones Used in These Studies

A previously described cDNA clone of the Mahoney strain of type I poliovirus, designated pT7-PV1$(A)_{80}$, was used as the parent clone for all poliovirus based constructs used in all studies herein (26). (i) pPV1ΔGUA$_3$ is a previously described construct which generates an RNA transcript [PV1ΔGUA$_3$ RNA] with a 5-nt deletion in the 3' NTR, known to inhibit negative-strand synthesis without affecting translation (26). (ii) pP23 is a previously described construct with a deletion of the P1 capsid coding region (104). RNA transcripts of this construct [P23 RNA] express all essential replication proteins from the P2 and P3 regions of the viral genome. These transcripts function as an RNA replicon, allowing for negative-strand, but not positive-strand synthesis. (iii) pRzP23 was generated from pP23 by inserting a hammerhead

ribozyme (Rz) downstream of the T7 promoter. Following transcription, this ribozyme removes itself from the 5' end of the transcript, yielding RNA transcripts with authentic poliovirus 5' ends (25, 141). These authentic ended transcripts function as replicons, capable of both positive- and negative-strand synthesis. (iv) pP23-5'CL(C24A) and pRzP23-5'CL(C24A) were engineered using site-directed mutagenesis. Transcripts of these constructs contain the mutant 5'CL^{C24A}, but translate all viral replication proteins. (vi) pP23-5'CL(MS2) was generated using site-directed mutagenesis, replacing nts 12-32 in pP23 (stem-loop b of 5'CL) with the cDNA for a 19 nt stem-loop from the MS2 bacteriophage genome sequence [ACATGAGGATTACCCATGT] (114). Proper folding of the resulting mutant 5'CL^{MS2} was verified using the Mfold RNA structure prediction program (220, 221). (vii) pF3 is a previously described construct in which the P1 and P2 coding regions were deleted, and a frameshift mutation was engineered near the beginning of the P3 coding region (183). Transcripts of this construct [F3 RNA] initiate translation at the 3A start codon but prematurely terminate translation. (viii) pF3-5'CL(C24A) was generated from pF3 using site-directed mutagenesis and transcripts of this construct contain the mutant 5'CL^{C24A}. (ix) pFS23 is derived from pP23 via the deletion of nucleotides 775-779 by restriction digest, blunting with the Klenow fragment of T4 DNA polymerase, and re-ligation. This deletion generated a reading frame shift causing transcripts of this construct [FS23] to initiate translation at the 2A start codon but prematurely terminate after the synthesis of a 65 amino acid peptide. (x) pP1-3D* is derived from pT7-PV1(A)$_{80}$ via insertion of a *Stu*I restriction site at position 3364 by site-directed mutagenesis and subsequent removal of the *Stu*I-*Dra*III fragment by restriction digest, blunting by T4 DNA polymerase, and re-ligation. The net effect of this process is an in-frame deletion of nucleotides 3365-6082, spanning the extreme 3' end of the P1 coding region through a 5' portion of the 3D coding region. Transcripts of this construct

[P1-3D* RNA] express a non-functional protein consisting of the majority of the P1 precursor (amino acids 1-874) fused to a large carboxy-terminal portion of 3D (amino acids 13-460). (xi) pFS1-3D* is derived from pP1-3D* via the deletion of nucleotides 1119-1122 by restriction digest, blunting with the Klenow fragment of T4 DNA polymerase, and re-ligation. This deletion generated a reading frame shift causing transcripts of this construct [FS1-3D* RNA] to initiate translation at the VP4 start codon but prematurely terminate after the synthesis of a 133 amino acid peptide. (xii) pP23-2A^{STOP} is derived from pP23 via insertion of two stop codons following the terminal Gln codon of the 2A coding sequence by site-directed mutagenesis. Transcripts of this construct [P23-2A^{STOP} RNA] retain the translation initiation context and all other RNA sequences of P23 RNA but translation terminates at the precise carboxy-terminus of 2A. (xii) pP23-2B^{STOP} is derived from pP23 via insertion of two stop codons following the terminal Gln codon of the 2B coding sequence by site-directed mutagenesis. Transcripts of this construct [P23-2B^{STOP} RNA] retain the translation initiation context and all other RNA sequences of P23 RNA but translation terminates at the precise carboxy-terminus of 2B. (xiv) pP23-2C^{STOP} is derived from pP23 via insertion of two stop codons following the terminal Gln codon of the 2C coding sequence by site-directed mutagenesis. Transcripts of this construct [P23-2C^{STOP} RNA] retain the translation initiation context and all other RNA sequences of P23 RNA but translation terminates at the precise carboxy-terminus of 2C. (xv) pP23-3A^{STOP} is derived from pP23 via insertion of two stop codons following the terminal Gln codon of the 3A coding sequence by site-directed mutagenesis. Transcripts of this construct [P23-3A^{STOP} RNA] retain the translation initiation context and all other RNA sequences of P23 RNA but translation terminates at the precise carboxy-terminus of 3A. (xvi) pP23-3B^{STOP} is derived from pP23 via insertion of two stop codons following the terminal Gln codon of the 3B coding sequence by

site-directed mutagenesis. Transcripts of this construct [P23-3B^{STOP} RNA] retain the translation initiation context and all other RNA sequences of P23 RNA but translation terminates at the precise carboxy-terminus of 3B. (xvii) pP23-3C^{STOP} is derived from pP23 via insertion of two stop codons following the terminal Gln codon of the 3C coding sequence by site-directed mutagenesis. Transcripts of this construct [P23-3C^{STOP} RNA] retain the translation initiation context and all other RNA sequences of P23 RNA but translation terminates at the precise carboxy-terminus of 3C. (xviii) pPV1p50 is derived from pT7-PV1(A)$_{80}$ via an in-frame deletion of nucleotides 867-6011 by digestion with *BstB*I and re-ligation of the vector fragment. Transcripts of this construct [PV1p50 RNA] utilize the authentic translational start and stop contexts and express a non-functional fusion protein (p50) between a short VP4 peptide (amino acids 1-41) and the majority of 3D (amino acids 9-460). (xix) p2BC-P3 is a previously described construct which contains the coding region for the 2BC-P3 precursor protein (104). Transcripts of this construct [2BC-P3 RNA] express the 2BC-P3 precursor protein. (xx) p2C-P3 is derived from two previously described constructs p2C and pP23 via removal of the *BamH*I fragment from p2C and subsequent ligation of that fragment into the corresponding sites of pP23 (104). Transcripts of this construct [2C-P3 RNA] express a 2C-P3 precursor protein. (xxi) pP3 is a previously described construct which contains the coding region for the entire P3 polyprotein precursor (104). Transcripts of this construct [P3 RNA] express the P3 polyprotein precursor. (xxii) p3BCD is derived from pP3 via site directed mutagenesis and subsequent removal of the 3A coding region. Briefly, a *Sma*I restriction site, Kozak's consensus sequence and AUG codon were introduced into pP3 immediately 5' of the initiating Gly codon of 3B. This mutant pP3 now contained tandem *Sma*I sites, one immediately upstream of the P3 start codon, and one immediately prior to the newly introduced 3B start codon. This subclone was digested with

*Sma*I, removing the 3A coding region, and subsequently re-ligated to form p3BCD. Transcripts of this construct [3BCD RNA] express the 3BCD precursor protein. (xxiii) p3CD is derived by an in-frame insertion of the 3C-3D(nt 1-247) protein coding sequence into the *Msc*I site of a previously described vector, pDJB2 (104). This vector retains the 5' and 3'NTR/poly(A) tail of full-length cDNA clone pT7PV1$(A)_{80}$, as well as a portion of 3D coding region, and contains the Kozak's consensus translational start site. Transcripts of this construct [3CD RNA] express proteolytically active $3CD^{pro}$ precursor protein. (xxiv) p3D is derived by an in-frame insertion of the 3D(nt 1-247) protein coding sequence into the *Msc*I site of pDJB2, as described above. Transcripts of this construct [3D RNA] express active $3D^{pol}$ alone. (xxv) To generate a series of PV polyprotein expression RNAs that would act as partial helper RNAs, the *Avr*II-*Mlu*I fragment from pPV1ΔGUA_3 was transferred into the corresponding sites of p3D, p3CD, pP3, and p2BC-P3, generating p3DΔGUA_3, p3CDΔGUA_3, pP3ΔGUA_3, and p2BC-P3ΔGUA_3, respectively. Each of these generates transcripts which express the indicated portion of the PV polyprotein but are defective for RNA replication. (xxvi) p3CD[3D-G327M]ΔGUA_3 and pP23[3D-G327M] were created by transferring the *BstB*I-*Avr*II fragment (containing the G327M mutation) to p3CDΔGUA_3 or pP23, from pT7-PV1$(A)_{80}$[3D-G327M] which had been generated previously in our laboratory. Transcripts of these constructs [3CD(G327M)ΔGUA_3 RNA or P23[3D-G327M] RNA] express 3CD which processes and binds RNA normally, however, the G327M mutation has disrupted the essential YGDD catalytic RNA polymerase motif, abolishing polymerase activity (98). (xxvii) p3CD[PM]ΔGUA_3 was created by mutagenic two-step PCR, using p3CDΔGUA_3 as a template. This mutant combines two previously described processing site mutations [T181K, Q182D] with two additional mutations [S183G, Q184N] designed to completely abrogate 3C-3D processing (12, 37, 88). Transcripts of this construct

[3CD(PM)ΔGUA$_3$ RNA] express 3CD which retains RNA binding and protease activity, but is unable to be processed into 3C and active 3D^{pol}. (xxviii) pP23[3CD(PM)] was created by transferring the *Bgl*II-*BstB*I restriction fragment from p3CD[PM]ΔGUA$_3$ into the corresponding sites of pP23. (xxix) p3CD[3C-R84S]ΔGUA$_3$ was created by mutagenic two-step PCR, using p3CDΔGUA$_3$ as a template. This mutation was previously identified to inhibit the RNA binding ability of 3C^{pro} (36). Transcripts of this construct [3CD(R84S)ΔGUA$_3$ RNA] express a 3CD with impaired RNA binding abilities, but retains the ability to release a fully wild-type 3D^{pol}. (xxx) pP23[3C-R84S] was created by transferring the *Bgl*II-*BstB*I restriction fragment from p3CD[PM]ΔGUA$_3$ into the corresponding sites of pP23. (xxxi) p3CD[3C-K12N/R13N]ΔGUA$_3$ and pP23[3C-K12N/R13N] were created by mutagenic two-step PCR, using p3CDΔGUA$_3$ or p23 as templates, respectively. These mutations were previously identified to inhibit the RNA binding ability of 3C^{pro} (36).

Poliovirus-Based Protein Expression Clones Used in These Studies

As described above, pDJB2 containing the ΔGUA$_3$ mutation was used as a PV expression vector to direct translation of a downstream reading frame (104). As before, all protein expression clones generate ΔGUA$_3$ RNA transcripts, which prevents the transcripts from functioning as RNA replicons (26). This vector can be digested with *Msc*I which cuts directly downstream from the IRES, prior to any initiating AUG codons. PCR products containing the Kozak's consensus translation initiation sequence and the coding region of a gene of interest can then be ligated into this vector, effectively replacing the PV coding sequence with that of the desired protein. (i) cDNA clones containing the PCBP1 and PCBP2 coding sequence were generously provided by Dr. Raul Andino (77). The PCBP1 and PCBP2 coding sequences were PCR amplified from plasmid DNA and cloned into the *Msc*I site of pDJB2ΔGUA$_3$ as described above, generating the PCBP1 and PCBP2 expression constructs pPCBP1ΔGUA$_3$ and

pPCBP2ΔGUA$_3$. (ii) The MS2 coding sequence (137) was synthesized by GeneArt, optimizing codon usage for both mammalian and bacterial expression. The synthetic DNA contained a 5' *Sma*I site as well as consensus Kozak's sequence upstream of the initiating AUG. For expression and cloning purposes, the MS2 coding sequence was tailed with a 3' RGSH linker (112) and the 5' nucleotides of the PCBP2 coding sequence through the preexisting *Ale*I site. This synthetic MS2 DNA was digested and cloned into the *Sma*I and *Ale*I sites of the pPCBP2ΔGUA$_3$ expression construct, generating an in-frame fusion of MS2 and PCBP2 (pMS2-PCBP2ΔGUA$_3$). Using two-step PCR, a second MS2 coding region was fused, in-frame, upstream of the original MS2-PCBP2 sequence, generating the p(MS2)$_2$PCBP2ΔGUA$_3$ expression construct, in which the two MS2 sequences were joined with a GAPGIHPGM peptide linker, described by Hook *et al*. (96). (iii) The (MS2)$_2$ expression construct [p(MS2)$_2$ΔGUA$_3$] was generated by introducing two stop codons in the (MS2)$_2$PCBP2ΔGUA$_3$ plasmid, following the RGSH linker sequence, using site-directed mutagenesis. The PCBP2 coding sequence was then removed from this construct by restriction digest and re-ligation. (iv) The (MS2)$_2$PCBP1 expression construct [p(MS2)$_2$PCBP1ΔGUA$_3$] was generated by semi-overlapping two-step PCR using p(MS2)$_2$ΔGUA$_3$ and pPCBP1ΔGUA$_3$ as templates. The resultant fused PCR product was ligated into the *Xma*I and *Xho*I sites of p(MS2)$_2$ΔGUA$_3$. (v) The PCBP2-KL and (MS2)$_2$PCBP2-KL expression constructs [pPCBP2-KLΔGUA$_3$ and p(MS2)$_2$PCBP2-KLΔGUA$_3$] were generated by deleting the cDNA corresponding to exon 8a in each parent clone using two-step mutagenic PCR. (vi) The (MS2)$_2$KH1[Region] expression construct [p(MS2)$_2$KH1[Region]ΔGUA$_3$] was generated by PCR amplification of the coding sequence for amino acids 1-91 of PCBP2 using a 5' phosphorylated (5'PO$_4$) primer and a 3' primer containing an *Xho*I site. This product was digested with *Xho*I and ligated into the *Ale*I and *Xho*I sites of

p$(MS2)_2$PCBP2ΔGUA_3, essentially replacing the PCBP2 coding sequence downstream of the RGSH linker. (vii) The $(MS2)_2$KH2[Region] expression construct [p$(MS2)_2$KH2[Region]ΔGUA_3] was generated by PCR amplification of the coding sequence for amino acids 90-233 of PCBP2 and subsequent cloning into the *Xho*I and *Ale*I sites of p$(MS2)_2$PCBP2ΔGUA_3, as described above. (viii) The $(MS2)_2$KH2[Region] expression construct [p$(MS2)_2$KH3[Region]ΔGUA_3] was generated by PCR amplification of the coding sequence for amino acids 234-364 of PCBP2 and subsequent cloning into the *Xho*I and *Ale*I sites of p$(MS2)_2$PCBP2ΔGUA_3, as described above. (ix) The $(MS2)_2$KH1/2[Region] expression construct [p$(MS2)_2$KH1/2[Region]ΔGUA_3] was generated by PCR amplification of the coding sequence for amino acids 1-233of PCBP2 and subsequent cloning into the *Xho*I and *Ale*I sites of p$(MS2)_2$PCBP2ΔGUA_3, as described above. (x) The $(MS2)_2$KH3[Domain] expression construct [p$(MS2)_2$KH3[Domain]ΔGUA_3] was generated by PCR amplification of the coding sequence for amino acids 269-357 of PCBP2 and subsequent cloning into the *Xho*I and *Ale*I sites of p$(MS2)_2$PCBP2ΔGUA_3, as described above. (xi) The $(MS2)_2$KH3-$\Delta\beta1$ expression construct [p$(MS2)_2$KH3-$\Delta\beta1\Delta GUA_3$] was generated by PCR amplification of the coding sequence for amino acids 280-357 of PCBP2 and subsequent cloning into the *Xho*I and *Ale*I sites of p$(MS2)_2$PCBP2ΔGUA_3, as described above. Transcripts of this construct express an $(MS2)_2$ fusion to the KH3 domain with the first β-strand of the domain deleted. (xii) The $(MS2)_2$KH3-$\Delta\alpha3$ expression construct [p$(MS2)_2$KH3-$\Delta\alpha3\Delta GUA_3$] was generated by PCR amplification of the coding sequence for amino acids 269-340 of PCBP2 and subsequent cloning into the *Xho*I and *Ale*I sites of p$(MS2)_2$PCBP2ΔGUA_3, as described above. Transcripts of this construct express an $(MS2)_2$ fusion to the KH3 domain with the last α-helix of the domain deleted. (xiii) The $(MS2)_2$KH1/2-ΔMD expression construct [p$(MS2)_2$KH1/2-ΔMD] was

generated by deleting the coding sequence for amino acids 125-158 of PCBP2 from the context of p$(MS2)_2$KH1/2[Region] using two-step mutagenic PCR. Transcripts of this construct express an $(MS2)_2$ fusion to the amino-terminal KH1/2 fragment of PCBP2 with a deletion in the multimerization domain of KH2.

To obtain cDNAs for the remaining PCBP family members (PCBP3, PCBP4, PCBP4A, and hnRNP-K), total cellular mRNA was obtained from 10^6 HeLa S3 suspension cells using TRIzol Reagent (Invitrogen) and subsequent ethanol precipitation. Using this purified cellular mRNA, 1st-strand cDNA was generated using SuperScript III Reverse Transcriptase (Invitrogen) with either Oligo$(dT)_{20}$ or DNA primers complimentary to the 3'NTR of the gene of interest. Digestion of the parent mRNA was achieved using RNase H (Invitrogen) and 2nd-strand cDNA was generated using PfuUltra Fusion Polymerase (Stratagene) with primers complimentary to the 5'NTR of the gene of interest. This newly synthesized cDNA was further amplified using PfuUltra Fusion Polymerase (Stratagene) and 5'PO_4 versions of the same 5' and 3' primers as were used for 1st and 2nd-strand cDNA synthesis. These specific PCR products were subcloned into the *EcoR*V site of pLITMUS39 (New England Biolabs) for blue/white screening. Following restriction enzyme screening, each coding sequence was PCR amplified from a correct subclone using 5' and 3' PO_4 primers specific to the precise gene start and stop. In addition, the 5' primer contained the Kozak's consensus sequence immediately prior to the initiating ATG, and the 3' primer contained an additional stop codon to prevent any potential translational read-through. In all cases, the PCR products were ligated into the *Msc*I site of pDJB2ΔGUA_3, generating the expression constructs pPCBP3ΔGUA_3, pPCBP4ΔGUA_3, pPCBP4AΔGUA_3, and pHnRNP-KΔGUA_3. The coding sequence for each of these PCBP family members was further fused to the $(MS2)_2$ coding sequence by semi-overlapping two-step PCR and ligation into the

*Xma*I and *Xho*I sites of p(MS2)$_2$ΔGUA$_3$. This resulted in the generation of the expression constructs p(MS2)$_2$PCBP3ΔGUA$_3$, p(MS2)$_2$PCBP4ΔGUA$_3$, p(MS2)$_2$PCBP4AΔGUA$_3$, and p(MS2)$_2$hnRNP-KΔGUA$_3$.

Bacterial Protein Expression Clones Used in These Studies

To inducibly express proteins of interest, the pET16b plasmid DNA was obtained from Novagen. Although this vector contains sequences encoding a previously inserted amino-terminal polyhistidine tag, these sequences were removed as a result of the cloning process. This would then result in the expression of fully wild-type, untagged protein following transfection and induction in expression cells. (i) To generate the bacterial expression constructs for PCBP1, PCBP2, PCBP2-KL, and PCBP3, the coding sequence for each protein was removed from the corresponding poliovirus based expression clone (described above) using *NcoI* and *XhoI*. The resultant fragment was ligated into the corresponding sites of similarly digested pET16b plasmid DNA, generating pET16-PCBP1, pET-PCBP2, pET16-PCBP2KL, and pET16-PCBP3. (ii) To generate the bacterial expression constructs for PCBP4 and PCBP4A, each coding sequence was amplified from each of the poliovirus expression constructs using a 5' primer containing a *BspH*I restriction site and a 3' primer containing an *Xho*I restriction site, since *BspH*I generates an *Nco*I-compatible overhang. Each PCR product was digested with *BspH*I and *Xho*I, and subsequently ligated into an *Nco*I/*Xho*I digested pET16b vector DNA, generating pET16-PCBP4 and pET16-PCBP4A. (iii) To generate the bacterial expression construct for hnRNP-K, pET16b was digested with *Xho*I, filled in with the Klenow fragment of T4 DNA polymerase, and then further digested with *Nco*I. The entire coding sequence for hnRNP-K was removed from the poliovirus expression construct by digestion with *Nco*I and *Pme*I (blunt cut). This fragment was subsequently ligated into the corresponding sites of the *Nco*I/*Xho*I-blunt pET16b vector DNA, generating pET16-hnRNPK

RNA Transcript Preparation and Purification

Prior to *in vitro* transcription, the run-off transcription template was prepared by digesting the desired plasmid DNA with *Mlu*I. Digestion with this enzyme resulted in linearization of the circular plasmid DNA via a single cut immediately following the poliovirus 3'NTR/poly(A) tail. Restriction digest reactions were phenol:chloroform extracted three times, chloroform extracted three times, and subsequently ethanol precipitated. Ethanol precipitated *Mlu*I cut template DNA was resuspended in TE, standardized to 0.5 µg/µL, and stored at -20°C.

Standard Transcription

Standard transcription conditions were used for generating all non-capped, non-ribozyme transcript RNAs. In these conditions, transcription reactions contained 1X transcription buffer [40 mM TrisHCl (pH=8), 6 mM $MgCl_2$, 2 mM spermidine], 10 mM DTT, 0.4 U/µL RNasin (Promega), 1000 µM of each NTP (ATP, CTP, GTP, UTP), and 15 ng/µL linearized template. Bacterially expressed recombinant T7 polymerase was purified by B. Joan Morasco, and approximately 1 µL of this purified T7 polymerase was used per 100 µL transcription reaction. Reactions were incubated at 37°C for 2 h and were stopped by the addition of 2.5 volumes of 0.5% SDS buffer [10 mM TrisHCl (pH=7.5), 100 mM NaCl, 1 mM EDTA, 0.5% sodium dodecyl sulfate].

For purification purposes, RNA transcripts were phenol:chloroform extracted three times, chloroform extracted three times, and subsequently precipitated by the addition of three volumes of 100% ethanol and incubation overnight at -20°C. Precipitated RNAs were further purified by desalting over Sephadex G-50 (GE Healthcare) gel filtration resin (0.5 x 15 cm column). Peak fractions containing RNA were identified and quantitated spectrophotometrically. All fractions containing significant quantities of RNA were pooled, aliquotted (10-20 µg/aliquot), and ethanol

precipitated. These purified, desalted transcript RNAs were stored, in ethanol, at -20°C and were only precipitated immediately prior to their use in translation/replication experiments.

Ribozyme Optimized Transcription

For RNA transcripts containing the Rz sequence, transcription conditions were altered to optimize Rz cleavage (141). These conditions are identical to those provided above for standard transcription, with the exception of the NTP concentrations. Here, each NTP (ATP, CTP, GTP, UTP) was included in the transcription reaction at 500 μM. It was determined experimentally that these conditions resulted in >95% ribozyme cleavage efficiency. Ribozyme optimized transcription reactions were stopped, extracted, desalted, and stored in the same manner as described above for standard transcription reactions.

5' Capping Transcription

To synthesize RNAs with a m^7G cap analog, transcription conditions were slightly altered to optimize the capping reaction. These conditions are identical to those provided above for standard transcription, with the exception that the GTP concentration was lowered to 200 μM, and 800 μM of m^7G[5']ppp[5']G cap analog (Epicentre) was added to the transcription reaction mixture (26). Under these conditions, ~80% of the transcript RNAs contain a 5' 7^mG cap. Capping transcription reactions were stopped, extracted, desalted, and stored in the same manner as described above for standard transcription reactions.

HeLa Extract Preparation

HeLa S3 cells were adapted to liquid suspension culture and were maintained in Joklik's modified Eagle medium supplemented with 5% bovine calf serum (Hyclone) and 2% FetalClone II (Hyclone). Cells were passaged as needed to maintain a cell density of less than 5×10^5 cells/mL. In cases where cells were being grown for the purposes of an S10 preparation, HeLa cells were pelleted and resuspended in fresh 18-24 h prior to their use in the S10

proceedure. The following procedures were originally developed in our laboratory by Barton *et al*, and are described in more detail in previous publications (21, 22, 24). Any deviation from these published procedures has been noted, where applicable.

S10 Preparation

HeLa cell density was determined by hemocytometer count, and approximately 10^9 HeLa suspension cells were pelleted by low speed centrifugation. This cell pellet was washed sequentially with 2 L of isotonic buffer [35 mM HEPES-KOH (pH=7.4), 146 mM NaCl, 5 mM dextrose], and was resuspended over 10 min on ice in 1.5 volumes of hypotonic buffer [20 mM HEPES-KOH (pH=7.4), 10 mM KCl, 1.5 mM $Mg(CH_3CO_2)_2$, 1 mM DTT] with gentle vortexing. Resuspended swollen cells were transferred to a glass dounce homogenizer and were dounced on ice using a type 'A' or tight pestle. Cell integrity was monitored by removing a small aliquot at various times during douncing and visually assessing percent lysis by light microscopy. Optimal lysis was defined as approximately 80% lysis with visibly intact nuclei and typically required 20-25 strokes of the dounce. The final volume of this mixture was determined and 1/9 volume of 10X S10 buffer [200 mM HEPES-KOH (pH=7.4), 1.2 M $K(CH_3CO_2)$, 40 mM $Mg(CH_3CO_2)_2$, 50 mM DTT] was added to make the final solution 1X. Following this addition, unlysed cells, nuclei, and other dense debris were removed by low speed centrifugation. The resultant semi-cleared supernatant was subsequently transferred to a siliconized corex tube and centrifuged at 12,000 x g for 15 min at 4°C. The supernatant from this centrifugation was treated with micrococcal nuclease (5 μg/mL, 20°C, 15 min) in the presence of $CaCl_2$ (1 mM) to degrade all endogenous cytoplasmic cellular mRNAs. After micrococcal nuclease treatment, the nuclease was inactivated by addition of EGTA (2 mM) to chelate the essential calcium. Any additional insoluble debris was the removed by a second 15 min centrifugation at 12,000 x g. The supernatant from this spin was divided into single use aliquots and stored at -80°C. This

supernatant is defined as HeLa S10 for the purposes of all experiments performed in the studies herein.

IF Preparation

The initial procedure for IF preparation is exactly the same as described above for S10 preparation with three significant changes: 1)Washed cell pellets were resuspended in 2 volumes of hypotonic buffer, rather than 1.5 volumes. 2)Swollen cells were dounced to 90-100% lysis, rather than 80%, however minimal disruption of nuclei is still ideal. 3)The supernatant from the first 12,000 x g centrifugation is not treated with micrococcal nuclease.

The supernatant from the first 12,000 x g centrifugation described above is transferred to an ultracentrifuge tube and centrifuged at 330,000 x g for 60 min at 4°C. The pellet from this spin contains the cytoplasmic ribosomes and ribosome associated protein components, as well as the smooth and rough endoplasmic reticulum, microsomes, exosomes, and other lipid related structures. The supernatant was removed and the ribosome containing pellet was resuspended in 1.5 mL of hypotonic buffer. Resuspension of this pellet was facilitated by the use of a magnetic micro stir bar and stir plate at 4°C, and typically required 30 min stir time. To standardize protein preparations, a 2 μL aliquot was removed, diluted 1:250, and the absorbance at 260 nm was obtained. This roughly reflects the concentration of ribosomal RNA in the preparation, and readings in the range of 0.7-0.9 (175-225 A_{260} units undiluted) reflect the optimal concentration range. Preparations that exceed this range were diluted appropriately with hypotonic buffer until the desired absorbance is reached. Once an optimal A_{260} reading was attained, the total volume was measured and 1/7 volume of 4 M KCl was added. This addition raised the final KCl concentration to 0.5 M, disrupting the ionic and electrostatic interactions necessary for initiation factor association with the larger ribosomal complex. To allow this dissociation to proceed, the mixture was incubated for 15 min at 4°C with stirring. The mixture was subsequently

centrifuged again at 330,000 x g for 60 min at 4°C. The resultant supernatant was removed and dialyzed against IF buffer [20 mM HEPES-KOH (pH=7.4), 120 mM K(CH_3CO_2), 5 mM $Mg(CH_3CO_2)_2$, 5 mM DTT] for 2 h at 4°C. The dialyzed supernatant was divided into single use aliquots and stored at -80°C. This dialyzed supernatant is defined as HeLa IF for the purposes of all experiments performed in the studies herein.

HeLa S10 Translation-RNA Replication Reactions

For all experiments, extract preparations are thawed on ice immediately prior to their use, and aliquots are never reused once thawed. Additionally, transcript RNAs are stored in ethanol and are precipitated, washed, resuspended and quantitated immediately prior to their use. Transcript RNAs, once precipitated, were never reprecipitated and reused for later experiments. In general, all reaction components are thawed and stored on ice during experimental setup. Both translation and replication reactions utilized single use aliquots of a 10X nucleotide reaction mix [155 mM HEPES-KOH (pH=7.4), 600 mM K(CH_3COOH), 300 mM creatine phosphate, 4 mg/mL creatine phosphokinase, 10 mM ATP, 2.5 mM GTP, 2.5 mM UTP]. This reaction mix includes optimal buffers and salts for PV translation and an ATP regenerating system, but excludes CTP. This omission allows for later use of [^{32}P]CTP to radiolabel RNA replication products.

RNA Programming and Translation

HeLa S10 translation reactions were prepared by combining 50% (by volume) HeLa S10 extract, 20% (by volume) HeLa IF, 10% (by volume) 10X nucleotide reaction mix, 2 mM guanidine hydrochloride (GuHCl), template RNA, and sterile/RNase-free water. Purified template RNA was precipitated, resuspended in sterile/RNase-free water, and quantitated spectrophotometrically. Unless otherwise specified in an individual experimental methodology, 4 pmol of purified template RNA was used to program the HeLa S10 translation reactions. In

cases where multiple RNAs were required (e.g. *trans*-replication experiments), 4 pmol total RNA was used. When RNA programmed translation reactions were assembled, a 10 µL aliquot was removed, to which 11 µCi (1 µL) of L-[^{35}S]-methionine (1,000 Ci/mmole; PerkinElmer) was added for metabolic labeling of newly synthesized proteins. Both the HeLa S10 translation reactions and the [^{35}S]-methionine labeling side reaction were incubated at 34°C for 3-4 h. Following incubation, the HeLa S10 translation reactions were centrifuged to isolate pre-initiation replication complexes (PIRCs), which is described below. Additionally, 5 µL of the [^{35}S]-methionine labeling side reaction was added to 45 µL of 1X Laemmli sample buffer (LSB; 112.5 mM TrisHCl (pH=6.8), 2% sodium dodecyl sulfate, 20% glycerol, 0.5% β-mercaptoethanol, 0.02% bromophenol blue). This mixture was stored at -20°C prior to analysis by SDS-PAGE.

PIRC Isolation and RNA Replication

Membrane associated PV translation in the HeLa S10 translation reactions resulted in the formation of replication complexes. The inclusion of GuHCl in the translation reaction allowed these complexes to form, however initiation of negative-strand synthesis was blocked. These pre-fire complexes have been defined as pre-initiation replication complexes (PIRCs). PIRCs can be obtained by centrifugation and isolation of the membrane pellet from HeLa S10 translation reactions. To do so, HeLa S10 translation reactions were centrifuged at 20,000 x g for 15 min at 4°C. Supernatants were carefully removed so as not to disturb the membrane pellet. PIRC pellets were gently resuspended in replication buffer, which contained 50% (by volume) S10 buffer (40 mM HEPES-KOH (pH=7.4), 120 mM K(CH_3CO_2), 5.5 mM Mg(CH_3CO_2)$_2$, 6 mM DTT, 10 mM KCl], 10% (by volume) 10X nucleotide reaction mix, 0.1 mg/mL puromycin, 5 µM CTP, and 30 µCi [α-^{32}P]CTP (800 Ci/mmol; PerkinElmer). Resuspension in a GuHCl-free buffer washed out the residual inhibitory GuHCl from the PIRCs,

and replication was allowed to proceed by incubation at 37°C for 1 h. Following incubation, RNA replication reactions were stopped with 6 volumes of 0.5% SDS buffer, and were treated with 20 μg of proteinase K for 15 min at 37°C. Digested RNA replication reactions were subsequently extracted three times with phenol:chloroform, extracted three times with chloroform, and precipitated by the addition of 3 volumes of 100% ethanol. Extracted product RNAs were stored in ethanol at -20°C for at least 12 h, or until analyzed by gel electrophoresis.

Analysis of Protein Synthesis by SDS-PAGE

Protein synthesis was analyzed by 9-18% gradient sodium dodecyl sufate polyacrylamide gel electrophoresis (SDS-PAGE). To do this, a vertical 0.75 mm 9-18% gradient resolving gel was cast using a gradient maker, and a 4% stacking gel was cast above the gradient gel. The ratio of acrylamide to *bis*-acrylamide used was 29:1, and the standard Tris-glycine discontinuous buffer system was also used. Samples were electrophoresed at constant current until the bromophenol blue dye front had exited the bottom of the resolving gel. Completed gels were fixed in 40% methanol/10% acetic acid for at least 15 min and rinsed with deionized water. Fixed gels were then impregnated with Amplify Fluorographic Reagent (GE Healthcare) by soaking for 10 min. Residual Amplify was rinsed away using deionized water and gels were transferred to chromatography paper for drying. Autoradiography was performed by exposure of dried gels to Kodak X-omat Blue XB-1 scientific imaging film at either -20°C or -80°C. Where applicable, quantitation of protein products was performed by phosphorimager using ImageQuant software (Molecular Dynamics).

Analysis of RNA Replication by Denaturing CH_3HgOH Gel Electrophoresis

Due to the uniquely elevated stability of an extended RNA-RNA duplex, complete denaturation of product RNA, particularly negative-strand RNA in a replicative form duplex, requires a powerful denaturant. For this reason, methyl mercury hydroxide (CH_3HgOH) agarose

gel electrophoresis was utilized to resolve and visualize RNA products from HeLa S10 translation-RNA replication reactions. Purified product RNA was recovered from ethanol precipitation by centrifugation, washing, and resuspension in 15 µL of sterile/RNase-free water. An equal volume of CH_3HgOH sample buffer [50 mM H_3BO_3/5 mM $Na_2B_2O_7$ (pH=8.2), 10 mM Na_2SO_4, 1 mM EDTA, 25% glycerol, 0.05% bromophenol blue, 50 mM CH_3HgOH] was then added to the resuspended replication product, and allowed to denature for 5-15 min at room temperature. Denatured RNA products were resolved on a vertical 1% Seakem LE agarose gel which contained 5 mM CH_3HgOH. Electrophoresis was performed at 70 mA constant current in 1X CH_3HgOH running buffer [50 mM H_3BO_3/5 mM $Na_2B_2O_7$ (pH=8.2), 10 mM Na_2SO_4, 1 mM EDTA]. For the first hour of electrophoresis, the buffer in the upper and lower buffer chambers were recirculated using a peristaltic pump to avoid depletion of buffering capacity. Electrophoresis was halted when the bromophenol blue dye front reached 1-2 cm from the bottom of the gel (typically 2.5 h total time). Gels were stained with 1.0 mg/mL ethidium bromide in 0.5 M $NH_4(CH_3COOH)$ for 10 min and visualized on a UV transilluminator to ascertain equal loading/recovery. Gels were subsequently transferred to chromatography paper for drying. Autoradiography was performed by exposure of dried gels to Kodak X-omat Blue XB-1 scientific imaging film at -80°C using a Biomax intensifying screen. Quantitation of RNA products was performed by phosphorimager using ImageQuant software (Molecular Dynamics).

Bacterial Protein Expression

Bacterial protein expression plasmids were maintained as DNA stocks in TE at -20°C and were only transformed into expression cells immediately prior to protein expression. Plasmid DNA was transformed into BL21(DE3) pLysS competent cells (Novagen) and a single colony was used to inoculate a 5.0 mL LB broth culture containing 50 µg/mL ampicillin and 34 µg/mL chloramphenicol. This culture was incubated overnight at 37°C with shaking. A fresh 50 mL

LB broth culture without antibiotic was then inoculated with 50 µL of the overnight culture and incubated at 25°C with shaking. Protein expression was induced for 2 h with 1 mM IPTG when the culture reached an OD_{600} of ~0.5. Cleared protein extracts were prepared as described in Andino *et al* (12). Briefly, cells were harvested, weighed, washed once with phosphate buffered saline, and resuspended using 5.0 mL/g wet weight in lysis buffer (10 mM HEPES-KOH (pH=7.9), 20 mM KCl, 25 mM EDTA, 5 mM DTT, 1% Triton X-100). The resuspended cell pellet was frozen and thawed, sonicated for 30 s, and centrifuged at 150,000 x g for 15 min. The supernatant from this centrifugation was supplemented with glycerol to a final concentration of 20%, aliquotted and stored at -80°C.

Electrophoretic Mobility Shift Assays

Riboprobe Synthesis

DNA templates containing the cDNA for the PV 5'CL were digested with *Hga*I, which cuts 30-nts past the 5'CL. Cut DNAs were purified by phenol:chloroform extraction and ethanol precipitation. Radiolabeled 5'CL probes were made by T7 transcription of *Hga*I cut DNA template as described above for ribozyme optimized transcription, with one exception. Rather than 500 µM CTP, a combination of 115 µM non-labeled CTP and 4 Ci/µL [α-^{32}P]CTP (400 Ci/mmol) was used. Probes were purified directly from the transcription reaction by passage over NucAway Spin Columns (Ambion), followed by a single phenol:chloroform extraction, single chloroform extraction, and ethanol precipitation. Riboprobes were stored in ethanol at -20°C until immediately prior to their use, and were only reprecipitated for a maximum of two additional experiments. For quantitation of precipitated radiolabeled riboprobes, TCA precipitation, filtering, and scintillation counting was performed. Calculations were subsequently performed based on the specific activity of the [^{32}P]CTP in the transcription reaction and the number of C residues in the given riboprobe.

Binding Reactions and Gel Electrophoresis

Electrophoretic mobility shift assays (EMSA) were performed based on a modified protocol described previously (13). Radiolabeled riboprobes were prepared as described above, and protein was either obtained from HeLa S10 translation reactions or as recombinant protein from clarified bacterial lysate. Binding reactions were performed by pre-incubating 1.5 μL of HeLa S10 translation reaction mixture or 0.5-3 μL of bacterial extract in a 9 μL reaction, containing binding buffer [5 mM HEPES-KOH (pH=7.9), 25 mM KCl, 2 mM $MgCl_2$, 3.8% glycerol, 1.5 mM ATP, 20 mM DTT], 20 μg yeast tRNA, and 40 U RNasin (Promega) at 30°C for 10 min. To this preincubation mix, 20 fmol of ^{32}P-labeled riboprobe was added to the reaction. The final binding reaction was incubated at 30°C for an additional 10 min prior to addition of 2 μL loading buffer [0.1% bromophenol blue, 50% glycerol]. A 5% polyacrylamide [40:1 acrylamide:bisacrylamide] native gel containing 5% glycerol was cast in 0.5X TBE buffer [176 μM TrisHCl, 176 μM H_3BO_3, 2 mM EDTA]. Prior to loading, the gel was pre-run at 4°C for 30 min at 30 mA with constant current using 0.5X TBE as the running buffer. Ribonucleoprotein complexes were resolved by electrophoresis at 4°C at 220 V with constant voltage. Electrophoresis was halted when the bromophenol blue dye front reached 3-4 cm from the bottom of the gel. The final gel was transferred to chromatography paper, dried, and visualized by autoradiography as described above.

CHAPTER 3
POLY(C) BINDING PROTEIN IS REQUIRED FOR EFFICIENT INITIATION OF POLIOVIRUS NEGATIVE-STRAND RNA SYNTHESIS

Introduction

The poly(C) binding proteins (PCBP; also called hnRNP E and αCP) represent a family of poly(rC/dC) binding proteins which include hnRNP K and PCBPs 1-4 (109, 121, 128, 133). In addition to their nucleic acid binding specificity, this protein family is characterized by the presence and positioning of three highly homologous hnRNP K Homology domains(KH domains) (80, 188). In the case of the PCBPs, the first and third KH domains contain the primary nucleic acid binding activity, although the second domain may enhance binding affinity and/or specificity (65, 67). It is thought that the structure of this domain is highly conserved, regardless of surrounding sequence context, acting as an independent cassette which can be evolutionarily tuned to a specific function. Although initially characterized as RNA binding proteins involved in pre-mRNA metabolism, more recent work has described an increasingly globalized set of essential cellular processes in which PCBPs participate. While there is some degree of overlap in the sequences bound by the PCBPs, the use of alternate binding partners together with modulation of binding specificity and affinity, results in an immense number of potential regulatory targets and functions.

As yet, the most extensively studied family members are hnRNP K, PCBP1, and PCBP2. Current work has firmly established the involvement of the PCBP protein family in mRNA stabilization, transcriptional regulation, translational control, and apoptotic program activation (reviewed by (129)). The mRNAs targeted by these proteins are diverse as well, including α-globin, 15-lipoxygenase, collagen αI, tyrosine hydroxylase, erythropoietin and androgen receptor (49, 64, 154, 162, 191, 211, 217). In addition, more recent work identified over 150 mRNAs in a hematopoietic cell line that interact, *in vivo*, with PCBP2 alone (208). A

number of interacting proteins have also been identified, including AUF1, HuR, SRp20 and Poly(A) Binding Protein, as well as other members of the PCBP family (6, 28, 49, 77, 93, 108, 110).

Given the abundance and multi-functional nature of these proteins, it is not surprising that multiple viruses, both RNA and DNA alike, have evolved to utilize these proteins during various stages of their replication. The ORF57 protein of Kaposi's Sarcoma-associated herpesvirus (KSHV) has been shown to interact with PCBP1, and this complex is capable of stimulating the translation of specific cellular and viral genes (147). In the case of human papillomavirus (HPV), PCBP1 interacts with one of the capsid protein mRNAs and down-regulates its translation (60). Interestingly, recent work revealed markedly decreased levels of PCBP1 in cervical epithelial cells transformed by HPV, and demonstrated a direct correlation between cellular PCBP1 levels and progression to cervical cancer (169). Hepatitis C virus (HCV) binds PCBP2 at both the 5' and 3' NTR of its genomic RNA (189, 200), however the role of these binding events is yet to be understood.

Many members of the family *Picornaviridae* have also been shown to utilize the PCBPs for their replication, including hepatitis A virus (HAV), human rhinovirus 14 (HRV-14), coxackievirus B3 (CVB3) as well as poliovirus (PV). One functional commonality is the requirement for PCBP2 in the cap-independent initiation of translation mediated by a type-I IRES (38, 66). Interestingly, although HAV does not have a classic type I IRES, PCBP2 is still utilized for translation initiation via interaction with an alternative sequence element in the 5' NTR (83). Even the type-II IRES of Encephalomyocarditis Virus (EMCV), which does not *require* PCBP, will still compete for PCBP binding (66). This suggests a more generalized function for the PCBPs in picornaviral translation initiation.

Poliovirus (PV), in addition to the IRES, possesses a 5'-terminal cloverleaf (5'CL) structure that is essential for RNA replication and is conserved among all members of the *Enterovirus* genus (12, 13, 26, 93, 126, 196, 213, 219). The 5'CL is divided into four domains: stem *a* and stem-loops *b*, *c*, and *d* (Figure 3-1A). Stem-loop *d* binds viral protein $3CD^{pro}$, and stem-loop *b* binds PCBP1 or PCBP2 (12, 13, 158). PCBP1/2 will bind to the 5'CL in the absence of viral proteins, however the concomitant binding of $3CD^{pro}$ results in a nearly 100-fold increase in PCBP binding affinity (79). While both the first and third KH domains bind poly(C) RNA with similar affinity, only the first KH domain of PCBP1/2 is required to bind to the 5'CL (65, 185, 209). The binding of PCBP1/2 and $3CD^{pro}$ to the 5' cloverleaf is believed to play an important role in viral RNA replication (12, 13, 79, 213), and in RNA stability (144). In addition, PV RNA replication is inhibited in Poly(C)-depleted HeLa S10 extracts, strongly suggesting that PCBP binding to the 5' cloverleaf is required in one or more steps of the viral RNA replication cycle (209).

In the current study, we investigated the role of the PCBP-5'CL RNP complex in PV RNA replication. Herein, we present data that demonstrates that the binding of PCBP to the 5'CL is required to form the replication complex used to initiate PV negative-strand RNA synthesis. Furthermore, we describe the novel application of a protein-RNA tethering system in the functional analysis of essential cellular protein involvement in virus replication. Using this system, we were able to overcome the difficulties presented in performing experiments involving RNAi, gene knockout, protein depletion or dominant negative inhibition of multi-functional, essential cellular proteins, such as the PCBPs. Moreover, we demonstrate the ability of this system to directly analyze and modify domains of a cellular protein, specifically as it pertains to virus replication.

Results

A Mutation in Stem-loop b of the 5' Cloverleaf Inhibits Negative-strand Synthesis

To clarify the role of PCBP binding to the 5'CL in PV RNA replication, we used a subgenomic PV RNA transcript [P23 RNA] which encodes all of the essential viral replication proteins and forms functional RNA replication complexes in cell-free reactions. We compared the replication of wild-type P23 RNA with the replication of the same RNA with a C24A mutation in stem-loop *b* of the 5' CL [P23-5'CL^{C24A} RNA] (Figure 3-1B). PV RNA replication was assayed using preinitiation RNA replication complexes (PIRCs) isolated from HeLa S10 translation-replication reactions as described in Chapter 2. To assay for negative-strand synthesis, we utilized P23 RNA transcripts which contain two 5' terminal non-viral G's that inhibit positive-strand initiation (25, 141).

To first examine the ability of the 5'CL^{C24A} to bind PCBP, we performed electrophoretic mobility shift assays (EMSA) using radiolabeled 5'CL riboprobes containing either a wild-type or C24A stem-loop *b*. The C24A mutation has been previously shown to inhibit the formation of the essential 5' RNP complex (12, 77, 144, 158), and as expected, the PCBP-5'CL RNP complex (complex I) was observed using 5'CL^{WT} RNA probe but not on 5'CL^{C24A} RNA probe. This demonstrated that PCBP2 does not bind to 5'CL^{C24A} RNA, as predicted. In RNA replication reactions containing P23-5'CL^{C24A} RNA, negative-strand synthesis was 10-20% of the amount observed with wild-type P23 RNA (Figure 3-2B). Additional work from our lab has shown that there is no defect in positive-strand synthesis of P23-5'CL^{C24A} RNA, despite the decreased levels of negative-strand synthesis (Sharma *et al*., unpublished results). Taken together, these experiments demonstrated that P23-5'CL^{C24A} RNA was defective for negative- but not positive-strand synthesis

$(MS2)_2$ Protein-RNA Tethering System

Tethered function assays have been used to study the activity of cellular proteins in mRNA metabolism and regulation apart from their RNA binding affinity and specificity (reviewed in 57). One system that is used for this type of assay takes advantage of the high-affinity interaction of the MS2 bacteriophage coat protein with its cognate RNA stem-loop structure (47, 58). The MS2 tethered function system requires the generation of an in-frame fusion of the MS2 coat protein with the protein of interest. At the same time, the native protein binding site in the target RNA is replaced with the MS2 RNA stem-loop structure (47). Co-expression of the MS2 fusion protein targets the protein of interest to the MS2 stem-loop structure in the target RNA. This system was used by Kong *et al*. to demonstrate that human α-globin mRNA is stabilized by tethering an isoform of murine PCBP2 (murPCBP2-KL) (112). Because the MS2 coat protein binds to the MS2 stem-loop as a dimer, Hook et al examined the use of a covalent dimer of the MS2 protein, first described by Peabody and Lim (96, 163). This head-to-tail covalent dimer of MS2 coat proteins, here termed $(MS2)_2$, results from the in-frame fusion of tandem MS2 open reading frames by a linker sequence. Using this approach, Hook et al. observed an increase in specificity and efficacy of the covalent dimer system, relative to that of a single MS2 fusion (96). For these reasons, we developed a protein-RNA tethering system using the $(MS2)_2$ covalent dimer to directly examine the role of PCBP2 tethered to the 5'CL in PV RNA replication.

In the case of wild-type PV RNA, PCBP1/2 binds to stem-loop *b* in the 5'CL and viral protein 3CD binds to stem-loop *d* (Figure 3-3A). By replacing the majority of stem-loop *b* with an equally sized MS2 stem-loop structure [$5'CL^{MS2}$] (Figure 3-1C), we removed the PCBP binding site, thereby preventing endogenous PCBP from binding to the $5'CL^{MS2}$. In addition, expression of the $(MS2)_2$PCBP2 covalent dimer fusion protein, in the presence of the $5'CL^{MS2}$ RNA, should tether PCBP2 to the $5'CL^{MS2}$ via the interaction of the $(MS2)_2$ covalent dimer with

the MS2 RNA stem-loop structure (Figure 3-3B). By extension, we predict that PV RNA transcripts containing the 5'CL^{MS2} will be defective for negative-strand synthesis, and that co-expression of the $(MS2)_2$PCBP2 fusion protein in the same reaction should restore negative-strand synthesis definitively showing that PCBP2 is required for negative-strand initiation.

$(MS2)_2$PCBP2 Binds Specifically to 5'CL^{MS2} RNA

To establish the functionality of the MS2 protein-RNA tethering system, we first performed electrophoretic mobility shift assays (EMSA) to examine the protein binding profile of the 5'CL^{MS2} relative to that of the 5'CL^{WT}. As expected, the 5'CL^{WT} RNA probe formed a previously characterized PCBP-5'CL RNP complex (complex I) with either endogenous PCBPs in HeLa S10 extracts or recombinant PCBP2 (rPCBP2) (Figure 3-4A, lanes 1-4) (12, 77, 158). In contrast, complex I was not formed in identical binding assays containing the 5'CL^{MS2} RNA probe (Figure 3-4A, lanes 5-8). This demonstrated that PCBP2 does not bind to 5'CL^{MS2} RNA probe, as predicted.

HeLa S10 translation-replication reactions were programmed with a non-translating RNA (mock translation) or protein expression RNAs which encoded either PCBP2, $(MS2)_2$ or $(MS2)_2$PCBP2. As expected, the PCBP-5'CL complex (complex I) was formed in binding assays containing the 5'CL^{WT} RNA probe (Figure 3-4B, lanes 2-5) but not in assays containing the 5'CL^{MS2} RNA probe (Figure 3-4B, lanes 7-10). The expression of exogenous PCBP2, $(MS2)_2$ or $(MS2)_2$PCBP2 had no significant effect on the formation of complex I with the 5'CL^{WT} probe (Figure 3-4B, lanes 3-5). However, the expression of either $(MS2)_2$ or $(MS2)_2$PCBP2 resulted in the formation of a new, slower-migrating RNP complex (complex II) with the 5'CL^{MS2} RNA probe (Figure 3-4B, lanes 9-10). This demonstrated that the $(MS2)_2$PCBP2 fusion protein binds specifically to 5'CL^{MS2} RNA and not wild-type RNA.

$(MS2)_2$PCBP2 Restores Negative-strand Synthesis on P23-5'CL^{MS2} RNA

To ascertain the effectiveness of the MS2 protein-RNA tethering system, we measured the levels of negative-strand synthesis observed with P23-5'CL^{MS2} RNA in presence or absence of $(MS2)_2$PCBP2. Negative-strand synthesis was measured in PIRCs isolated from HeLa S10 reactions that contained either P23 RNA or P23-5'CL^{MS2} RNA and an equimolar amount of a protein expression RNA which expressed either $(MS2)_2$, PCBP2 or $(MS2)_2$PCBP2. In the reactions that contained P23 RNA, the co-expression of $(MS2)_2$ or $(MS2)_2$PCBP2 had little effect on negative-strand synthesis (Figure 3-5, lanes 1 & 3). There was a detectable increase in negative-strand synthesis in the presence of exogenous PCBP2 (Figure 3-5, lane 2), which again is indicative of PCBP2 involvement in negative-strand synthesis. In the reactions containing P23-5'CL^{MS2} RNA, negative-strand synthesis was reduced to barely detectable levels in the reactions that contained either the $(MS2)_2$ or PCBP2 expression RNAs (Figure 3-5, lanes 4-5). In contrast, a large increase in negative-strand synthesis was observed in the reaction containing the $(MS2)_2$PCBP2 expression RNA (Figure 3-5, lane 6). In this reaction, negative-strand synthesis increased approximately 100-fold over the levels observed in the $(MS2)_2$ or PCBP2 control reactions (Figure 3-5, compare lane 6 with 4 & 5). Therefore, these results clearly established the effectiveness of the MS2 protein-RNA tethering system and showed that PCBP2, either directly bound or tethered to the 5'CL, is required for efficient initiation of PV negative-strand RNA synthesis.

Deletion Analysis of PCBP2 Using the $(MS2)_2$ Protein-RNA Tethering System

To define the region of PCBP2 involved in the protein-protein or protein-RNA interactions relevant to the initiation of negative-strand synthesis, we performed a deletion analysis of PCBP2, followed by a test of function using the MS2 protein-RNA tethering system. The PCBP2 coding sequence was divided into three regions, each region containing one of the three

conserved KH domains (Figure 3-6A). The coding sequence for each of these regions was expressed as an $(MS2)_2$ fusion protein in reactions containing P23-5'CL^{MS2} RNA. As before, significant levels of negative-strand RNA synthesis was observed in the presence of $(MS2)_2$PCBP2 compared to those observed in the $(MS2)_2$ and PCBP2 reactions (Figure 3-6B, lanes 1-3). Neither expression of the $(MS2)_2$KH1[Region] nor the $(MS2)_2$KH2[Region] fusion proteins were able to support negative-strand synthesis above background levels (Figure 3-6B, lanes 4-5). In contrast, the expression of the $(MS2)_2$KH3[Region] fusion protein restored negative-strand synthesis to levels slightly higher than those observed with $(MS2)_2$PCBP2 (Figure 3-6B, lanes 1 & 6). This suggested that the dominant domain in PCB2 that is required for negative-strand initiation resides in the C-terminal 130 amino acids of PCBP2, which includes the KH3 domain.

A recent structural analysis of the KH domains of PCBP2 revealed an intramolecular interaction between the KH1 and KH2 domains that was predicted to influence the function of one or both of the domains (67). In consideration of this potential effect on the functional activity, the amino terminal region of PCBP2, including both KH1 and KH2 domains, was fused to $(MS2)_2$ [KH1/2[Region]], and the replication of P23-5'CL^{MS2} RNA was measured in the presence of this fusion protein. In this reaction, negative-strand synthesis was restored to about 70-80% of the levels observed with $(MS2)_2$PCBP2 and about 50-60% of the levels observed with $(MS2)_2$KH3[Region] (Figure 3-6C, lanes 1, 4 & 5). Therefore, the results of this replication assay were consistent with the results of the structural studies which predicted a functional relevancy for the intramolecular interaction between the individual KH1 and KH2 domains of PCBP2 (67).

To ensure that the differences in replication efficiency observed in Figure 3-6 were not a secondary result of variations in the synthesis (or stability) of the $(MS2)_2$ fusion proteins or the viral replication proteins, we measured the amount of protein synthesized in each reaction. Labeled proteins were synthesized in HeLa S10 translation reactions containing [^{35}S]-methionine and were examined by SDS-PAGE and autoradiography (Figure 3-7). The results of this experiment indicated that all of the $(MS2)_2$ fusion proteins were synthesized in similar amounts as full-length, intact proteins, and similar levels of the labeled viral proteins were synthesized in each reaction (Fig. 7). Taken together, these results indicated that the observed differences in negative-strand synthesis that were a direct result of the efficacy of the given $(MS2)_2$ fusion protein and not a result of differences in the levels of protein synthesis or protein stability.

The Conserved KH3 Domain is Sufficient to Support Negative-strand Synthesis

Since the C-terminal KH3 containing fragment supported the highest levels of negative-strand synthesis, we chose to analyze this region further. To determine if the KH3 domain itself was responsible for the observed activity, the residual N- and C-terminal amino acid sequences outside of the KH3 domain were deleted to form the KH3[Domain] fusion protein construct (Figure 3-8A). Separate N- and C-terminal deletions were also made within the KH3 domain, removing the N-terminal β-strand and the C-terminal α-helix respectively (Figure 3-8A). Due to the structurally conserved nature of the KH domain, these deletions would be expected to perturb the tertiary structure of the KH3 domain and to disrupt structurally dependent protein interaction surfaces. The coding sequences for each of these mutants was fused to $(MS2)_2$, and the replication of P23-5'CL^{MS2} RNA was measured in the presence of the individual fusion proteins. Similar levels of protein synthesis were verified as before by SDS-PAGE (data not shown). As expected, expression of the $(MS2)_2$PCBP2 and $(MS2)_2$KH3[Region] fusion proteins supported significant levels of negative-strand synthesis. Removal of the amino acids

flanking the KH3 domain had no inhibitory effect on levels of negative-strand synthesis observed (Figure 3-8B, lanes 3 & 4), however, deletions in the KH3 domain itself (i.e. KH3Δβ1 and KH3Δα3) completely inhibited negative-strand synthesis (Figure 3-8B, lanes 5 & 6). Therefore, the intact KH3 domain was required to support high levels of negative-strand synthesis.

To confirm that the observed differences in negative-strand synthesis were not due to an unexpected change in a given $(MS2)_2$ fusion protein's ability to bind to 5'CL^{MS2} RNA, an EMSA was performed using 5'CL^{MS2} RNA probe and each of the PCBP2 fragment $(MS2)_2$ fusion proteins (Figure 3-9A). In each case, the labeled probe was shifted to form a slower migrating RNP complex similar to complex II in Figure 3-4B. We also examined the expression and integrity of each individual $(MS2)_2$ fusion proteins by SDS-PAGE and autoradiography (Figure 3-9B). The results of these experiments clearly showed that the $(MS2)_2$ protein acts as a functional cassette to efficiently tether a fusion protein to the 5'CL, regardless of that proteins identity. Additionally, all $(MS2)_2$ fusion proteins appear to be synthesized in the similar amounts as stable, full-length proteins.

Therefore, these results demonstrate that, when tethered to the RNA, the KH3 domain alone was sufficient to support initiation of PV negative-strand synthesis. This activity was not an artifact of increased protein concentration or binding affinity, and from deletion experiments, this activity appears to be dependent on the intact tertiary structure of the KH domain.

The Combined KH1-KH2 Domain Fragment Does Not Utilize PCBP Dimerization to Promote Negative-strand Synthesis

PCBP2 dimerization has been shown to be required for PCBP2's function in PV IRES translation, and an approximate dimerization domain within the KH2 domain was identified (29). This intermolecular dimerization could potentially be influenced by the previously discussed

intramolecular interaction between the KH1 and KH2 domains (67). In this case, it is possible that the $(MS2)_2$KH1/2 fusion protein, when tethered to the RNA, forms heterodimers with endogenous full-length PCBP2 in the HeLa extracts. If so, the negative-strand synthesis observed in RNA replication reactions could be a result of the function of this additional molecule of PCBP, rather than a direct function of the KH1/2 domains.

To determine if multimerization with endogenous PCBP was responsible for the observed activity of the KH1/2 fragment, we deleted the 23 amino acid multimerization domain (MD; amino acids 125-158 of PCBP2) from the KH2 domain, in the context of the $(MS2)_2$KH1/2 fragment [$(MS2)_2$KH1/2-ΔMD] (Figure 3-10A) (29). Again, due to the structurally conserved nature of the KH domain, this deletion would be expected to significantly perturb the tertiary structure of the KH2 domain. Replication of P23-5'CL^{MS2} RNA was measured in the presence of the $(MS2)_2$PCBP2, $(MS2)_2$, $(MS2)_2$KH1/2[Region] and $(MS2)_2$KH1/2-ΔMD fusion proteins. Similar levels of protein synthesis were verified as before by SDS-PAGE (data not shown). As expected, expression of the $(MS2)_2$PCBP2 and $(MS2)_2$KH1/2[Region] fusion proteins supported relative levels of negative-strand synthesis comparable to previous experiments (Figure 3-10B, lanes 1 & 3). Surprisingly, deletion of the MD did not abolish the ability of the KH1/2 fusion protein to promote negative-strand synthesis, although the level of RNA product observed were decreased slightly. Therefore, the intact KH1/2 region, when tethered to the RNA, does not require multimerization to promote negative-strand synthesis.

Multiple PCBP Isoforms Support Initiation of Negative-strand RNA Synthesis

Given the high degree of sequence conservation among members of the PCBP family, particularly within the KH domains, it was likely that multiple PCBP isoforms may share the ability to promote PV negative-strand initiation. Additionally, it was already known that PCBP1 could bind to the 5'CL and could also restore PV replication in Poly(C)-depleted cell extracts

(77, 209). Further, the dominant splice variant of PCBP2, PCBP2-KL, only differs by the exclusion of 31 amino acids encoded by exon 8a, suggesting that PCBP2-KL would likely function similarly (Figure 3-11A) (76, 128). Together, PCBP1, PCBP2, PCBP2-KL represent the most closely related and highly abundant members of this protein family (48, 127), and we would therefore predict that each of these isoforms would function at some level to restore negative-strand RNA synthesis in the $(MS2)_2$ tethering system.

To determine the efficiency with which PCBP1 could function in this system, we measured the levels of negative-strand synthesis of P23-5'CL^{MS2} RNA in the presence of either PCBP1, $(MS2)_2$PCBP1, PCBP2 or $(MS2)_2$PCBP2. As before, negative-strand synthesis was measured in PIRCs using equimolar amounts of P23-5'CL^{MS2} RNA and the individual protein expression RNA. In the reactions that contained P23-5'CL^{MS2} RNA, co-expression of PCBP1 or PCBP2 alone was unable to promote negative-strand synthesis (Figure 3-11B, lanes 1 & 3). As predicted, $(MS2)_2$PCBP1 was able support negative-RNA synthesis, and interestingly, the levels of negative-strand synthesis were slightly higher (~1.5-fold) than those observed in reactions containing $(MS2)_2$PCBP2 (Figure 3-11B, lanes 2 & 4).

To determine the efficiency with which PCBP2-KL could function in the $(MS2)_2$ tethering system, we measured the levels of negative-strand synthesis of P23-5'CL^{MS2} RNA in the presence of either PCBP2, $(MS2)_2$PCBP2, PCBP2-KL or $(MS2)_2$PCBP2-KL. Here again, negative-strand synthesis was measured in PIRCs using equimolar amounts of P23-5'CL^{MS2} RNA and the individual protein expression RNA. In reactions that contained P23-5'CL^{MS2} RNA, co-expression of PCBP2 or PCBP2-KL alone was unable to promote negative-strand synthesis (Figure 3-11C, lanes 1 & 3). As expected, $(MS2)_2$PCBP2-KL was able support levels

of negative-RNA synthesis similar to those observed in reactions containing $(MS2)_2$PCBP2 (Figure 3-11C, lanes 2 & 4).

Not All PCBP Family Members Support Negative-strand synthesis

Although their potential role in PV replication has never been investigated, the more distantly related members of the PCBP family (PCBP3, PCBP4, PCBP4A, and hnRNP K) are all expressed to varying levels in different tissue types (128). More importantly, we were able to detect mRNA corresponding to each protein in HeLa cell total RNA by RT-PCR, indicating the presence of each of these less abundant isoforms in HeLa cell extracts. HnRNP K is the most distantly related to all other PCBPs, and undergoes significant nucleo-cytoplasmic shuttling (135), but is predominantly localized to the nucleus except during cell-cycle signaling (118). PCBP3 and PCBP4/4A exhibit cytoplasmic localization and appear to be excluded from the nuclear compartment (48), indicating their availability to participate in cytoplasmic PV replication. PCBP4A is a splice variant of PCBP4, differing only in the carboxy-terminal amino acids, but contains an identical KH1, KH2, variable region, and 90% of KH3 (128). Despite a higher degree of amino acid similarity within individual KH domains, PCBP3/4/4A are significantly divergent from PCBP1/2 and may not retain all necessary functions relative to PV replication (Figure 3-12A).

To determine the relative abilities of the various PCBP family members to function in the $(MS2)_2$ tethering system, we measured the levels of negative-strand synthesis of P23-5'CL^{MS2} RNA in the presence of either $(MS2)_2$, $(MS2)_2$PCBP1, $(MS2)_2$PCBP2, $(MS2)_2$PCBP2-KL, $(MS2)_2$PCBP3, $(MS2)_2$PCBP4, $(MS2)_2$PCBP4A, or $(MS2)_2$hnRNP-K. As before, negative-strand synthesis was measured in PIRCs using equimolar amounts of P23-5'CL^{MS2} RNA and the individual protein expression RNA. As before, $(MS2)_2$PCBP1, $(MS2)_2$PCBP2, or $(MS2)_2$PCBP2-KL were all able to promote negative-strand RNA synthesis of P23-5'CL^{MS2}

RNA to similar levels (Figure 3-12, lanes 2-4). The $(MS2)_2$ fusion of the most distantly related, predominantly nuclear hnRNP K was unable to support significant levels of negative-strand synthesis, as may have been expected (Figure 3-12, lane 8). Surprisingly, the distantly related PCBP4, and to a lesser extent PCBP4A, functioned better than PCBP1, 2, or 2KL, whereas the more closely related PCBP3 appeared to support very modest levels of negative-strand RNA synthesis (Figure 3-12, lanes 5-7).

To further determine if these more distantly related PCBPs could plausibly be involved in natural PV replication, the ability of each of the isoforms was assayed for its ability to bind the wild-type 5'CL. RNA binding was ascertained by EMSA using a 5'CL riboprobe and bacterially recombinant PCPBs as described in Chapter 2. Since the splice variants PCBP2-KL and PCBP4A maintain the same RNA binding determinants as their parental proteins, only PCBP2 and PCBP4 were assayed. As previously observed, both PCBP1 and PCBP2 were able to form RNP complexes with the PV 5'CL, and corresponding with its significant divergence, no RNP complex was formed in the presence of hnRNP K (Figure 3-13, lanes 2, 3, & 6). Interestingly, both PCBP3 and PCBP4 were able to form RNP complexes with the PV 5'CL (Figure 3-13, lanes 4 & 5), suggesting that these isoforms have the potential to, if present, form an RNP complex with viral RNA and participate in negative-strand initiation.

Discussion

The work presented here demonstrated the requirement for PCBP in the initiation of PV negative-strand synthesis. Furthermore, we established that a *direct* PCBP-RNA interaction was not required to mediate this function by developing and using the $(MS2)_2$ protein-RNA tethering system to investigate PV negative-strand synthesis. We demonstrated the utility of this system in analyzing regions in an essential cellular protein, relative to PV replication, without affecting other viral and cellular processes in which the protein is involved. In doing so, we have shown

the KH3 domain of PCBP2, when tethered to the RNA, was able to support the initiation of negative-stand RNA synthesis. This suggests that a structurally conserved protein-protein or protein-RNA interaction surface which is required for negative-strand initiation exists within this conserved domain. We have also noted the functional redundancy of the combined KH1/2 domains of PCBP2 relative to PV RNA replication, consistent with recent work demonstrating the *in vitro* functionality of PCBP2 with the KH3 domain deleted (165).

Prior Indications of PCBP Involvement in Poliovirus RNA Replication

Initial *in vivo* studies identified an RNP complex formed at the 5' end of PV genomic RNA which appeared to be involved at some stage of RNA replication (13). Further investigation of this complex revealed the presence of both a viral (3CD) and cellular (PCBP2) protein, and showed that disruption of this complex inhibited RNA replication (12, 158). Further *in vitro* analysis using a PCBP binding site point mutant (C24A) revealed an additional role for PCBP in PV RNA stability (144). Using an alternative approach, Walter et al. showed that replication of a dicistronic PV RNA replicon was inhibited in cell extracts which were depleted for PCBPs (209). However, the above work was either unable to directly account for effects on RNA stability or to differentiate between defects in negative- and positive-strand synthesis.

Our results showed that the C24A mutation, which inhibits PCBP binding, also inhibits negative-strand synthesis without inhibiting positive-strand synthesis. Using a *trans*-replication assay, we showed definitively that this defect was not a secondary effect of a deficiency in either protein synthesis or RNA stability. Therefore, these findings suggested but did not prove that PCBP is a co-factor in the initiation of PV negative-strand synthesis.

$(MS2)_2$ Protein-RNA Tethering Assay Demonstrated that PCBP is Required for Poliovirus Negative-strand Synthesis

We directly addressed the role of PCBP2 in the initiation of PV negative-strand synthesis, by developing a protein-RNA tethering system. This system utilized the high affinity interaction of MS2 bacteriophage coat protein with its cognate RNA stem-loop (47, 58). We modified this system as described by Hook et al. to take advantage of the added specificity and efficacy conferred by using an MS2 protein covalent dimer, $(MS2)_2$ (96). By replacing the natural PCBP binding site in the 5'CL of PV genomic RNA with the MS2 stem-loop (5'CL^{MS2}), we were able to target the $(MS2)_2$PCBP2 fusion protein to the 5'CL^{MS2} RNA.

This system has many significant advantages over other approaches used to functionally characterize cellular protein involvement in virus replication. It is very difficult to isolate individual functions of multi-functional cellular proteins using techniques such as RNAi, gene knockout, protein depletion and dominant-negative inhibition, which can result in a broad spectrum of downstream effects unrelated to the function of interest. In addition, some of these techniques are not feasible in certain systems, while others present significant technical challenges. The $(MS2)_2$ protein-RNA tethering system could be adapted for *in vivo* and *in vitro* use, and functional analysis with this system can be performed with minimal disruption of other normal cellular processes. In the PV life-cycle, PCBP2 is used in both IRES-dependent translation and RNA replication. Our analysis of PCBP2's role in replication using the $(MS2)_2$ protein-RNA tethering system can be performed without affecting PCBP2 binding to the IRES, since the fusion protein is targeted specifically to the 5'CL. The system also permits us to precisely define the protein bound to the 5'CL, thereby providing a platform to perform mutagenic analysis of protein function in a straightforward manner.

Using the $(MS2)_2$ protein-RNA tethering system, we observed a significant defect in negative-strand synthesis of a 5'CL^{MS2} template RNA, concurrent with the loss of PCBP binding to the 5'CL^{MS2}. We then demonstrated a restoration of negative-strand synthesis upon co-expression of the $(MS2)_2$PCBP2 protein. This conclusively showed that the presence of PCBP2 at the 5'CL of PV genomic RNA is required for the initiation of negative-strand synthesis. Furthermore, PCBP's function is not mediated through direct protein-RNA interaction with the 5'CL, since tethered PCBP2 was capable of restoring RNA replication.

The requirement for PCBP in negative-strand initiation is consistent with the current model of PV replication complex formation involving genome circularization mediated by protein-protein interactions between RNP complexes formed at the 5' and 3' ends of PV genomic RNA (26, 93, 126, 196). By this model, PCBP2 bound or tethered to the 5'CL interacts with PABP bound to the poly(A) tail, thereby circularizing the genome and allowing the subsequent initiation of negative-strand synthesis.

The Combined KH1 & KH2 Fragment or the KH3 Domain of PCBP2 is Required for Negative-strand Initiation

An important application of the tethered function assay is mutational analysis of the tethered protein to determine the regions involved in protein-protein interactions. This illustrates yet another advantage of this system in that functional analysis of PCBP fragments can be performed without requiring direct binding to the 5'CL. Using this system, we were able to show that the KH3 domain of PCBP2 contains sequences and structures sufficient for the functional interactions involved in the initiation of negative-strand RNA synthesis. Based on the current circularization model, the key protein-protein interactions would be between PCBP, PABP and 3CD, however it is also possible that other proteins are involved, or that PCBP interacts with an as yet unknown RNA element in the 3' end of the viral genome.

We were also able to observe a functional redundancy in PCBP2 residing in the amino-terminal KH1 and KH2 domains that was capable of mediating similar critical interactions. This function was not observed when either the KH1 or KH2 domains were used separately, consistent with recent NMR structural data, which indicated structural differences between the PCBP2 KH1 or KH2 domains individually and a tandem KH1/2 construct (67). Multiple studies from Du *et al.* have identified large hydrophobic faces on KH1 and KH2 which would allow the two domains to interact intramolecularly, further intertwining the function of the KH1 and KH2 domains (67, 68). These results are also consistent with the recent work by Perera *et al.* which demonstrated the ability of PCBP2 with a KH3 deletion to restore PV RNA replication in Poly(C)-depleted cell extracts (165). A dimerization domain in PCBP2 has been identified and it was shown that this sub-domain within KH2 was required for IRES function (29). This domain was deleted from the KH1/2 fusion protein and was shown to be dispensable for negative-strand synthesis, indicating that the activity of KH1/2 fragment does not require multimerization.

The fully functional KH3 fragment does not contain any established dimerization sequences; so here again, dimerization of PCBP2 does not appear to be required to mediate the interactions required for negative-strand initiation. This does not rule out the possibility that dimerization of PCBP may be involved in physiologic PCBP binding to the 5'CL, since this interaction has been bypassed using the protein-RNA tethering system.

A Subset of PCBP Isoforms Support Initiation of Negative-strand RNA Synthesis

The PCBPs represent a family of poly(rC/dC) binding proteins which include hnRNP K and PCBPs 1-4, and two additional predominant splice variants, PCBP2-KL and PCBP4A (109, 121, 128, 133). This protein family is characterized by the presence and positioning of three highly homologous KH domains (80, 188), which were originally characterized as RNA binding

domains (65, 67) but have been evolutionarily retuned to perform additional or alternative functions. Given the high degree of sequence conservation among members within the PCBP family, particularly between corresponding KH domains, it was likely that some functional overlap between different isoforms of PCBP. Specifically, different PCBP isoforms could share the ability to promote PV negative-strand initiation. Both PCBP1 and PCBP2 are able to bind to the 5'CL and were able restore PV replication in poly(C)-depleted cell extracts (77, 209). Since PCBP2 and its splice variant PCBP2-KL share the same RNA binding determinants and only differ by 31 amino acids, it is likely that PCBP2-KL functions similarly (76, 128). Through the application of the $(MS2)_2$ protein-RNA tethering system, we have shown that PCBP1, PCBP2, and PCBP2-KL all share similar functionality relative to PV RNA replication and can support similar levels of negative-strand synthesis.

Despite a higher degree of amino acid similarity within individual KH domains, PCBP3, PCBP4, and PCBP4A are significantly divergent from PCBP1/2/2KL and may not retain all necessary functions relative to PV replication. Even within the KH domains, hnRNP K is clearly the most divergent and distantly related PCBP isoform, and would be predicted to share very little functional similarity with the other family members (128). We have shown by RT-PCR that the more distantly related and less abundant PCBP isoforms are in fact expressed in HeLa cells, and have further shown that PCBP3 and PCBP4/4A, but not hnRNP K, are capable of forming critical RNP complexes with the PV 5'CL. Again, using the $(MS2)_2$ tethering system, we have shown that PCBP4 and PCBP4A are capable of supporting higher levels of negative-strand synthesis than the levels supported by PCBP1/2/2KL. Interestingly, PCBP3 was only able to support minimal levels of negative-strand synthesis, suggesting that PV RNA replication may be inhibited in cells which express high levels of PCBP3. Taken together this

suggests that during natural PV infection, PCBP3, PCPB4 or PCBP4A would each possess the ability to bind to the 5'CL and incorporate into the RNP complexes critical for initiation of negative-strand RNA synthesis. Furthermore, PCBP3 could potentially act as an inhibitor of viral RNA replication by forming a non-functional RNP complex with the 5'CL of PV RNA.

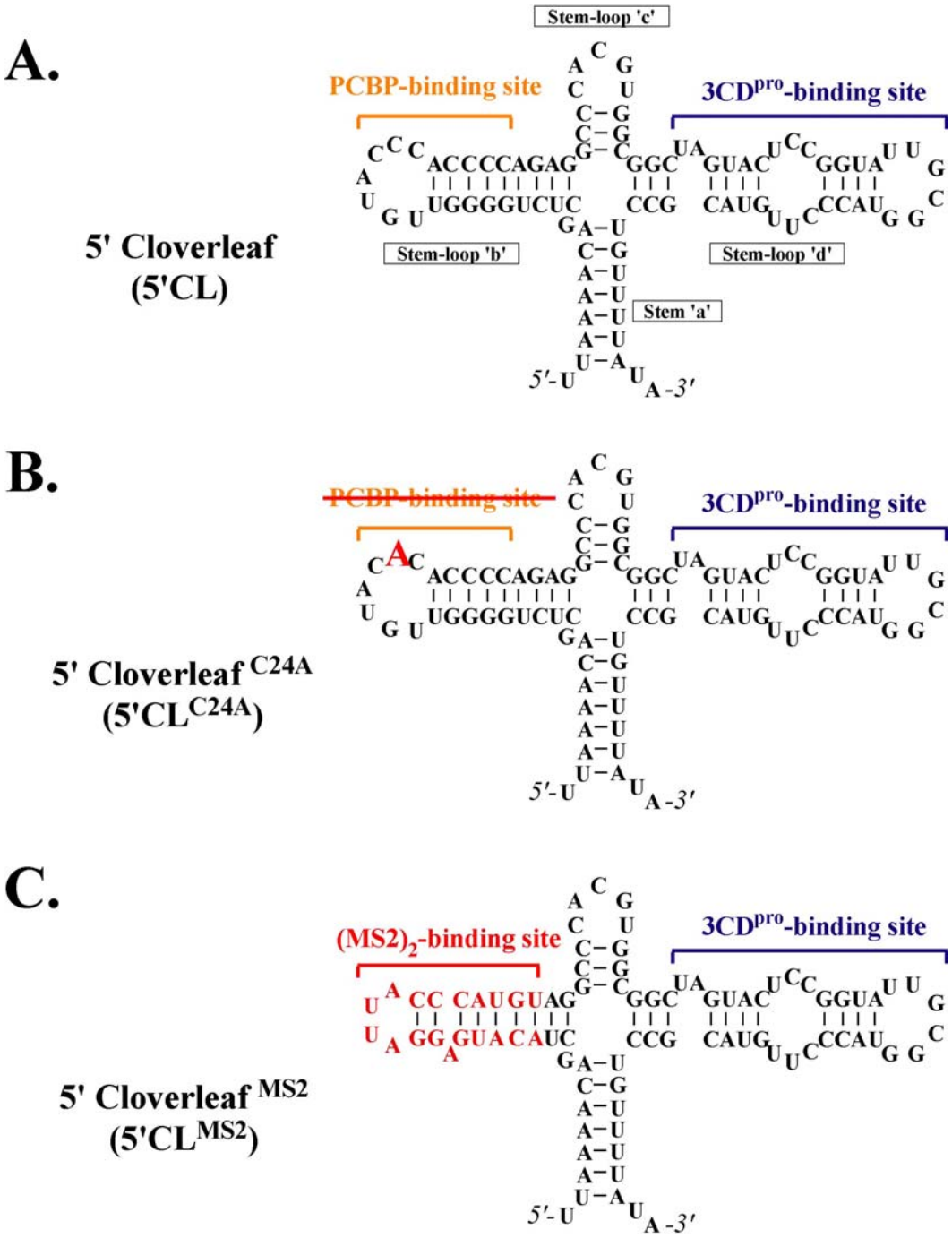

Figure 3-1. Diagrams of the wild-type and mutant 5' cloverleaf. A) The PV 5'CL is divided into four domains: stem *a*, and stem-loops *b*, *c*, and *d*. A region of stem-loop *b* functions as the PCBP binding site, whereas $3CD^{pro}$ binds to structural elements in stem-loop *d*. B) The $5'CL^{C24A}$ contains a single mutation (indicated in red) in the PCBP binding site of stem-loop *b*. C) The $5'CL^{MS2}$ has had the majority of stem-loop *b* replaced with the MS2 bacteriophage coat protein binding site (MS2 stem-loop).

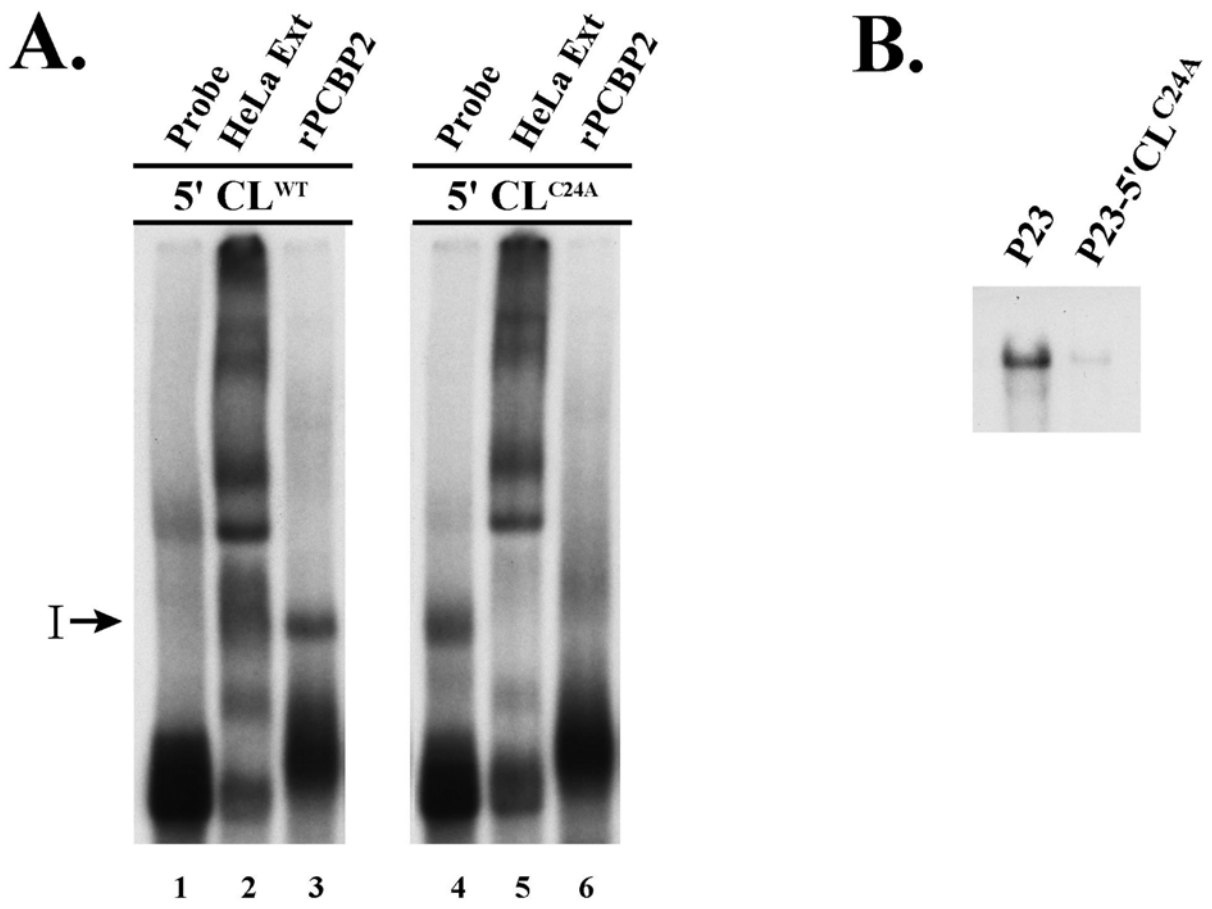

Figure 3-2. The C24A mutation inhibits PCBP binding and negative-strand RNA synthesis. A) Electrophoretic mobility shift assay (EMSA) using radiolabeled RNA probes, either 5'CL^{WT} RNA (lanes 1-3) or 5'CL^{C24A} RNA (lanes 4-6). The RNA probe was either run alone (lanes 1 & 4), with HeLa S10 extracts (lanes 2 & 5), or with bacterially expressed rPCBP2 (lanes 3 & 6). The specific RNP complex formed with the 5'CL^{WT} RNA probe and cellular PCBP is labeled as complex I. B) Replication of P23 RNA and P23-5'CL^{C24A} RNA was measured using PIRCs isolated from HeLa S10 reactions. Radiolabeled product RNA was visualized by denaturing CH_3HgOH-agarose gel electrophoresis and autoradiography. These P23 RNA transcripts allow only negative-strand synthesis due to the presence of two non-viral G residues at the 5' end as a result of T7 transcription.

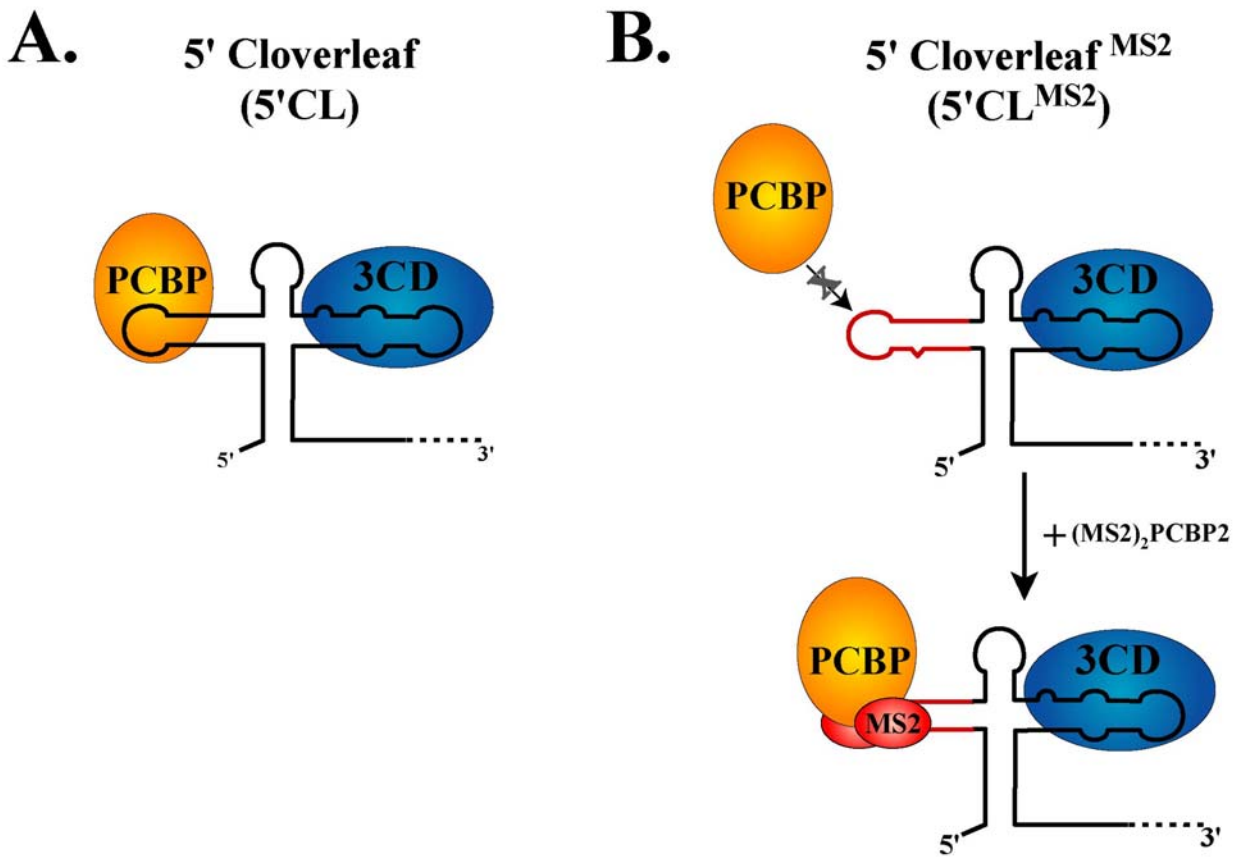

Figure 3-3. Schematic of the $(MS2)_2$ protein-RNA tethering system. A) Schematic of the wild-type 5'CL RNP complex. This complex consists of PCBP bound to stem-loop *b* and $3CD^{pro}$ bound to stem-loop *d*. B) Schematic of the $5'CL^{MS2}$ RNP complex. Endogenous PCBP in cell extracts (or recombinant PCBP) is no longer able to bind to the 5'CL because stem-loop *b* has been replaced with the MS2 stem-loop. In the absence of PCBP binding, $3CD^{pro}$ can still bind to the $5'CL^{MS2}$, but at lower affinity. When the $(MS2)_2$PCBP2 fusion protein is provided, it is recruited to the $5'CL^{MS2}$ via the $(MS2)_2$ interaction with its cognate stem-loop. This effectively tethers PCBP2 to the 5'CL, forming a surrogate 5'CL RNP holocomplex.

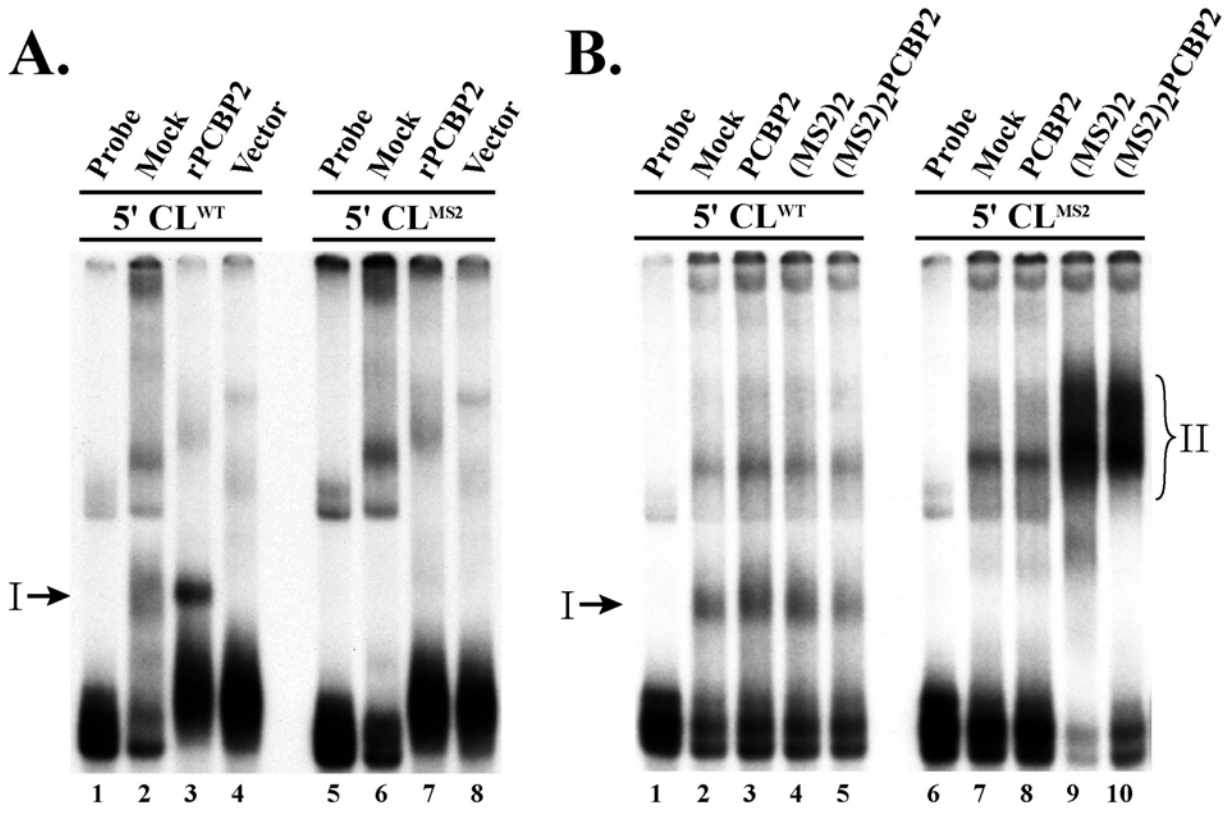

Figure 3-4. The 5'CL^{MS2} binds $(MS2)_2$ fusion proteins but does not bind PCBP2.
A) Electrophoretic mobility shift assay (EMSA) using radiolabeled RNA probes, either 5'CL^{WT} RNA (lanes 1-4) or 5'CL^{MS2} RNA (lanes 5-8). The RNA probe was either run alone (lanes 1 & 5), with HeLa S10 mock translation reactions (lanes 2 & 6), with bacterially expressed rPCBP2 (lanes 3 & 7) or a vector control bacterial extract (lanes 4 & 8). The specific RNP complex formed with the 5'CL^{WT} RNA probe and endogenous cellular PCBP is labeled as complex I. B) EMSA using either 5'CL^{WT} RNA probe (lanes 1-5) or 5'CL^{MS2} RNA probe (lanes 6-10). The probe was either run alone (lanes 1 & 6), with a HeLa S10 mock translation reaction (lanes 2 & 7), or with HeLa S10 translation reactions in which the indicated proteins were expressed (lanes 3-5, 8-10). Specific RNP complexes were formed with the 5'CL^{WT} RNA and endogenous cellular PCBP (complex I), or with the 5'CL^{MS2} RNA and $(MS2)_2$ or $(MS2)_2$PCBP2 (complex II).

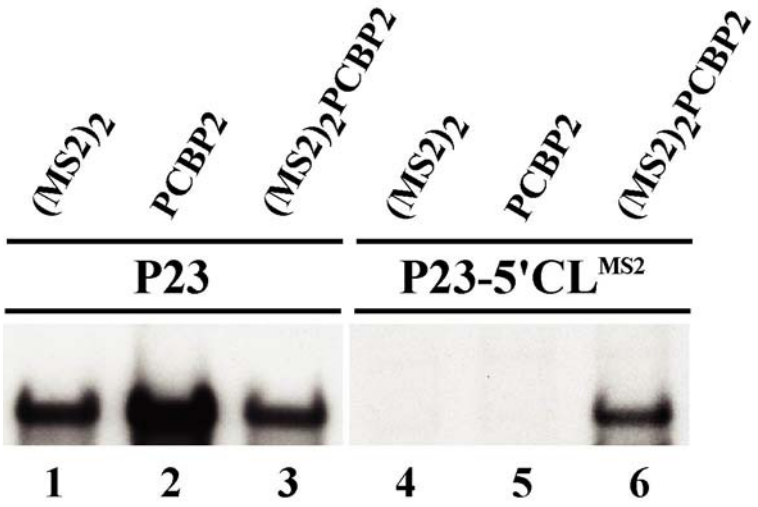

Figure 3-5. The $(MS2)_2$PCBP2 fusion protein restores negative-strand synthesis of a 5'CL^{MS2} RNA template. Negative-strand synthesis was measured in reactions containing either P23 RNA (lanes 1-3) or P23-5'CL^{MS2} RNA (lanes 4-6) using PIRCs isolated from HeLa S10 reactions. Each reaction contained either P23 RNA or P23-5'CL^{MS2} RNA and an equimolar amount of a protein expression RNA which expressed either $(MS2)_2$, PCBP2 or $(MS2)_2$PCBP2, as indicated. Both template RNAs were capped to ensure equal template stability. Radiolabeled product RNA was visualized by denaturing CH_3HgOH-agarose gel electrophoresis and autoradiography

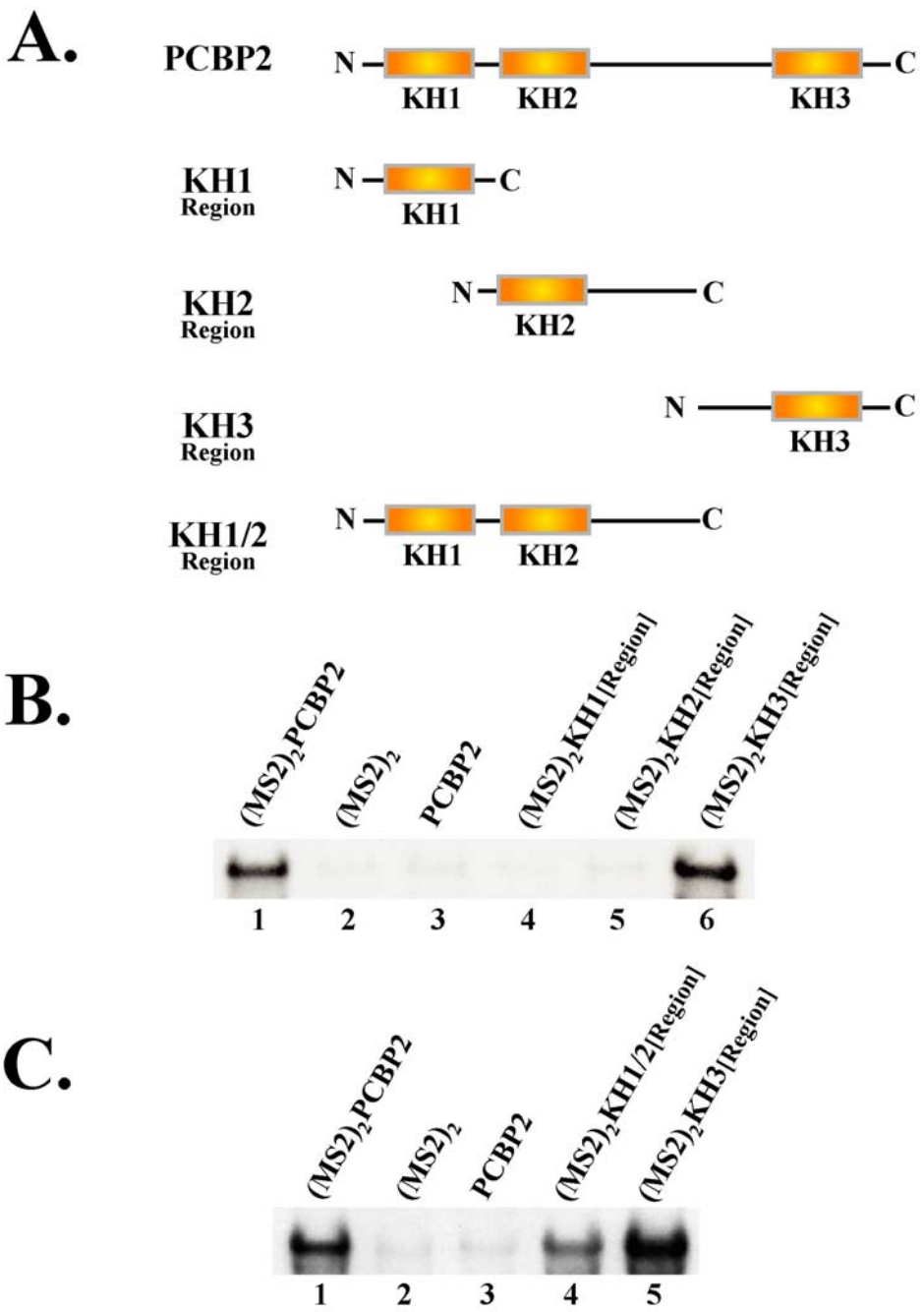

Figure 5-6. Identification of the functional domains within PCBP2 that restore negative-strand RNA synthesis of a 5'CL^{MS2} template RNA. A) Schematic of the domain structure of PCBP2, including the conserved KH1, KH2 and KH3 domains. Each PCBP2 region depicted was fused to $(MS2)_2$ and assayed in replication reactions.
B & C) Negative-strand synthesis was measured in reactions containing P23-5'CL^{MS2} RNA and an equimolar amount of an RNA which expressed the indicated RNA. The total molar RNA concentration and molar RNA ratio were maintained in each reaction, and the input template RNA contained a 5' cap.

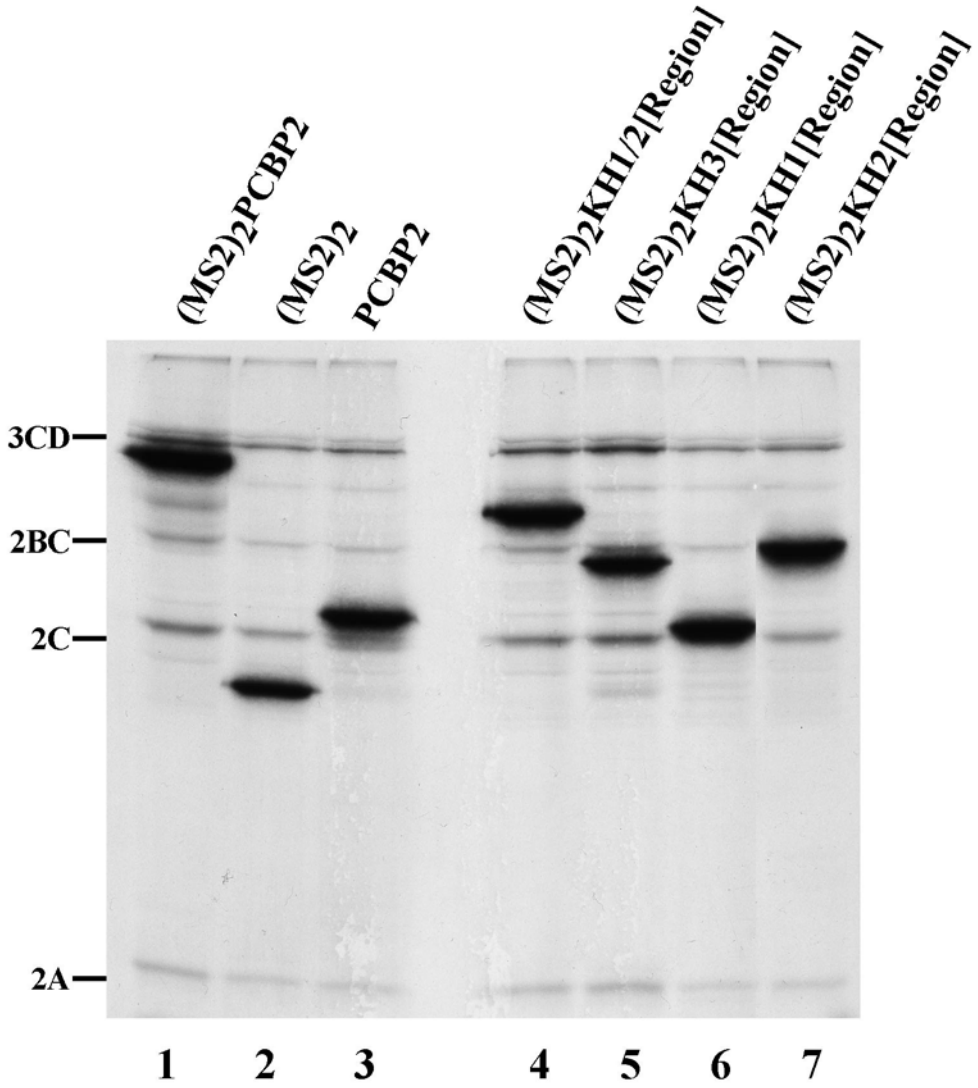

Figure 3-7. Levels of protein synthesis observed in the $(MS2)_2$ protein-RNA tethering replication reactions. HeLa S10 translation reactions which correlate to those described in Figure 5-6 were incubated with [^{35}S]methionine to metabolically label all newly synthesized protein products. The labeled proteins synthesized in these reactions were analyzed by SDS-PAGE and autoradiography. Each reaction contained an equimolar amount of P23-5'CL^{MS2} RNA and the indicated $(MS2)_2$ fusion protein expression RNA.

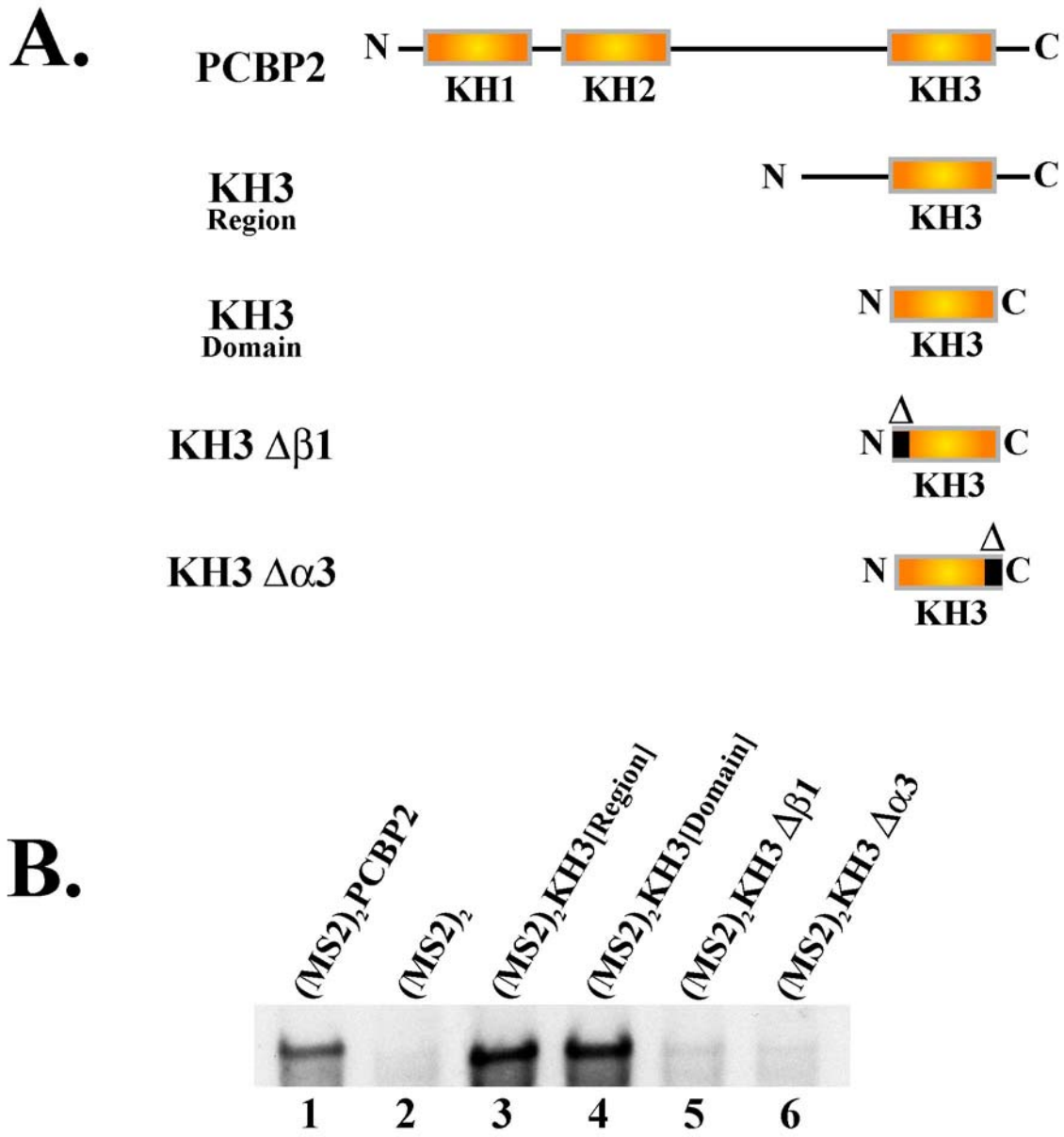

Figure 3-8. Characterization of the KH3 domain using the $(MS2)_2$ protein-RNA tethering system. A) Schematic of PCBP2 and the KH3 domain deletion mutants used in this experiment. B) Negative-strand synthesis was measured using PIRCs isolated from HeLa S10 reactions containing P23-5'CL^{MS2} RNA and an equimolar amount of a protein expression RNA as indicated above. The total molar RNA concentration and molar RNA ratio were maintained in each reaction, and the input template RNA contained a 5' cap.

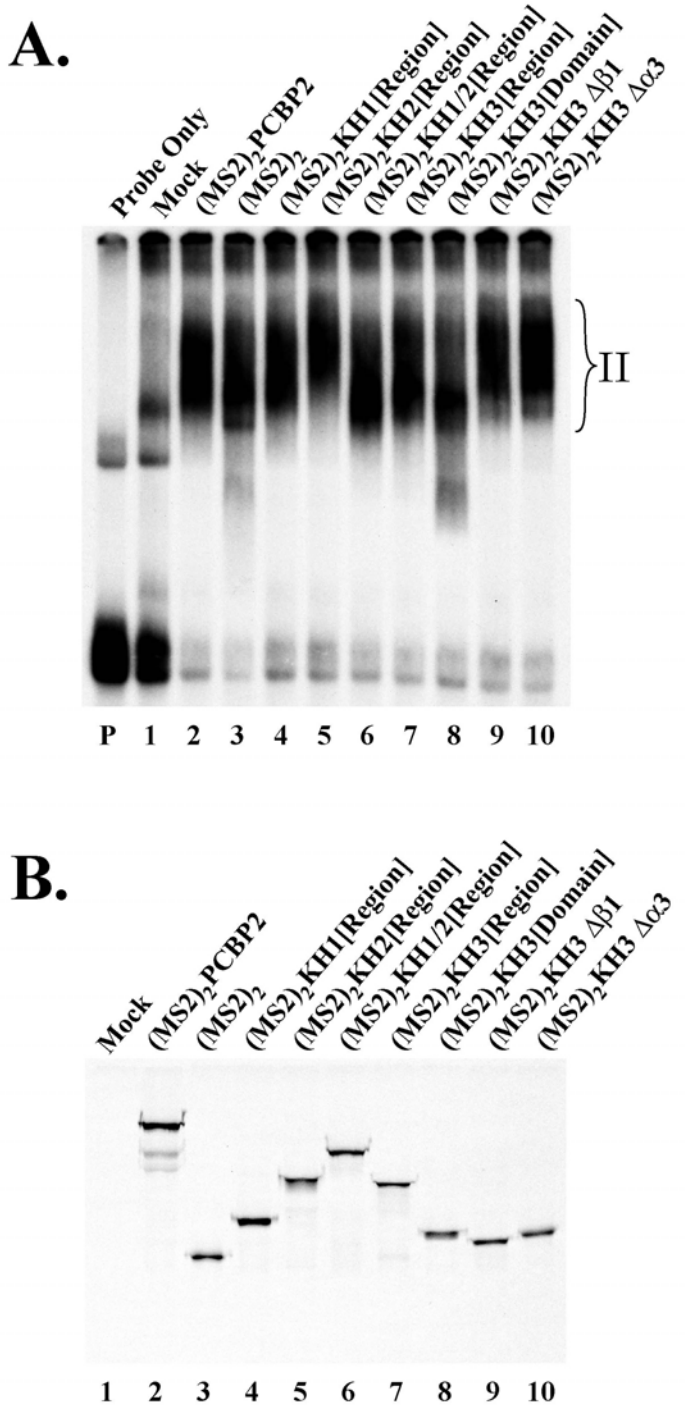

Figure 3-9. The $(MS2)_2$ fusion proteins are evenly expressed, stable, and bind to 5'CL^{MS2} with similar affinity. A) An EMSA was performed using a radiolabeled 5'CL^{MS2} RNA probe. The probe was either run alone (lane 1), with a HeLa S10 mock translation reaction (lane 2), or with HeLa S10 translation reactions in which the indicated proteins were expressed (lanes 3-11). B) Portions of the same HeLa S10 translation reactions used above were incubated with [^{35}S]methionine, and the labeled protein products were analyzed by SDS-PAGE and autoradiography.

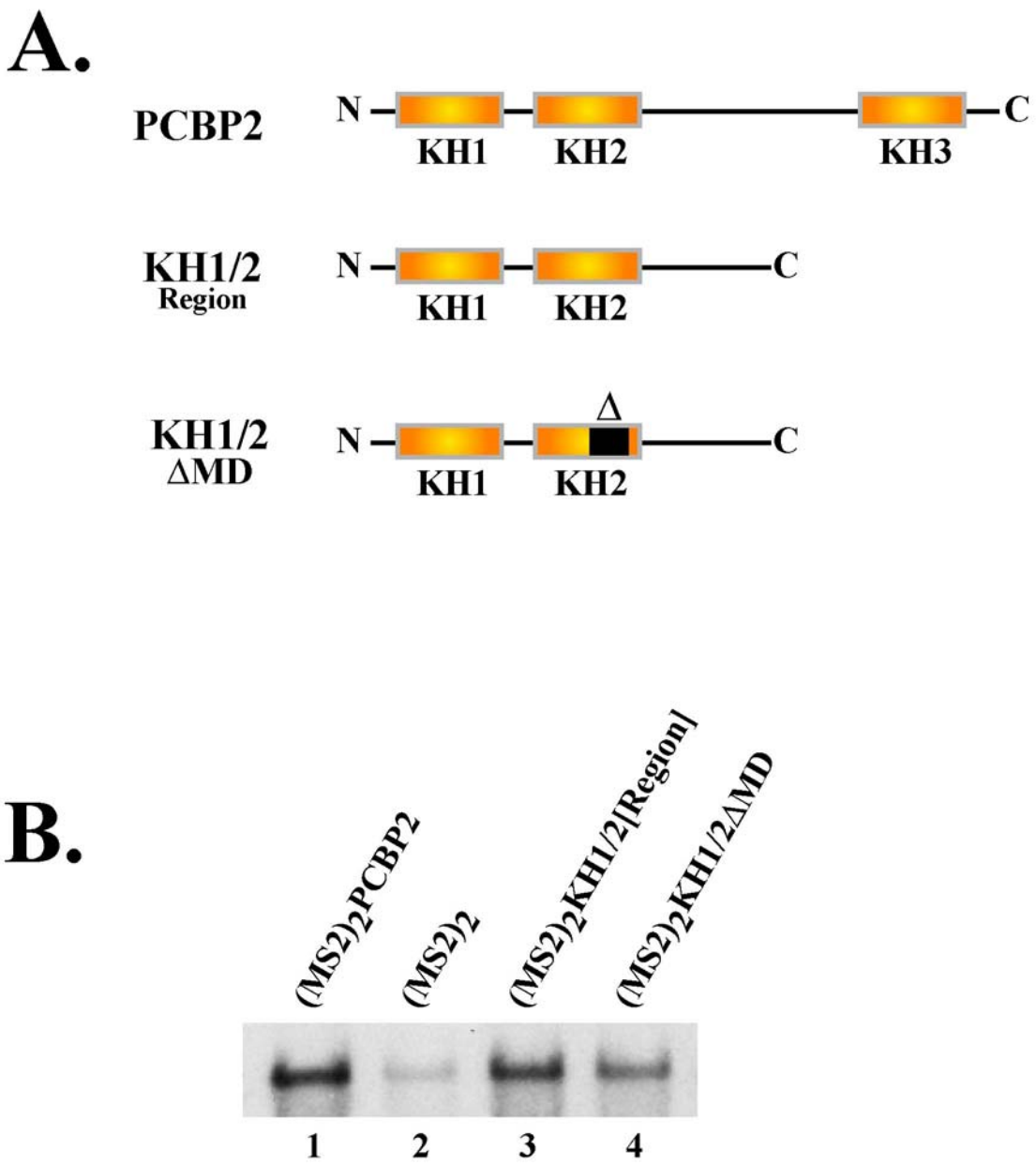

Figure 3-10. The ability of the combined KH1/2 domains to restore negative-strand synthesis does not require the multimerization domain. A) Schematic of PCBP2, KH1/2 region, and the multimerization domain deletion mutant used in this experiment. B) Negative-strand synthesis was measured using PIRCs isolated from HeLa S10 reactions containing P23-5'CL^{MS2} RNA and an equimolar amount of a protein expression RNA as indicated above. The total molar RNA concentration and molar RNA ratio were maintained in each reaction, and the input template RNA contained a 5' cap.

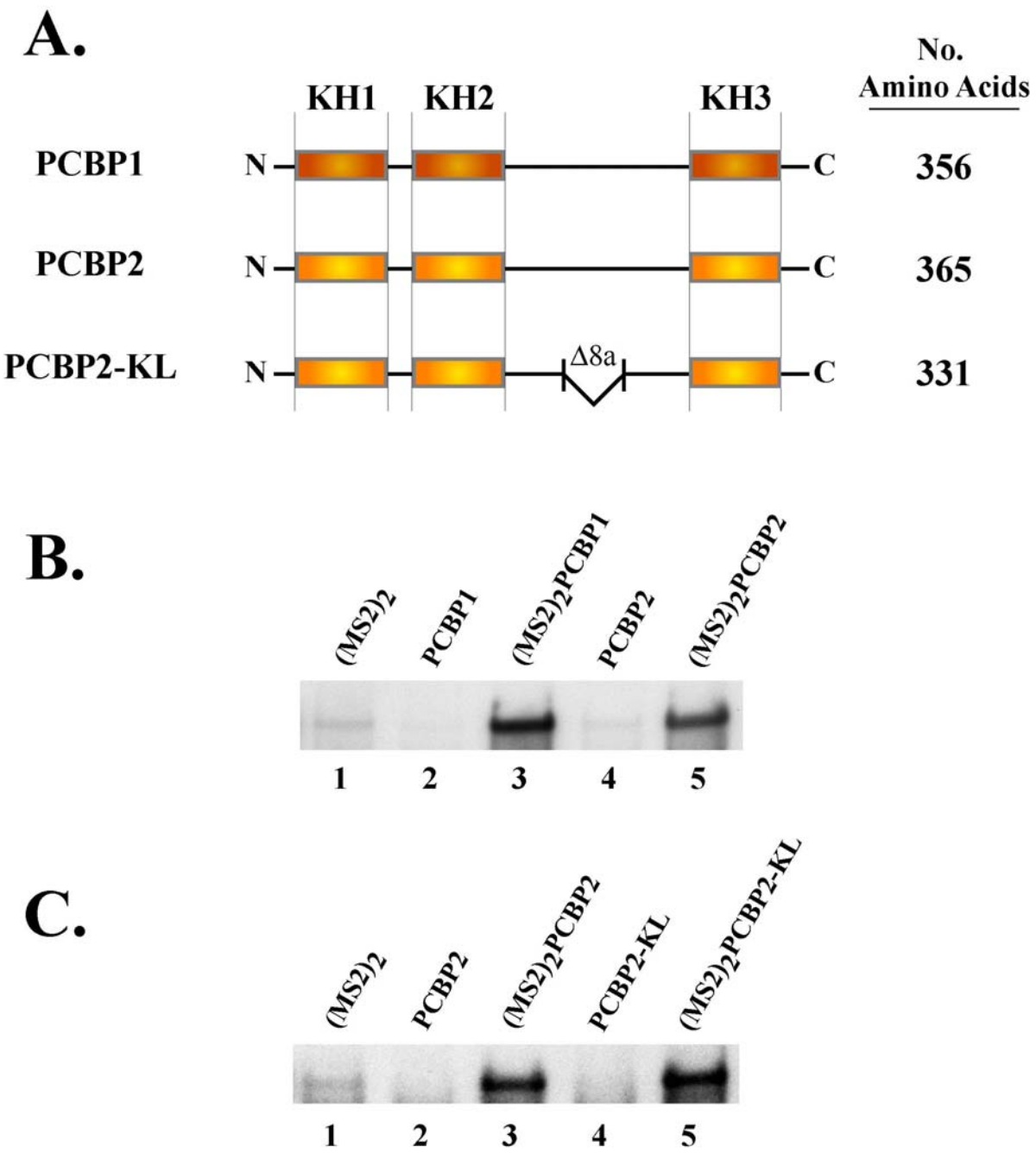

Figure 3-11. PCBP1, PCBP2, and PCBP2-KL restore negative-strand synthesis to similar levels in the $(MS2)_2$ protein-RNA tethering system. A) Schematic of the domain structure of PCBP1, PCBP2 and PCBP2-KL. Each PCBP isoform depicted, as well as its corresponding $(MS2)_2$ fusion protein, was assayed in replication reactions. B & C) Negative-strand synthesis was measured in reactions containing P23-5'CL^{MS2} RNA and an equimolar amount of an RNA which expressed the indicated protein. The total molar RNA concentration and molar RNA ratio were maintained in each reaction, and the input template RNA contained a 5' cap.

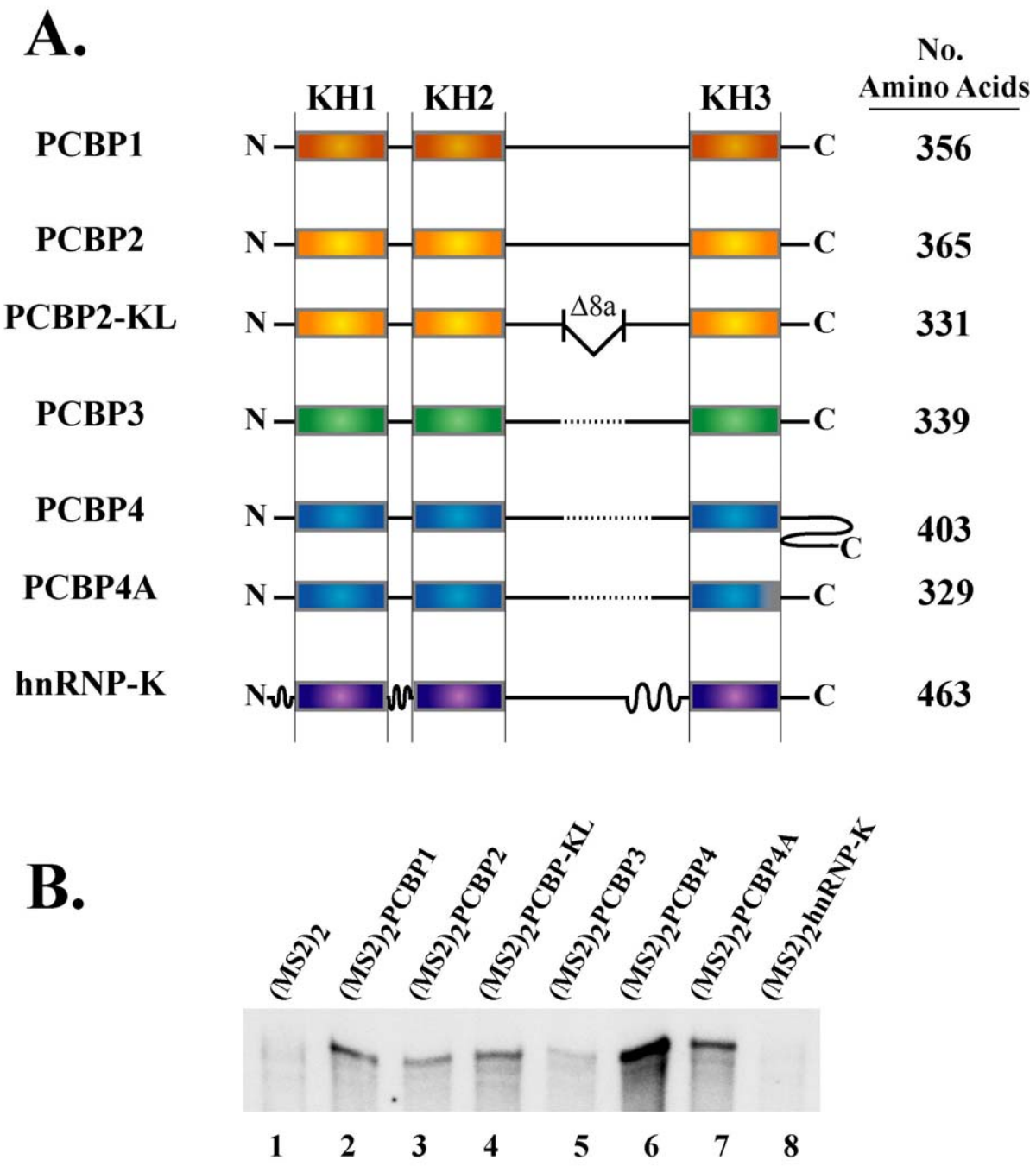

Figure 3-12. PCBP4/4A, but not PCBP3 or hnRNP K, restores negative-strand synthesis in the $(MS2)_2$ protein-RNA tethering system. A) Schematic of the domain structure of the PCBPfamily. Each PCBP isoform depicted was fused to $(MS2)_2$ and assayed in replication reactions. B) Negative-strand synthesis was measured in reactions containing P23-5'CL^{MS2} RNA and an equimolar amount of an RNA which expressed the indicated protein. The total molar RNA concentration and molar RNA ratio were maintained in each reaction, and the input template RNA contained a 5' cap.

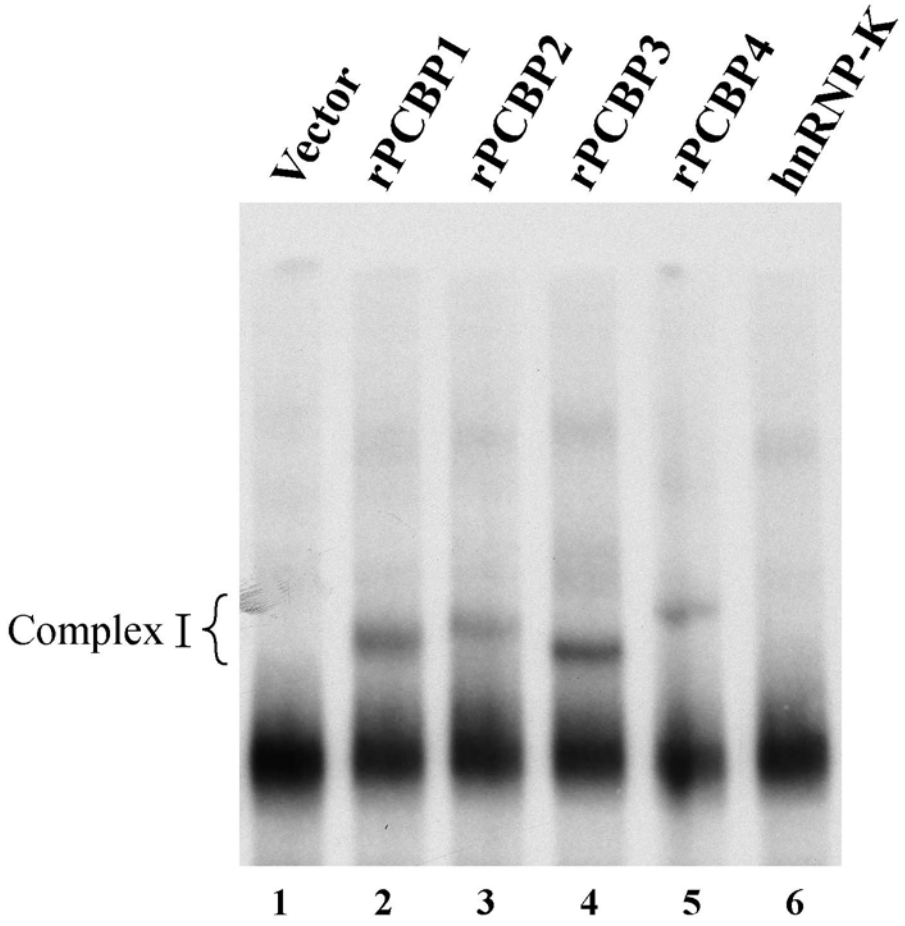

Figure 3-13. All PCBP family proteins, except hnRNP-K, bind to the PV 5'CL. A) An EMSA was performed using radiolabeled 5'CL^{WT} RNA probe and clarified bacterial recombinant protein extract. The RNA probe was incubated with a vector only expression control (lane 1) or with a bacterially expressed recombinant PCBP isoform as indicated (lanes 2 & 6). The specific RNP complexes formed with the 5'CL^{WT} RNA probe and the various PCBP is isoforms are indicated as isotypes of complex I

CHAPTER 4
2BC-P3 IS THE CRITICAL *CIS*-ACTING VIRAL PROTEIN PRECURSOR DIRECTING INITIATION OF POLIOVIRUS NEGATIVE-STRAND RNA SYNTHESIS

Introduction

Each stage of the viral life-cycle must be carefully orchestrated, both spatially and temporally, to optimize total virus yield. The evolutionary imperative to do so is met by a myriad of obstacles at every step, yet viruses have developed multiple mechanisms to overcome these challenges and replicate efficiently. One common theme among these adaptations is a close coupling between sequential steps of viral replication; predicating the initiation of one step, not simply on completion of the previous step, but also on the spatial availability and functionality of the products of that previous step. The primary means by which many viruses accomplish this is through extensive rearrangement of the host cell architecture and the creation of structures known as virus inclusions or virus factories (reviewed by (145)). While the creation of these structures is well established, the mechanisms which drive the coupling of the viral life-cycle *within* these structures continue to be of great interest.

Poliovirus infection has been shown to causes dramatic membrane rearrangements resulting in the formation of characteristic vesicles within the host cell cytoplasm (44). For PV, the cytoplasmic surface of these membrane vesicles serves as the site of viral replication complex assembly, RNA replication, and infectious particle assembly (34, 35, 43-45, 51, 167). Recent data from Egger & Bienz suggest a tight coupling between viral translation at the endoplasmic reticulum and the formation of these membrane vesicles as well as concurrent replication complex formation (70, 71). Furthermore, PV defective interfering particles all maintain the correct reading frame and harbor deletions within the capsid coding region, suggesting that active translation and RNA replication are linked (85, 115). This coupling was further substantiated by Novak and Kirkegaard who showed that *cis* translation of mutant viral

RNA is a prerequisite to the replication of that particular RNA (151). Additionally, RNA replication is functionally coupled to infectious particle assembly, such that only newly synthesized positive-strand virion RNA is encapsidated efficiently (152). Taken together, these studies depict a highly organized and well coordinated process by which PV infection progresses, each step inextricably tied to the initiation of the next, in an effort to maximize replication efficiency and virus yield.

While it is clear that PV does adhere to a tightly coupled replication strategy, the various molecular mechanisms by which this coupling occurs remain unclear. In an effort to characterize some of these mechanisms, we utilized the HeLa S10 translation-replication system to probe the relationship between viral translation and initiation of RNA replication. To do this, we performed *trans*-complementation of PV subgenomic RNAs expressing discrete polyprotein precursors and assayed for the ability of these subgenomic RNAs to serve as templates for negative-strand RNA synthesis. Herein, we show that the coupling of translation to subsequent negative-strand synthesis is not simply due to the act of translation itself, but the function of a specific gene product(s). Furthermore, we identify the critical region(s) of the PV polyprotein as that which includes 2B and $3D^{pol}$ proteins and/or their precursors. This data, in combination with previous observations, strongly indicates that it is the translation of the 2BC-P3 precursor in *cis* that drives template selection for membrane associated negative-strand RNA synthesis.

Results

To determine if the marked coupling of translation and RNA replication observed during *in vivo* PV infection was recapitulated in cell-free replication reactions, we performed a series of *trans* complementation experiments utilizing the HeLa S10 translation-replication system. In all cases, two RNAs were present in these reactions: the template RNA, which acts as the RNA

replication template, and the helper RNA, which acts as the *trans* protein provider but does not itself act as a replication template.

Efficient PV Negative-strand Synthesis Requires Translation of Viral Template RNA

We and others have established that neither the capsid proteins nor the capsid protein coding region is required for PV genome translation and RNA replication both *in vitro* and *in vivo* (61, 85, 106, 115). With this in mind, the template RNA used was either a subgenomic RNA which expressed all PV replication proteins [P23 RNA] or a similar RNA containing a frameshift mutation and subsequent early termination codons [FS23 RNA] (Figure 4-1A). In both cases, a full-length PV helper RNA was included in the reaction to provide all PV proteins and polyprotein precursors in *trans*. This full-length helper RNA contains a five nucleotide deletion in the 3' NTR which has been previously shown to inhibit negative-strand synthesis without affecting translation [PV1ΔGUA$_3$ RNA] (26). In all cases, detected product RNA represents only negative-strand synthesis as a result of two non-viral G residues at the 5'end of all template RNAs used in this study.

PV negative-strand RNA synthesis was assayed using preinitiation replication complexes (PIRCs) isolated from HeLa S10 translation-replication reactions as previously described in Chapter 2. Equimolar amounts of template RNA [P23 or FS23] and helper RNA [PV1ΔGUA$_3$] were co-translated and subsequent negative-strand synthesis was measured by [α-^{32}P]CTP incorporation and visualized by denaturing CH_3HgOH-agarose gel electrophoresis and autoradiography. As shown in Figure 4-1B, negative-strand synthesis from the non-translating FS23 template RNA was reduced 5 to 10-fold relative to that observed from the P23 template RNA, which translated all replication proteins in *cis*. As expected, there were slightly increased levels of the viral P23 proteins produced in the reaction containing both P23 and PV1ΔGUA$_3$

RNAs relative to that produced in the reaction containing the non-translating FS23 RNA. However, in reactions in which the amount of helper RNA was doubled to approximate reaction conditions with elevated replication proteins, the levels of negative-strand synthesis in reactions containing FS23 RNA remained significantly lower than those observed with P23 RNA (data not shown). Additionally, if proteins coming in *cis* and in *trans* contributed equally to RNA replication, one would expect the levels of negative-strand synthesis supported by proteins coming only in *trans* to be half of that observed when proteins are provided both in *cis* and in *trans*, rather than the 10-15% that was experimentally determined (Figure 4-1B, compare lanes 1 & 2). Therefore, these data indicate that the observed difference in negative-strand synthesis between P23 and FS23 RNA templates was predominantly due to the translation status of the RNA being replicated.

In many translation systems, RNAs harboring premature termination codons or RNAs that are translationally inactivated are often subject to nonsense mediated decay or other forms of RNA degradation (56, 146). To determine if the observed negative-strand synthesis defect of FS23 was an indirect effect of RNA instability we performed RNA stability assays under conditions identical to those used to assay for negative-strand RNA synthesis. Radiolabeled input RNA, either P23 or FS23 RNA, was co-translated with PV1ΔGUA$_3$ RNA and the amount of input RNA remaining was assessed at various times by CH_3HgOH-agarose gel electrophoresis and autoradiography. There was no detectible defect in the stability of FS23 input RNA relative to P23 RNA (Figure 4-1C, compare lanes 1-4 to lanes 5-8), despite premature translation termination on FS23 RNA. This result confirmed that the difference in the levels of negative-strand synthesis observed between P23 and FS23 RNA templates was not due to a secondary stability defect arising from the absence of elongating ribosomes.

Template RNA Translation Alone is Not Sufficient to Promote Efficient PV Negative-strand RNA Synthesis

To determine if translation of an entire reading frame and/or translation termination in the authentic context was required for efficient initiation of negative-strand synthesis, a PV1 subgenomic RNA was constructed in which the sequences coding for 2A through 3C and a portion of 3D were deleted (P1-3D* RNA; Figure 4-2A). This RNA is actively translated to produce a fusion of the P1 capsid precursor protein and a carboxy terminal fragment of 3D, but does *not* produce any active $3D^{pol}$, and terminates translation in the authentic context. A derivative of this subgenomic RNA was then constructed by the addition of a frameshift mutation at nucleotide 1119 of P1-3D* RNA (FS1-3D* RNA; Figure 4-2A). Translation of this RNA initiates properly but terminates prematurely, resulting in synthesis of a truncated protein product and incomplete ribosomal transit of the template RNA.

Negative-strand RNA synthesis was assayed as described above in reactions containing either P1-3D* or FS1-3D* template RNA and an equimolar amount of PV1ΔGUA$_3$ helper RNA. As shown in Figure 4-2B, no significant difference in the levels of negative-strand synthesis was observed between reactions containing P1-3D* or FS1-3D* RNA. Additionally, the amount of negative-strand synthesis observed from both reactions is significantly reduced from those observed from P23 RNA which translates all viral replication proteins in *cis* (data not shown). These data clearly show that neither complete ribosome translocation through a template RNA, nor termination of translation in the authentic context, is sufficient to direct efficient negative-strand synthesis from that template. Furthermore, this result strongly suggests that the previously observed *cis*-translation enhancement of negative-strand synthesis is primarily due to the activity of a viral translation product in *cis*.

Translation through the 3D Coding Region in *cis* is Necessary for Efficient PV Negative-strand Synthesis

To determine which viral protein product or products were required in *cis* for efficient PV negative-strand synthesis, a series of subgenomic template RNAs was constructed based on the P23 RNA used above. For each construct, two stop codons were inserted after the terminal amino acid residue of the desired protein within the context of the entire polyprotein coding region of P23 RNA (Figure 4-3A). These constructs all maintained the identical RNA sequences and structures (with the exception of the stop codons) as the parent P23 RNA, but translated only a defined amino-terminal portion of the PV polyprotein. Translation of these RNAs initiated with 2A and progressed normally until reaching the inserted stop codons, whereby P23-2A^{STOP} translated 2A, P23-2B^{STOP} translated 2AB, P23-2C^{STOP} translated 2ABC, and so forth (Figure 4-3A). In all reactions, the full-length PV helper RNA provided all PV proteins and naturally occurring polyprotein precursors in *trans*.

Negative-strand synthesis was assayed as described above from reactions containing one of the template RNAs depicted in Figure 4-3A with an equimolar amount of PV1ΔGUA$_3$ helper RNA. Interestingly, RNA templates which translated anything less than the complete P23 polyprotein exhibited a significant defect in their ability to support efficient negative-strand synthesis (Figure 4-3B, compare lanes 1-6 to lane 7). The replication deficient P23-3C^{STOP} RNA and the replication competent P23 RNA only differ by the inclusion of the 3D coding region, implicating 3D^{pol} or a 3D-precursor as the *cis* protein requirement. Since the majority of the 3D coding region was present in the replication deficient P1-3D* RNA (Figure 4-2), it is highly unlikely that physical ribosome transit through this region is responsible for the observed effect. Taken together, these data strongly indicate that efficient PV negative-strand synthesis requires *cis* translation of 3D^{pol}, 3CD^{pro}, and/or another 3D containing precursor.

Translation of the 2BCP3 Protein Precursor in *cis* is Sufficient for Efficient PV Negative-strand Synthesis

To determine if efficient PV negative-strand synthesis requires *cis* translation of $3D^{pol}$ alone or the translation of a larger 3D containing precursor, a second series of RNA templates was constructed. These constructs all contain the same 5' and 3' NTRs, however each RNA in the series contains the coding sequence for a successively larger 3D containing precursor that has been previously associated with PV replication (Figure 4-4A) (104, 119, 159). In addition to these template RNAs, an additional control RNA was generated which contained an in-frame deletion of nucleotides 867-6011 from full-length PV1 RNA [PV1p50 RNA]. This RNA retains the entire PV 5' and 3' NTRs, utilizes the authentic start/stop codons and codon contexts, and translates a non-functional 50 kDa protein (p50), serving as an additional control for the effect of ribosome transit through the RNA. Here again, the full-length PV helper RNA provided all PV proteins and naturally occurring polyprotein precursors in *trans*.

Negative-strand synthesis was assayed as described above from reactions containing one of the template RNAs depicted in Figure 4-4A with an equimolar amount of $PV1\Delta GUA_3$ helper RNA. As shown in Figure 4-4B, RNAs which translated p50, $3D^{pol}$, $3CD^{pro}$, 3BCD, or P3 proteins in *cis* were all unable to efficiently serve as RNA templates for negative-strand synthesis (Figure 4-4B, compare lanes 1-5 to lane 7). Strikingly, template RNA which translated the 2BC-P3 precursor protein in *cis* supported negative-strand synthesis to levels greater than that observed with P23 RNA (Figure 4-4B, compare lane 7 to lane 8). These data clearly demonstrate that neither *cis* translation of $3D^{pol}$ alone nor ribosomal transit through the 3D coding region of a template RNA is sufficient to promote efficient PV negative-strand synthesis on that template. The replication deficient P3 RNA and the replication competent 2BC-P3 RNA only differ by the inclusion of the 2BC coding region, which indicates strongly that efficient PV

negative-strand synthesis requires *cis* translation of either the full 2BC-P3 precursor protein or a combination of individual, discrete protein functions within the 2BC-P3 polyprotein.

If efficient PV negative-strand synthesis requires *cis* translation of multiple discrete proteins/precursors, one of the most likely candidate proteins (in addition to $3D^{pol}$/$3CD^{pro}$) is protein 2C. Protein 2C has been directly implicated in negative-strand initiation and has been shown to specifically bind to PV RNA (17, 18, 122, 170, 202). Therefore, a 2C-P3 expressing template RNA was constructed and tested as was described above (Figure 4-5A), despite the fact that a 2C-P3 precursor protein has neither been observed nor postulated to play a role in PV replication. Negative-strand synthesis was assayed as described above from reactions containing P3, 2C-P3, or 2BC-P3, as well as an equimolar amount of PV1ΔGUA$_3$ helper RNA. As shown in Figure 4-5B, the 2C-P3 expressing template RNA supported nearly identical levels of negative-strand synthesis as the replication deficient P3, and supported significantly lower levels of negative-strand synthesis compared to those observed from the 2BC-P3 template RNA. Taken together, these results strongly implicate *cis* translation of the 2BC-P3 precursor as the primary requirement for efficient PV negative-strand synthesis. Multiple discrete proteins or protein precursors derived from 2BC-P3 which include the 2B and $3D^{pol}$ polypeptides may function synergistically to achieve efficient initiation of negative-strand synthesis. However, given the obligatorily sequential nature of the PV polyprotein, the 2BC-P3 precursor would be the minimum *cis* translation product required in either case for efficient negative-strand RNA synthesis.

Discussion

The work presented here has clearly established a close coupling of PV translation and initiation of negative-strand RNA synthesis in the *in vitro* HeLa S10 translation-replication

system, mirroring the characteristics of PV infection *in vivo*. Moreover, we have demonstrated that this coupling is due to a marked *cis* preference of viral protein function, rather than the result of RNA template preparation induced by ribosomal transit. Through the use of *trans* complementation RNA replication assays in the cell-free system, we have defined this *cis* acting protein product as the 2BC-P3 precursor polyprotein. This result, in combination with previous observations by our lab and others, allows us to propose a model whereby the translation of the 2BC-P3 precursor in *cis* is followed rapidly by a concerted association with newly formed membrane vesicles as well as its template RNA, initiating the critical process of replication complex assembly. This model provides mechanistic insight into the functional coupling of PV translation and initiation of RNA replication.

PV Translation in *cis* is a Prerequisite for Efficient RNA Replication

Using the HeLa S10 translation-replication reactions, we have observed that PV subgenomic RNA which translates all its replication proteins in *cis* [P23 RNA] exhibits approximately 5 to 10-fold higher levels of negative-strand RNA synthesis than the similar frameshifted RNA [FS23 RNA], which obtains its replication proteins in *trans*. These observations are consistent with the previous finding that all naturally occurring defective interfering (DI) PV genomes maintain the translational reading frame, despite containing various deletions in the P1 coding region (115). Additionally, previous work by our lab and others has shown that maintaining the reading frame of PV RNAs through the majority of the P23 coding sequence was required for efficient RNA replication in cell culture, even in the presence of a helper RNA or helper virus (61, 151, 197). This phenomenon has also been observed in cell culture during PV infection, in that genomes whose RNA replication has been arrested by guanidine will, following release of the guanidine block, return to the ER to re-start translation prior to RNA replication, despite the presence of sufficient PV proteins (70). In total, these data

strongly indicate that PV RNA replication requires not only newly translated replication proteins, but that these nascent proteins be translated in *cis* from the PV genome which will subsequently begin negative-strand RNA synthesis.

It is possible that the observed replication defect of PV RNAs resulting from prematurely aborted translation is a secondary effect of decreased RNA stability. It is known that cellular mRNAs which are improperly translated are subject to a wide range of RNA degradative machinery, including nonsense mediated decay (56, 146). Recent work by Kempf and Barton has also indicated that polyribosome assembly on PV RNA imparts some protection from endogenous exoribonucleases, suggesting that the absence of polysomes would result in RNA degradation (107). Interestingly, we observed no increase in the degradation of RNAs which prematurely terminated translation. This observation is again consistent with previous observations by our lab and others that premature termination of PV RNA does not result in RNA instability (105, 151; Ogram *et al*., unpublished results). These results show that the RNA replication defect observed in frameshifted PV RNAs is not a secondary effect of decreased RNA stability, but instead is a direct result of the incomplete *cis* translation of the replicating RNA.

Complete Ribosome Transit Through a Template RNA is Not Sufficient to Promote High Levels of Negative-strand RNA Synthesis

Because initiation of negative-strand RNA synthesis and termination of translation both occur at the extreme 3' end of the PV genome, it is possible that complete ribosomal transit and translation termination in the authentic RNA context is required for preparing the 3' end of the genome for efficient initiation of negative-strand synthesis. Using constructs which contain the authentic translation termination context but do not translate any functional replication proteins, we observed no significant difference between RNA which translated its entire open reading

frame (P1-3D*) compared to an RNA which terminated translation prematurely (FS1-3D*). This clearly showed that neither complete ribosome transit, nor authentic translation termination, conferred the ability to efficiently initiate negative-strand RNA synthesis.

A set of very elegant *in vivo* experiments was performed by Novak and Kirkegaard using PV RNAs containing premature amber stop codons in which replication was assayed in both non-permissive and amber-suppressor cells (151). Using this system, Novak and Kirkegaard observed a severe replication defect in PV RNAs which prematurely terminated translation and proposed a series of potential models to explain their results. One such model proposes that the act of ribosomal transit through a critical region of the template RNA promotes efficient negative-strand synthesis by affecting RNA secondary structure or by affecting protein association with the RNA template. We observed that the *cis* translation of the P23-3C^{STOP} RNA or 2C-P3 RNA did not result in efficient initiation of negative-strand synthesis, yet these two RNAs together contain the entire RNA sequence which comprises the critical region identified by Novak & Kirkegaard. This indicates that the efficient initiation of negative-strand RNA synthesis observed on fully translated template RNAs is a result of the *cis* action of a viral protein product(s) rather than the physical result of ribosomal transit through a specific region of the PV RNA.

Poliovirus RNA Replication Requires Translation of the 2BC-P3 Precursor in *cis*

By providing all essential PV proteins and naturally occurring precursors in *trans* from a helper RNA, we assayed for negative-strand synthesis from PV subgenomic RNA expressing sequentially larger portions of the PV replication polyprotein. Using this additive approach, we determined that the protein product required in *cis* for efficient negative-strand synthesis was either 3D^{pol} or a 3D-containing precursor protein. By assaying for negative-strand synthesis from RNAs expressing increasingly larger 3D-containing precursor proteins, we determined that

the 2BC-P3 precursor was the minimal PV polyprotein precursor required in *cis* to efficiently initiate negative-strand synthesis. This concept is consistent with previous work which showed that deletions extending past the $2A^{pro}$ coding sequence are lethal *in vivo*, and that providing $2A^{pro}$ in *trans* is sufficient to fully complement a $2A^{pro}$ deficient PV replicon RNA (61, 104, 105). Under conditions where $2A^{pro}$ is being provided in *trans*, such as those in Figure 4-4, the addition of the 2A polypeptide to the *cis* precursor (i.e. comparing 2BC-P3 to P23) actually is disadvantageous, forcing an additional cleavage step prior to generation of the ideal precursor. This would explain the observation that 2BC-P3 RNA replicates better than P23 RNA when in the presence of a helper RNA.

It remains possible that, rather than the 2BC-P3 precursor in its entirety, it is the function of multiple distinct proteins or protein precursors within 2BC-P3 that are required in *cis*. However, studies from the laboratory of Eckhard Wimmer showed that a dicistronic PV RNA containing the EMCV IRES between the 2A and 2B coding sequence generated viable virus and showed no abnormal polyprotein processing, whereas insertion of the EMCV IRES at any other intergenic position in the replicase polyprotein was lethal (139, 160). These studies clearly show that an intact 2BC-P3 precursor is essential for efficient PV RNA replication. Previous work from our lab further establishes the critical nature of the 2BC-P3 precursor by showing that a lethal mutation in protein 2C (2C[P131N]) could only be complemented efficiently by 2BC-P3 and not by a smaller precursor (104). It is critical to note, however, that despite the ability of the 2BC-P3 precursor to complement in *trans*, the ability of 2BC-P3 to promote negative-strand RNA synthesis is still dramatically more efficient in *cis* than in *trans*. Taken together, these observations indicate that the entire 2BC-P3 precursor as the essential *cis* acting viral protein factor required for the efficient initiation of negative-strand RNA synthesis.

A Model for PV RNA Replication Complex Formation Dependent on *cis* Translation of the 2BC-P3 Precursor Polyprotein

Poliovirus replication occurs on membranous vesicles induced upon infection by a combination of hydrophobic viral proteins and protein precursors. Interestingly, when these vesicles are induced via heterologous expression of these proteins, they are not utilized for RNA replication by a superinfecting virus (71). As the authors of this previous study concluded, this indicates that membrane vesicles must be induced immediately prior to RNA replication, by the proteins produced from the genome about to be replicated. This would require at least *cis* translation of $2C^{ATPase}$ and/or 2BC, since it has been shown that characteristic membrane rearrangements are induced by these two proteins (9, 20, 50). It is also of note that the PV polyprotein is subject to two distinct processing cascades as described by Lawson & Semler, one soluble pathway and one which is membrane associated (119). The membrane associated processing pathway initiates with the creation of the 2BC-P3 precursor, which we have identified here as the critical *cis* acting PV protein responsible for efficient initiation of negative-strand RNA synthesis. Furthermore, given the significantly short half-life of the 2BC-P3 precursor observed by Lawson & Semler, we assert that the *trans* acting capability of the 2BC-P3 precursor is severely restricted both by its inherently transient nature, as well as its membrane association. Based on our results presented above as well as work performed by multiple other laboratories, we propose a replication model whereby the PV polyprotein precursor 2BC-P3 acts in *cis* to bind its genomic RNA and simultaneously induce and associate with membrane vesicles, forming an active PV replication complex. This concerted process acts to functionally couple viral translation, membrane vesicle induction, and RNA replication, and represents a critical transition in the PV life-cycle from genomic translation to RNA replication.

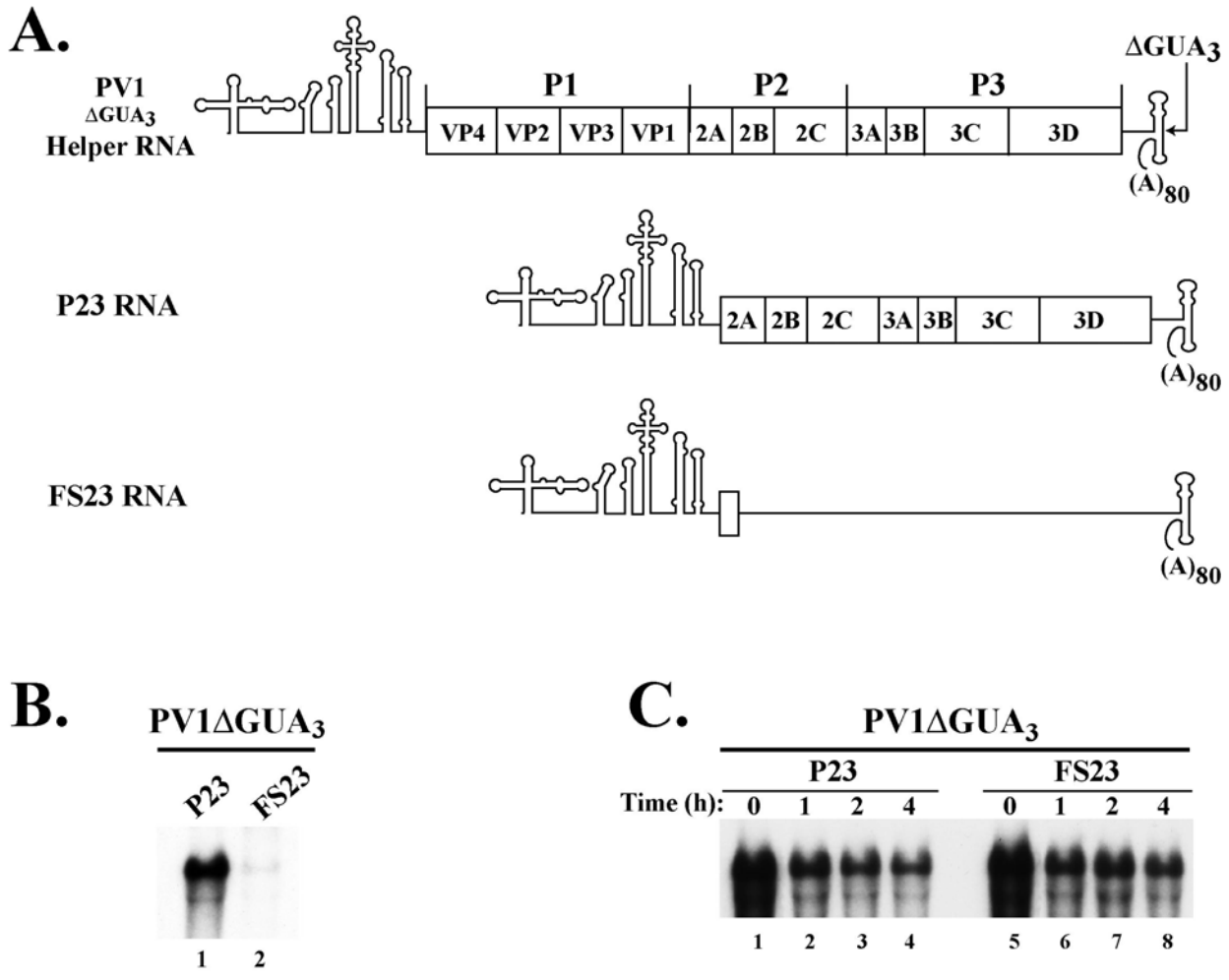

Figure 4-1. Translation of a PV RNA template is a prerequisite for efficient negative-strand synthesis. A) Schematic of poliovirus RNAs used in these experiments. PV1ΔGUA$_3$ helper RNA contains the entire PV RNA sequence with a mutation in the 3'NTR, rendering it incapable of RNA replication. P23 RNA encodes all essential viral replication proteins, and FS23 RNA contains a frameshift mutation in the 2A coding region of P23 RNA and does not express any functional protein B) Replication of P23 RNA and FS23 RNA was measured using PIRCs isolated from HeLa S10 reactions and RNA product was analyzed by CH_3HgOH gel electrophoresis and autoradiography as described in Chapter 2. Each transcript RNA contained two non-viral 5' G residues which permits only negative-strand RNA synthesis. Equimolar amounts of PV1ΔGUA$_3$ RNA were included in each reaction to provide all naturally occurring viral proteins in *trans*. C) The stability of uniformly radiolabeled P23 RNA or FS23 RNA in HeLa S10 reactions was measured as described in Chapter 2. Aliquots of the reaction mixtures were removed after the indicated incubation time and the full-length RNA remaining was analyzed by denaturing CH_3HgOH gel electrophoresis and autoradiography. As before, an equimolar amount of PV1ΔGUA$_3$ RNA was included in each reaction to recapitulate replication reaction conditions. Gels depicted in panels B & C were generated by Dr. Nidhi Sharma.

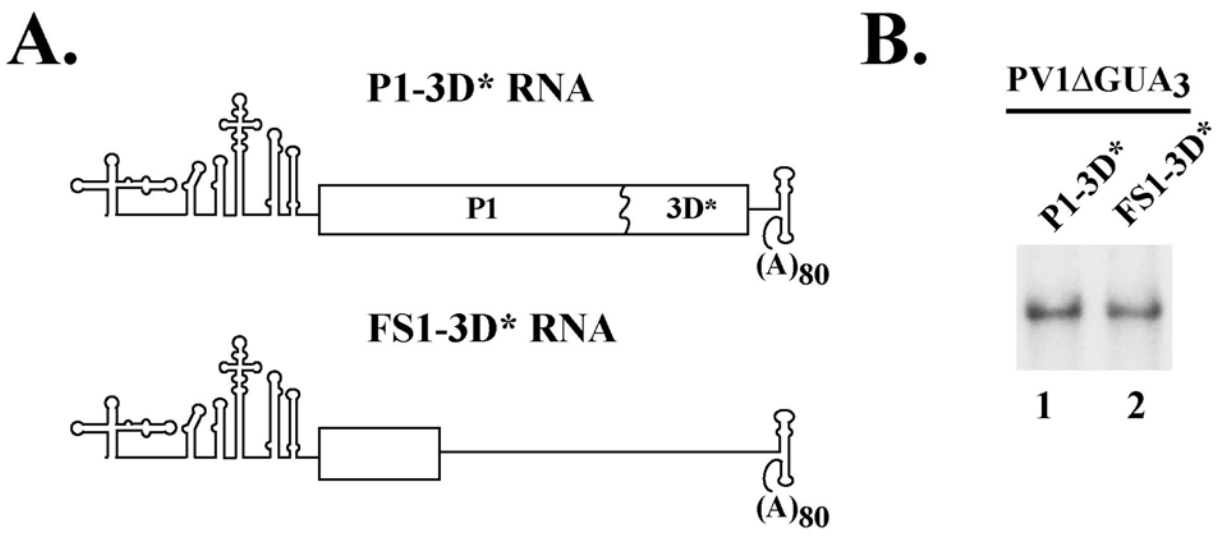

Figure 4-2. Physical ribosome transit of a template RNA is not sufficient to promote efficient initiation of negative-strand synthesis. A) Schematic of poliovirus RNAs used in this experiment. P1-3D* RNA encodes a fusion protein between the P1 coding region and a non-functional carboxy-terminal portion of 3D. During translation of P1-3D* ribosomes completely transit the length of the template and terminate translation in the authentic RNA context. FS1-3D* RNA contains a frameshift mutation early in the P1 coding region of P1-3D* RNA and terminates translation prematurely, without completely transiting the RNA template. B) Replication of P1-3D* and FS1-3D were assayed in the presence of equimolar amounts of PV1ΔGUA$_3$ helper RNA using PIRCs isolated from HeLa S10 reactions as described in Chapter 2. RNA product was visualized by denaturing CH_3HgOH gel electrophoresis and autoradiography. The gel depicted in panel B was generated by Dr. Nidhi Sharma.

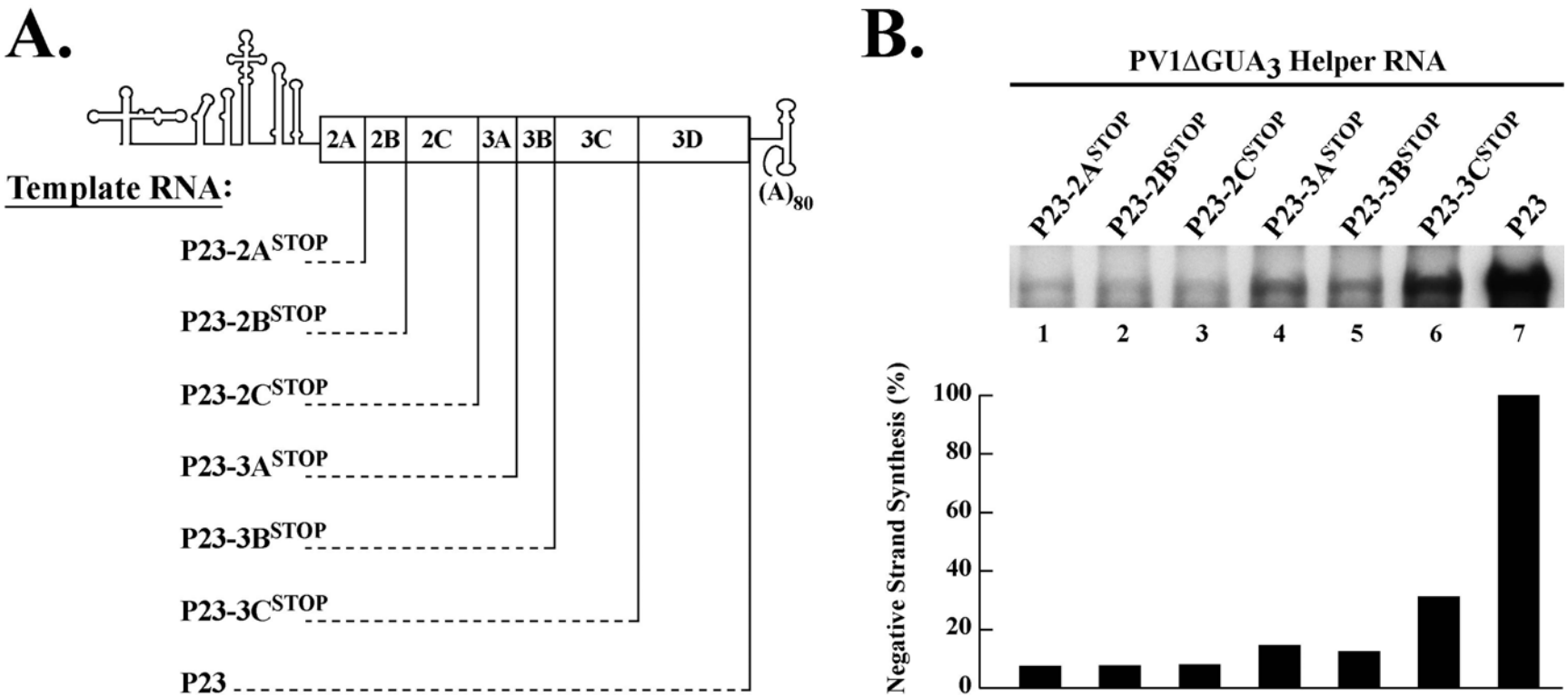

Figure 4-3. Translation of 3D or a 3D precursor is required in *cis* for efficient initiation of negative-strand synthesis. A) Schematic of poliovirus RNAs used in this study. Each successive template RNA encodes one additional protein component of the PV replication polyprotein (P23), such that P23-2A^{STOP} encodes only 2A, P23-2B^{STOP} encodes 2AB, P23-2C^{STOP} encodes 2ABC, and so on. All RNAs used in these experiments are identical in length, and differ in sequence only by the inclusion of two stop codons at the indicated position in the coding region. B) Replication of each template RNA indicated above was assayed in the presence of equimolar amounts of PV1ΔGUA$_3$ helper RNA as described previously. Full length product RNA was analyzed by denaturing CH_3HgOH gel electrophoresis and levels of negative-strand synthesis were quantitated by phosphorimager. The level of negative-strand synthesis of each RNA were scaled relative to those observed with P23 RNA and represented graphically below the autoradiograph. The gel depicted in panel B was produced by Dr. Sushma Ogram.

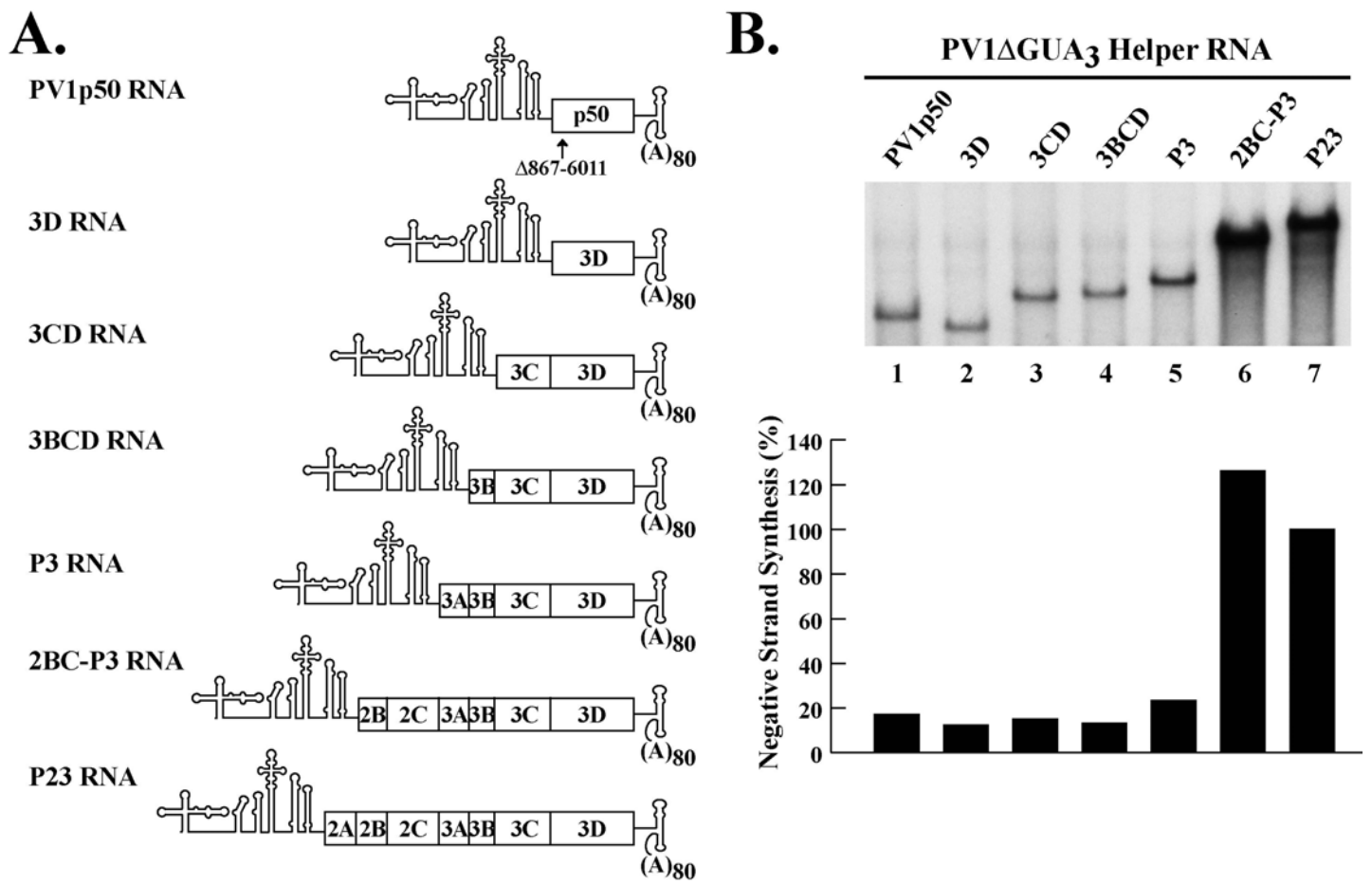

Figure 4-4. Efficient initiation of negative-strand synthesis requires translation of 2B or a 2B precursor in *cis*. A) Schematic of poliovirus RNAs used in this study. Each RNA encodes a successively larger $3D^{pol}$ precursor as indicated by the template name listed at left. PV1p50 RNA acts as a control RNA, translating a non-functional 50 kDa protein and utilizing the authentic translational start and stop contexts. B) Replication of each template RNA indicated above was assayed in the presence of equimolar amounts of $PV1\Delta GUA_3$ helper RNA as described previously. Full length product RNA was analyzed by denaturing CH_3HgOH gel electrophoresis and quantitated by phosphorimager. The levels of negative-strand synthesis of each RNA were scaled relative to P23 RNA and are represented graphically below the autoradiograph.

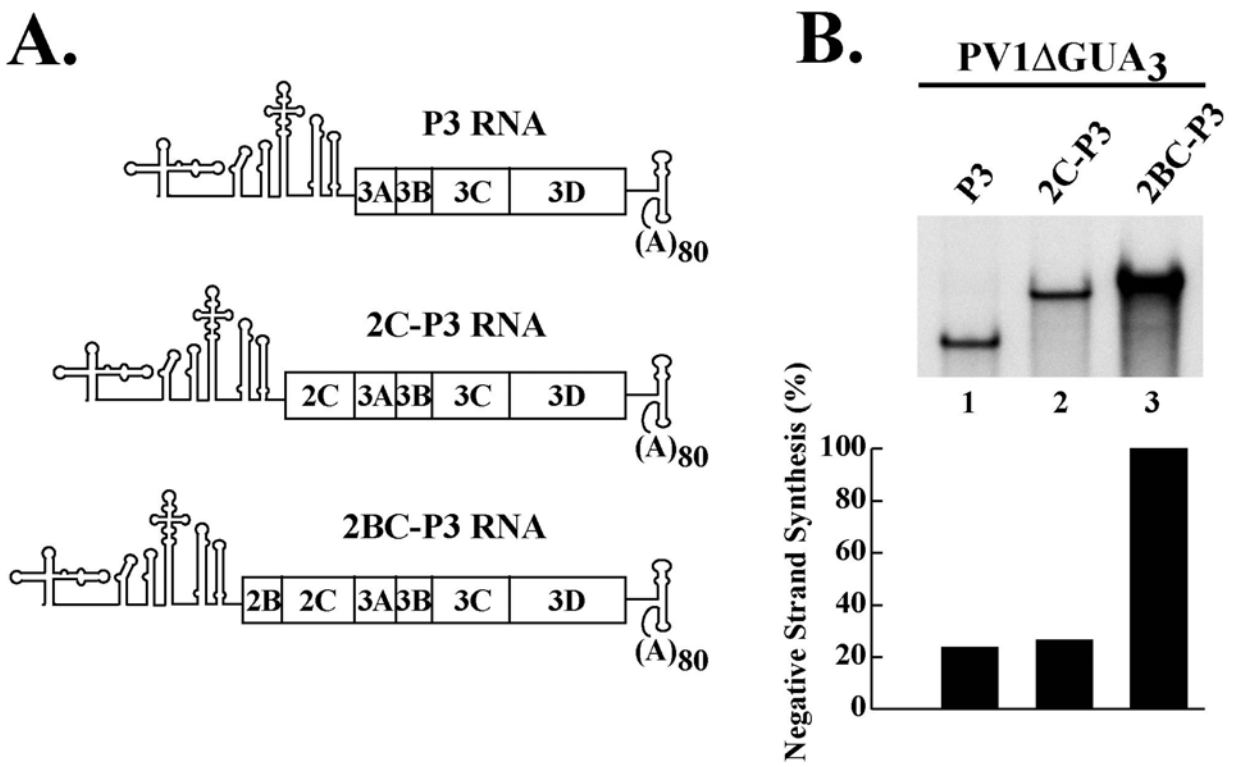

Figure 4-5. Poliovirus RNA replication requires translation of the 2BC-P3 polyprotein precursor in *cis*. A) Schematic of the poliovirus RNAs used in this study. P3 RNA encodes the P3 polyprotein precursor, 2C-P3 RNA encodes the 2C-P3 precursor, and 2BC-P3 RNA encodes the 2BC-P3 precursor. B) Replication of each template RNA indicated above was assayed in the presence of equimolar amounts of PV1ΔGUA$_3$ helper RNA as described previously. Full length product RNA was analyzed by denaturing CH_3HgOH gel electrophoresis and quantitated by phosphorimager. The levels of negative-strand synthesis of each RNA were scaled relative to 2BC-P3 RNA and are represented graphically below the autoradiograph.

CHAPTER 5
MUTLIPLE MOLECULES OF THE 3CD VIRAL PROTEIN PRECURSOR PERFORM DISCRETE FUNCTIONS IN THE INITIATION OF POLIOVIRUS NEGATIVE-STRAND RNA SYNTHESIS

Introduction

The differential use of polyprotein precursors and their products is a key strategy employed by poliovirus (PV) to perform the many diverse functions required during viral replication using limited sequence space. An extension of this is the evolution of multiple activities within a single protein or protein precursor. The PV precursor $3CD^{pro}$ exemplifies both of these concepts in that it performs multiple functions as a precursor and these activities are functionally distinct from is processed products $3C^{pro}$ and $3D^{pro}$.

As a precursor, $3CD^{pro}$ exhibits no polymerase acitivity, however its processed product $3D^{pol}$, acts as the RNA-dependent RNA polymerase (RdRp) (73, 74, 88). The $3CD^{pro}$ precursor also has the ability to bind to stem-loop *d* of the 5'CL, and while this ability is partially retained by its processed product $3C^{pro}$, the binding affinity of $3C^{pro}$ for the 5'CL is 10-fold lower than that of $3CD^{pro}$ (12). And while both $3CD^{pro}$ and $3C^{pro}$ are proteases, their cleavage specificities and activity levels are different, and this difference is particularly apparent in the processing of the viral capsid precursor (P1) and at the 3C-3D junction (157). In these cases, $3C^{pro}$ processing of P1 and 3CD were 1000-fold and 100-fold less efficient than the processing observed by $3CD^{pro}$. Interestingly, there are very few structural differences between $3C^{pro}$ and $3D^{pol}$ alone and within the $3CD^{pro}$ precursor as determined by x-ray crystallography.(130).

The current model of PV replication complex formation invokes genomic circularization mediated by RNP complexes formed at the 5'CL and 3'NTR/poly(A) tail to promote initiation of negative-strand synthesis (26, 93, 126, 196). Given that $3CD^{pro}$, in the presence of PCBP and/or 3AB, was observed to form RNP complexes with the 5'CL as well as the 3'NTR (12, 14, 89,

158, 213), these circular models also included two molecules of $3CD^{pro}$. It has been established that the formation of the 5'CL-$3CD^{pro}$ RNP complex is required for negative-strand synthesis (12, 158, 213), but the functional role of $3CD^{pro}$ bound to the 3'NTR is yet to be elucidated. The consequences of differential interactions between $3CD^{pro}$ and either 3AB or PCBP have also not yet been addressed. Additionally, it has not yet been determined if the molecule binding to the 5'CL is the same as that which binds the 3'NTR or if these are indeed two different molecules as has been modeled.

Although it has been established that the above described activities of $3CD^{pro}$ are required for PV RNA replication, the precise molecular mechanisms which drive these requirements have not been delineated (12, 89, 158, 213). In an effort to more directly characterize some of these mechanisms, we utilized the HeLa S10 translation-replication system to examine the complementation profiles of functionally defined mutants in the PV protein precursor $3CD^{pro}$. To do this, we performed *trans* complementation analysis of PV subgenomic RNA replicons containing lesions in the $3CD^{pro}$ coding sequence. These mutant RNAs were assayed for their ability to assemble functional replication complexes and initiate negative-strand synthesis in the presence of complementing protein expression RNAs. Herein, we demonstrate that $3D^{pol}$ must be admitted into the replication complex as its immediate precursor $3CD^{pro}$ and that binding to the 5'CL is not required for this activity. In addition, we provide compelling evidence that at least two molecules of $3CD^{pro}$ are present in the PV replication complex and these individual precursors perform multiple distinct functions. Lastly, we show that the 5'CL RNP complex essential for initiation of negative-strand synthesis is likely formed by a molecule of $3CD^{pro}$ which enters the replication complex in the form of its precursor P3.

Results

Mutations Which Prevent the Production of Active $3D^{pol}$ are Rescued by $3CD^{pro}$

To begin to analyze the role of $3CD^{pro}$ in the formation of the PV replication complex used to initiate negative-strand RNA synthesis, we first needed to establish the phenotypes of each specific $3CD^{pro}$ mutants in the HeLa S10 translation-replication system. The first subtype of $3CD^{pro}$ mutants examined were those which failed to generate active $3D^{pol}$. The first of these was a previously described mutant in the highly conserved YGDD motif of RNA-dependent RNA polymerases, where the Gly327 of PV $3D^{pol}$ was mutated to Met (3D[G327M]) (98). This mutation was shown to abolish all polymerase activity in bacterially expressed recombinant PV $3D^{pol}$. The second mutant $3CD^{pro}$ examined contained four sequential mutations of the 3C-3D cleavage site, all on the $3C^{pro}$ side of the junction in positions P1-P4, thereby maintaining the integrity of the $3D^{pol}$ amino acid sequence. This processing mutant (3CD[PM]) combines two previously described processing site mutations [T181K, Q182D] with two additional mutations [S183G, Q184N] designed to completely abrogate 3C-3D processing (12, 37, 88). This extensive mutagenesis is required to completely inhibit processing of $3CD^{pro}$, as individual mutations as well as combinations thereof have been shown to reduce, but not eliminate processing ((88); data not shown). Because the $3CD^{pro}$ precursor does not possess any of the polymerase activity of its progeny $3D^{pol}$, the abrogation of 3CD processing also functionally inactivates polymerase activity (73, 74, 88). Since both 3CD[G327M] and 3CD[PM] would be unable to generate a functional $3D^{pol}$, PV RNAs containing these mutations should be unable to replicate.

Each mutant $3CD^{pro}$ was assayed for its ability to support negative-strand RNA synthesis of a previously described subgenomic PV RNA replicon (P23 RNA) which contained the above described mutations in the 3CD coding region. Negative-strand synthesis was assayed using

PIRCs isolated from HeLa S10 translation-replication reactions as described in Chapter 2. Radiolabeled full-length product RNA was visualized by denaturing CH_3HgOH gel electrophoresis and autoradiography as previously described. As expected, P23 RNA which expresses wild-type $3CD^{pro}$ generated significant amounts of negative-strand product RNA (Figure 5-1A, lane 1). However, P23 RNAs which express a $3CD^{pro}$ that cannot generate active $3D^{pol}$ are unable to generate detectible levels of negative-strand synthesis (Figure 5-1A, lanes 2-3).

To ensure that the observed RNA replication phenotype of these mutants was not the result of defects in translation or processing, protein synthesis in the replication reactions was analyzed by [^{35}S]methionine incorporation, SDS-PAGE, and autoradiography. As shown in Figure 5-1B, both mutant P23 RNAs generate similar levels of protein synthesis. Further, there are no significant differences in the pattern of polyprotein processing, except where $3C^{pro}$ and $3D^{pol}$ were absent from reactions expressing the 3CD[PM], as expected (Figure 5-1B, lane 3). These data confirm that mutations which prevent the generation of active $3D^{pol}$ block PV negative-strand RNA synthesis, and the mutations tested do not affect translation or polyprotein processing.

To determine if these $3D^{pol}$ deficient mutations can be complemented in *trans*, negative-strand synthesis of P23-3D[G327M] RNA or P23-3CD[PM] RNA was assayed in the presence of non-replicating helper RNAs encoding sequentially larger 3D containing precursors. Levels of negative-strand synthesis were assessed as described above. Interestingly, expression of wild-type $3D^{pol}$ alone was not sufficient to rescue negative-strand synthesis to significant levels for either of the $3D^{pol}$ deficient mutants (Figure 5-2A/2C, lane 1). However,

negative-strand synthesis of these mutants was efficiently restored by complementation with $3CD^{pro}$ or a larger precursor (Figure 5-2A/2C, lane 2-4).

Protein synthesis and polyprotein processing in the replication reactions was also analyzed by [^{35}S]methionine incorporation, SDS-PAGE, and autoradiography. Despite the presence of a disproportionate excess of polymerase in reactions which expressed solely $3D^{pol}$ (Figure 5B/5D, lane 1), only minimal levels of negative-strand synthesis were observed in complementation assays. Furthermore, there is direct correlation between the amounts of $3CD^{pro}$ present and the level of *trans* complementation observed in RNA replication assays. Taken together, these data suggest that the active $3D^{pol}$ is delivered to the replication complex in the form of its immediate precursor, $3CD^{pro}$.

Complementation of $3D^{pol}$ Deficient Mutations Requires the Intact $3CD^{pro}$ Precursor

To further characterize the complementation of the $3D^{pol}$ deficient mutations by $3CD^{pro}$, negative-strand synthesis of P23 RNAs expressing either 3CD[G327M] or 3CD[PM] was assayed in the presence of a combination of $3C^{pro}$ and $3D^{pol}$ expression RNAs or an RNA which expresses the heterologous mutant 3D/3CD. Levels of negative-strand synthesis were assessed as described above. As before, complementation of both $3D^{pol}$ deficient mutants by $3CD^{pro}$ was significantly more efficient than complementation by $3D^{pol}$ (Figure 5-3A/3C, lanes 1-2). Complementation using a combination of $3C^{pro}$ and $3D^{pol}$ expression RNAs was slightly less efficient than using a $3D^{pol}$ expression RNA alone, and negative-strand synthesis was undetectable in complementation reactions containing the heterologous 3D/3CD mutant expression RNA (Figure 5-3A/3C, lanes 3-4). Analysis of protein synthesis and polyprotein processing showed equal levels of protein synthesis and processing, except where expected for additional proteins expressed in *trans* (Figure 5-3B/3D). These results clearly show that the

active $3D^{pol}$ used to initiate negative-strand RNA synthesis is delivered to the PV replication complex in the form of its intact $3CD^{pro}$ precursor.

Mutations Which Disrupt $3C^{pro}/3CD^{pro}$ Binding to the 5'CL Block RNA Replication and Affect Polyprotein Processing

To further analyze the role of $3CD^{pro}$ in the formation of the PV replication complex used to initiate negative-strand RNA synthesis, we generated mutants in the RNA binding region of $3C^{pro}/3CD^{pro}$ and determined the replication and translation phenotypes of these mutants in the HeLa S10 translation-replication system. Three distinct regions of the 3C primary sequence have been implicated in binding to the 5'CL, an N-terminal region (Y6, K12, R13), a central region (K82, F83, R84, D85, I86, R87), and a C-terminal region (T154, G155, K156) (12, 33, 36, 132, 142). The residues included in the C-terminal RNA binding region have also been implicated VPg uridylylation on the *cre*(2C) hairpin and overlap a predicted protein-protein interaction site (130), making this region unattractive for mutagenesis. The residues in the central region represent a highly conserved picornaviral KFRDIR 3C-RNA binding motif, and a previously described mutant, 3C[R84S], has been included in this analysis as a prototypic example of mutations in this region(36). Lastly, a double mutant in the N-terminal RNA binding region of $3C^{pro}$ was also created which combined two adjacent previously described RNA binding mutations, 3C[K12N/R13N] (36).

Each 3CD RNA binding mutant (RBM) was assayed for its ability to support negative-strand RNA synthesis of P23 RNA which contained one the above described mutations in the 3CD coding region. The levels of negative-strand synthesis from isolated PIRCs were assessed as described above. As shown previously, P23 RNA which expresses wild-type $3CD^{pro}$ generated significant amounts of negative-strand product RNA (Figure 5-4A, lane 1). However,

P23 RNAs which express a $3C^{pro}/3CD^{pro}$ that cannot bind the 5'CL are unable to generate detectible levels of negative-strand synthesis (Figure 5-4A, lanes 2-3).

To determine the translational and processing phenotypes of these mutants, protein synthesis in the replication reactions was analyzed by [^{35}S]methionine incorporation, SDS-PAGE, and autoradiography. As shown in Figure 5-4B, both mutant P23 RNAs generate similar levels of protein synthesis, however, both mutants exhibited differences in the pattern of polyprotein processing (Figure 5-1B, lane 2-3). In reactions containing P23-3C[R84S], there was a significant accumulation of unprocessed high molecular weight precursors. Likewise, every mutation tested within the conserved KFRDIR motif exhibited some degree of polyprotein processing defect (data not shown), which complicates the interpretation of RNA replication phenotypes. In reactions containing P23-3C[K12N/R13N], there was a moderate but detectable increase in the efficiency of 3C-3D processing, however this is likely benign, particularly since all other polyprotein processing seems unaffected. These data, particularly the 3C[K12N/R13N] mutant, indicate that mutations which disrupt the binding of $3C^{pro}/3CD^{pro}$ to the 5'CL block PV negative-strand RNA synthesis

Complementation of $3C^{pro}/3CD^{pro}$ RNA Binding Mutants Requires the Intact $3CD^{pro}$ Precursor

Although $3C^{pro}$ can bind RNA, it has been shown that the $3CD^{pro}$ precursor has a 10-fold higher affinity for the PV 5'CL than does $3C^{pro}$ alone (12). And given the significant excess of $3CD^{pro}$ over $3C^{pro}$ that exists during PV infection, the most likely 5'CL RNP complex is one which contains $3CD^{pro}$ rather than $3C^{pro}$ alone. To test this assumption, complementation assays were performed using P23 RNA containing either the 3C[K12N/R13N] or 3C[R84S] mutations, in combination with non-replicating helper RNAs expressing either $3C^{pro}$ alone or its precursor

3CD^{pro}. In addition, the mutant P23 RNAs were each complemented with a combination of 3C^{pro} and 3D^{pol} expressing RNAs or an RNA which expressed the heterologus 3CD^{pro}[RBM].

As predicted, the defect in negative-strand synthesis of both P23[RBM] RNAs were unable to be complemented by 3C^{pro} alone or 3C^{pro} and 3D^{pol} in combination (Figure 5-5A, lanes 1, 3, 5, and 7). In contrast, expression of the 3CD^{pro} precursor was able to complement both P23-3C[K12N/R13N] as well as P23-3C[R84S], while the heterologous 3CD[RBM] was unable to do so (Figure 5-5A, lanes 2, 4, 6, and 8). It is of note, however, that the efficiency of rescue differed significantly between the two mutants, most likely as a result of interference by the defective polyprotein processing exhibited by 3CD[R84S].

Analysis of protein synthesis in these reactions shows appropriate expression of all complementing proteins as well as similar levels of protein synthesis for both P23[RBM] RNAs (Figure 5-5B/5C). Interestingly, some of the polyprotein processing defect exhibited by P23-3C[R84S] is complemented in *trans* by 3C^{pro}/3CD^{pro}, and this complementation is even greater in the reaction which expressed 3CD[K12N/R13N] which exhibited elevated processing activity (Figure 5-5C). Despite these minor processing irregularities, these results clearly show that the intact 3CD^{pro} precursor is required to complement a 3C^{pro} RNA binding mutation. Moreover, this confirms that 3CD^{pro}, and not 3C^{pro}, is a component of the 5'CL RNP complex required for the initiation of negative-strand synthesis.

Complementation Between Two Functionally Distinct 3CD^{pro} Mutants

Work by Cornell *et al.* showed reciprocal complementation between an RNA expressing a non-functional chimeric polymerase and an RNA expressing a P3 precursor which contained a 3C/3CD RNA binding mutation (62). The authors therefore concluded that viral proteins capable of binding RNA and initiating replication complex formation, can recruit complementing proteins to the replication via protein-protein interactions. In the context of the current

investigation, this would predict that a $3D^{pol}$ deficient $3CD^{pro}$ mutant which retained RNA binding ability could be complemented by a 3CD[RBM] which could generate functional polymerase. Replication complexes would therefore require the presence of at least two molecules of $3CD^{pro}$ for such a complementation to occur, and the potential replication complex models for this are depicted in Figure 5-6.

To determine if reciprocal complementation of two functionally distinct $3CD^{pro}$ mutants was possible, negative-strand RNA synthesis was assayed in reactions containing P23-3CD[G327M] RNA in combination with a helper RNA which expressed a wild-type or mutant $3CD^{pro}$. For the purposes of these complementation experiments, 3CD[K12N/R13N] was the RNA binding mutant of choice due to the severe processing defects exhibited by 3CD[R84S]. In reactions containing P23-3D[G327M], efficient complementation was observed in the presence of wild-type or K12N/R13N $3CD^{pro}$ RNA, but not in the presence of the synonymous 3CD[G327M] RNA (Figure 5-7A, lanes 1-3). When the complementation was reversed, P23-3CD[K12N/R13N] was able to be complemented by both wild-type and G327M $3CD^{pro}$ RNA, but not by the synonymous 3CD[K12N/R13N] RNA (Figure 5-7A, lanes 4-6). However, the reversed complementation efficiency was significantly reduced relative to the original complementation, even in the presence of wild-type $3CD^{pro}$ helper RNA.

To determine if the above complementation would also occur for the similarly $3D^{pol}$ deficient 3CD[PM], negative-strand RNA synthesis was assayed in reactions containing P23-3CD[PM] RNA in combination with a helper RNA which expressed a wild-type or mutant $3CD^{pro}$. As expected, efficient complementation was observed in reactions containing P23-3D[G327M] RNA in the presence of wild-type or K12N/R13N $3CD^{pro}$ RNA, but not in the presence of the synonymous 3CD[PM] RNA (Figure 5-7C, lanes 1-3). And here too, when the

complementation was reversed, the same pattern and decrease in efficiency of complementation was observed as was for the 3CD[G327M] mutation (Figure 5-7C, lanes 4-6).

To determine if the differences in complementation efficiencies were caused by abnormalities in translation and/or polyprotein processing, protein synthesis was monitored by [^{35}S]methionine incorporation and assessed by SDS-PAGE and autoradiography as before. As shown in Figures 5-7B and 5-7D, overall protein synthesis was nearly identical in all reactions and polyprotein processing showed no abnormalities (except for expected differences for 3CD[K12N/R13N] and 3CD[PM] as previously discussed).

These results clearly show that two distinct mutations in essential functions of the 3CD^{pro} precursor can be reciprocally complemented to restore replication complex formation and negative-strand synthesis. Therefore, two or more molecules of the 3CD^{pro} precursor must be simultaneously present in the PV replication complex, such as diagrammed in Figure 5-6D.

High Efficiency Complementation of 3C[K12N/R13N] Requires the P3 Precursor

Interestingly, although the same pattern of complementation was present, we observed a significant decrease in complementation efficiency when the template RNA contained the 3CD[K12N/R13N] mutations. This could result from either a dominant negative effect of a larger 3CD[K12N/R13N] containing precursor, a more stringent requirement for proteins in *cis* to bind the 5'CL, or the requirement of a larger precursor to provide RNA binding in *trans*. To test this, we first assessed the ability of P23-3C[K12N/R13N] RNA to be complemented by RNAs expressing sequentially larger 3C^{pro} containing precursors. As before, in reactions containing P23-3C[K12N/R13N] RNA and 3C^{pro} expression RNA, levels of negative-strand synthesis were undetectable, whereas complementation was observed in the presence of RNA which expressed 3CD^{pro} (Figure 5-8A, lanes 1-2). Surprisingly, higher levels of negative-strand synthesis were observed when P23-3C[K12N/R13N] RNA was complemented with P3 or

2BC-P3 expression RNA (Figure 5-8A, lanes 3-4). Aside from the expected increases in the levels of additional viral proteins expressed in *trans*, there were no significant alterations in the translation or polyprotein processing profile in any of the replication reactions (Figure 5-8B). These results clearly show that high efficiency complementation of a $3CD^{pro}$ RNA binding mutant requires the presence of a P3 precursor. Moreover, these data suggest that the P3 precursor delivers $3CD^{pro}$ to the 5'CL during the formation of the 5'CL RNP complex which is essential for the initiation of negative-strand RNA synthesis.

Discussion

The work presented here has clearly illustrated the multifunctional nature of the viral $3CD^{pro}$ precursor, particularly as it pertains to the initiation of negative-strand RNA synthesis. By performing *trans* complementation assays using the HeLa S10 translation-replication system, we have further defined the role of $3CD^{pro}$, as well as its precursors and processed products, in the formation of a functional PV replication complex. Using this approach, we have clearly shown that $3D^{pol}$ is admitted to the replication complex in the form of its intact immediate precursor $3CD^{pro}$ and that binding to the 5'CL is not a prerequisite for this activity. Furthermore, by performing reciprocal complementation using two $3CD^{pro}$ mutants in distinct, essential functions, we have shown that there are at least two molecules of $3CD^{pro}$ present in the PV replication complex which perform discrete functions. Lastly, we have shown that the $3CD^{pro}$ which forms the essential 5'CL RNP complex is likely admitted to the replication complex in the form of its precursor P3.

Active $3D^{pol}$ is Admitted to the PV Replication Complex in the Form of its Polymerase-inactive Precursor $3CD^{pro}$

Although $3CD^{pro}$ contains the entire $3D^{pol}$ peptide, it contains none of the associated polymerase activity (73, 74, 88). This is most likely due to changes in positioning of the

N-terminus of $3D^{pol}$ that occur subsequent to processing (95, 130, 180, 199). This strategy allows PV to synthesize large amounts of $3CD^{pro}$ prior to replication without risking the generation of non-specifc dsRNA products on cellular mRNAs which could activate innate immune pathways. Here, the $3CD^{pro}$ precursor functions as a pro-enzyme which can be synthesized to high-levels and activated rapidly on demand. We were able to show that mutants in either 3C-3D processing or the conserved $3D^{pol}$ RdRp motif could only be rescued efficiently by an intact $3CD^{pro}$ or a 3CD containing precursor. This indicates that $3CD^{pro}$ is recruited into the PV replication complex in an inactive form, and its activation by processing represents the "firing" of replication complexes and marks the initiation of negative-strand synthesis. Additionally, this recruitment does not require direct binding of the $3CD^{pro}$ precursor to RNA, since mutations which disrupted conserved RNA binding residues in 3C were able to complement $3D^{pol}$ deficient RNA replicons.

RNA Binding and Protease Activities of $3CD^{pro}$ are Functionally Linked

Each RNA binding mutation tested, in addition to its replication phenotype, also exhibited altered patterns of polyprotein processing. In most cases, this alteration was detrimental and resulted in accumulation of unprocessed precursors, however in one case (3C[K12N/R13N]) the mutations resulted in increased processing efficiency. The effect of the latter mutations was mild and manifested primarily as an increased proportion of processed $3C^{pro}$ and $3D^{pol}$ in replication reactions. These observations are consistent with recent structural work by Claridge *et al.*, who showed that RNA binding by rhinovirus $3C^{pro}$ induced conformational changes in regions involved in proteolysis (53). In this manner, one face of $3C^{pro}/3CD^{pro}$ communicates with the other to transmit information regarding RNA binding status to the proteolytic machinery. This has significant implications for the PV life-cycle, since the rapid polyprotein processing that is observed in the membrane associated processing cascade may actually be performed by the

5'CL-3CD^{pro} RNP complex. Since this processing pathway is associated with RNA replication, polyprotein processing, membrane association, and replication complex formation may be additionally coupled by enhanced proteolysis by RNA-associated 3C^{pro}/3CD^{pro}. By this model, most RNA binding mutations which disrupt processing may essentially lock 3C^{pro}/3CD^{pro} in an unbound conformation, whereas the K12N/R13N mutant induces conformational shifts that simulate the bound conformation in the absence of RNA.

Multiple 3CD^{pro} Peptides are Present in the PV RNA Replication Complex Used to Initiate Negative-strand RNA Synthesis

Current models of initiation of PV negative-strand RNA synthesis involve interaction of the 5' and 3' ends of genomic RNA, mediated by RNP complexes, to form a circular replication complex (26, 93, 126, 196). It was known that 3CD^{pro}, in the presence of PCBP and/or 3AB, could form RNP complexes with both the 5'CL and the 3'NTR (12, 14, 89, 158, 213). Based on this, in combination with our own 3D complementation data, our model for circular replication complex formation included two molecules of 3CD^{pro}. Later studies by Cornell *et al.* showed that negative-strand synthesis of an RNA encoding an inactive chimeric 3D^{pol} could be complemented by expressing a P3 precursor with an RNA binding mutation (62). However, the authors did not characterize in which function the chimeric polymerase was defective and examined only the P3 precursor for its ability to complement in *trans*. From this data it is difficult to draw precise conclusions about replication complex formation and composition. Using precise mutations which inactivated single functions of the 3CD^{pro} precursor, we demonstrated reciprocal complementation of 3D^{pol} deficient mutants (3CD[G327M] and 3CD[PM]) with an RNA binding mutant (3CD[K12N/R13N]). Each of the mutants blocks negative-strand RNA synthesis as each represents a mutation(s) in a discrete but essential function of the PV replication complex. Since both functions are required simultaneously in the

initiation of negative-strand synthesis, complementation of these mutants requires that at least one copy of each mutant $3CD^{pro}$ be present at the time of replication initiation. This represents the first conclusive functional evidence that multiple molecules of the $3CD^{pro}$ polypeptide are present and perform discrete functions within the PV replication complex that is used to initiate negative-strand RNA synthesis.

The $3CD^{pro}$ Bound to the 5'CL is Admitted to the PV Replication Complex in the Form of its Precursor P3

We observed that, although functional, RNAs expressing $3CD^{pro}$, 3CD[G327M], or 3CD[PM] were only capable of minimally complementing P23-3CD[K12N/R13N] RNA. This was significant because when the complementation had been reversed, 3CD[K12N/R13N] expression RNA was capable of complementing P23-3D[G327M] and P23-3CD[PM] RNAs to significantly higher levels. Upon examining the ability of larger $3C^{pro}$ precursors to rescue negative-strand synthesis of P23-3C[K12N/R13N] RNA, we showed that complementation efficiency was significantly higher in the presence of either P3 or 2BC-P3 expression RNAs. Given that expression of P3 resulted in the highest level of negative-strand synthesis, and that expression of 2BC-P3 also provides P3, we conclude that the $3CD^{pro}$ which forms the essential RNP complex with the 5'CL is first admitted into the replication complex in the form of the P3 precursor. This is particularly interesting, since $3CD^{pro}$ has been shown to bind to the 5'CL in the presence of the 3AB precursor (89, 213). Together, 3AB and $3CD^{pro}$ comprise the P3 precursor, which may enter the replication complex intact and subsequently process upon binding to the 5'CL. Furthermore, since VPg(3B) serves as protein primer for RNA synthesis, the 3AB generated from above described P3 processing, could serve as the precursor for the VPg used to prime negative-strand synthesis. This model is consistent with previous work which

showed that mutations in VPg which blocked its priming ability could only be complemented in *trans* by P3 or in *cis* as an intragenic fusion to a $3CD^{pro}$containing precursor (124).

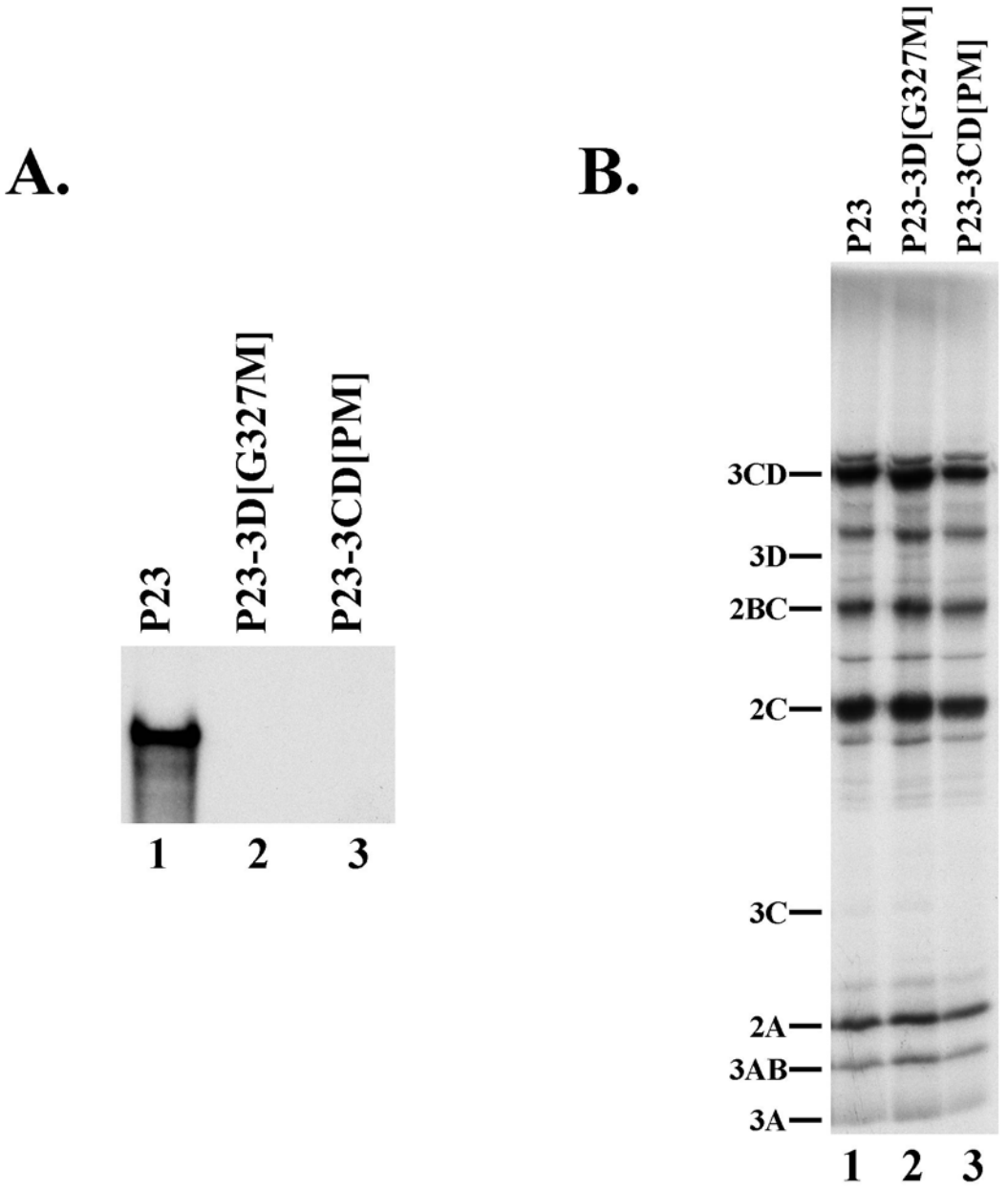

Figure 5-1. Mutations which prevent the generation of active $3D^{pol}$ block RNA replication. A) Negative-strand synthesis was assayed using PIRCs isolated from HeLa S10 reactions as described in Chapter 2. Reactions contained subgenomic P23 RNA containing either a wild-type or mutant 3CD coding region (3D[G327M] or 3CD[PM]). Full length RNA product was analyzed by denaturing CH_3HgOH gel electrophoresis and autoradiography. B) A portion of the HeLa S10 reactions described in (A) was metabolically labeled with [^{35}S]methionine to assay for protein synthesis. These reactions were analyzed by SDS-PAGE and autoradiography. Viral proteins are indicated at left.

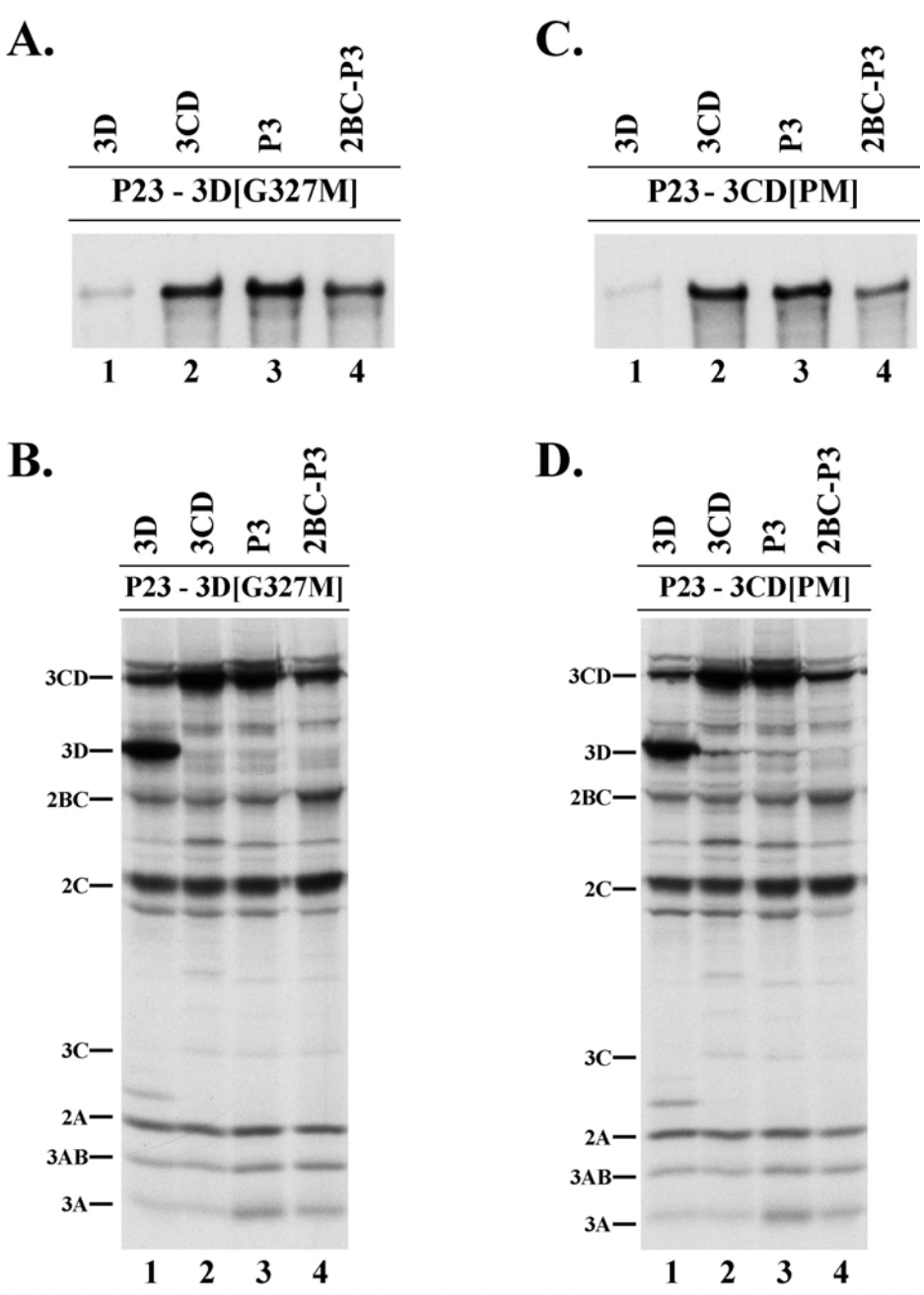

Figure 5-2. Viral Precursor $3CD^{pro}$ complements both 3D[G327M] and 3CD[PM] in *trans*. A & C) Negative-strand synthesis was assayed using PIRCs isolated from HeLa S10 reactions as described in Chapter 2. Reactions contained P23 RNA with a mutated 3CD coding region (3D[G327M] or 3CD[PM]) and a second complementing RNA expressing the indicated protein. All complementing RNAs contain the ΔGUA_3 mutation which inhibits negative-strand synthesis. Product RNA was analyzed by denaturing CH_3HgOH gel electrophoresis and autoradiography. B & D) A portion of the reactions described above was metabolically labeled with [^{35}S]methionine and these reactions were analyzed by SDS-PAGE and autoradiography. Viral proteins are indicated at left.

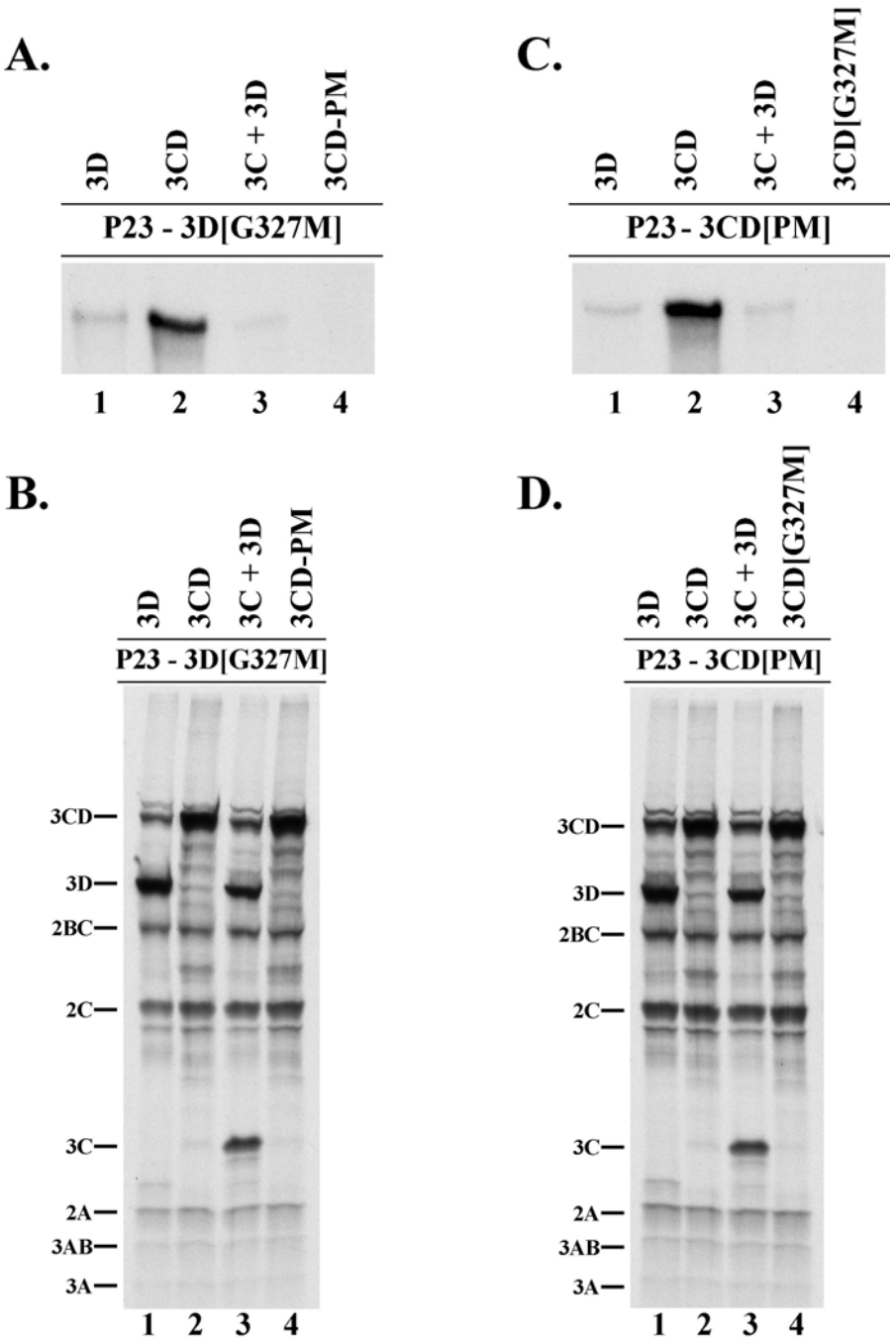

Figure 5-3. Complementation of 3D[G327M] or 3CD[PM] requires the intact $3CD^{pro}$ precursor. A & C) Negative-strand synthesis was assayed using PIRCs isolated from HeLa S10 reactions as described in Chapter 2. Reactions contained P23 RNA with a mutated 3CD coding region (3D[G327M] or 3CD[PM]) and a second complementing RNA expressing the indicated protein(s). All complementing RNAs contain the ΔGUA_3 mutation which inhibits negative-strand synthesis. Product RNA was analyzed by denaturing CH_3HgOH gel electrophoresis and autoradiography. B & D) A portion of the reactions described above was metabolically labeled with [^{35}S]methionine and these reactions were analyzed by SDS-PAGE and autoradiography. Viral proteins are indicated at left.

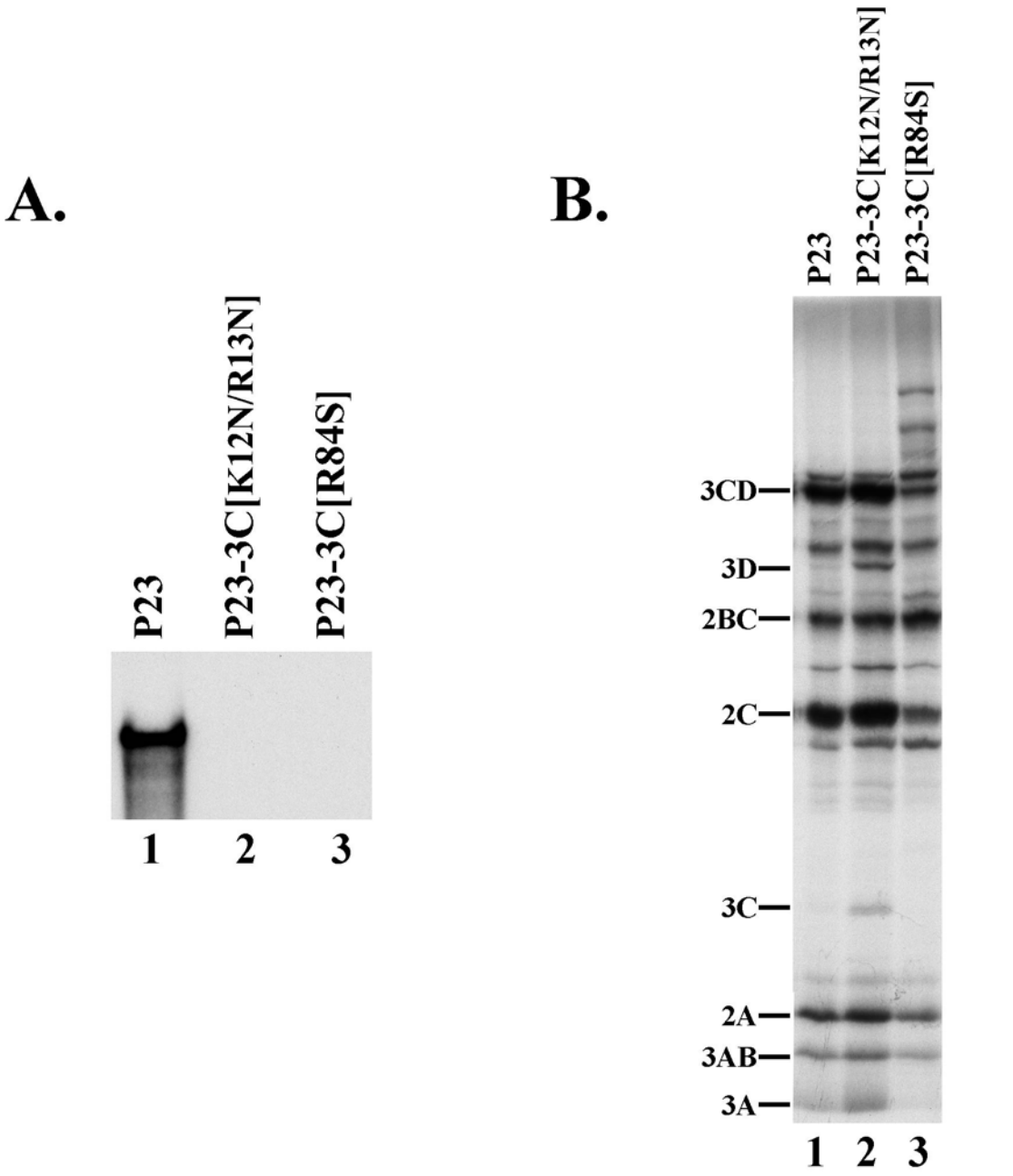

Figure 5-4. Mutations which disrupt $3C^{pro}$/$3CD^{pro}$ binding to the 5'CL block RNA replication. A) Negative-strand synthesis was assayed using PIRCs isolated from HeLa S10 reactions as described in Chapter 2. Reactions contained subgenomic P23 RNA containing either a wild-type or mutant 3C coding region (3C[K12N/R13N] or 3C[R84S]). RNA product was analyzed by denaturing CH_3HgOH gel electrophoresis and autoradiography. B) A portion of these reactions described was metabolically labeled with [^{35}S]methionine to assay for protein synthesis. These reactions were analyzed by SDS-PAGE and autoradiography. Viral proteins are indicated at left.

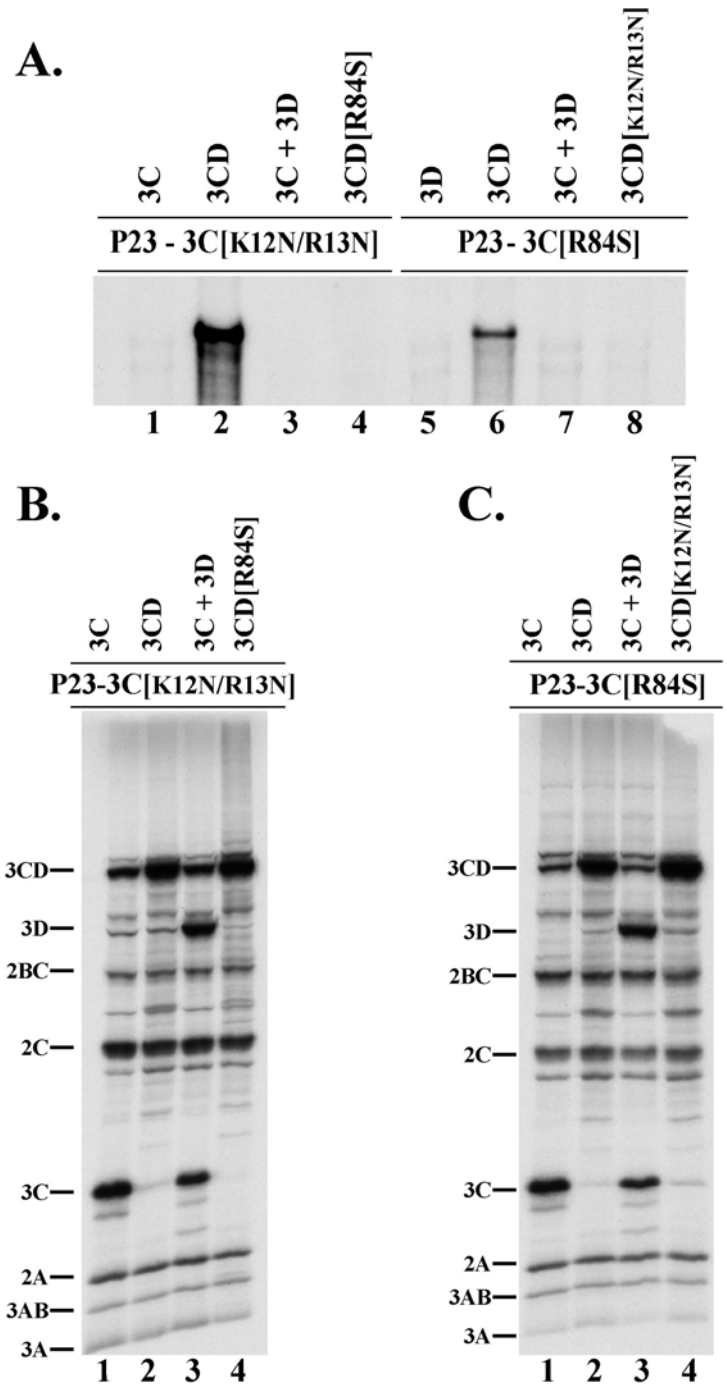

Figure 5-5. Complementation of 3C[K12N/R13N] or 3C[R84S] requires the intact $3CD^{pro}$ precursor. A) Negative-strand synthesis was assayed using PIRCs isolated from HeLa S10 reactions as described in Chapter 2. Reactions contained subgenomic P23 RNA containing a mutant 3C coding region (3C[K12N/R13N] or 3C[R84S]) and a second complementing RNA expressing the indicated protein(s). RNA product was analyzed by CH_3HgOH gel electrophoresis and autoradiography. B-C) A portion of the above reactions was metabolically labeled with [^{35}S]methionine to assay for protein synthesis. These reactions were analyzed by SDS-PAGE and autoradiography. Viral proteins are indicated at left.

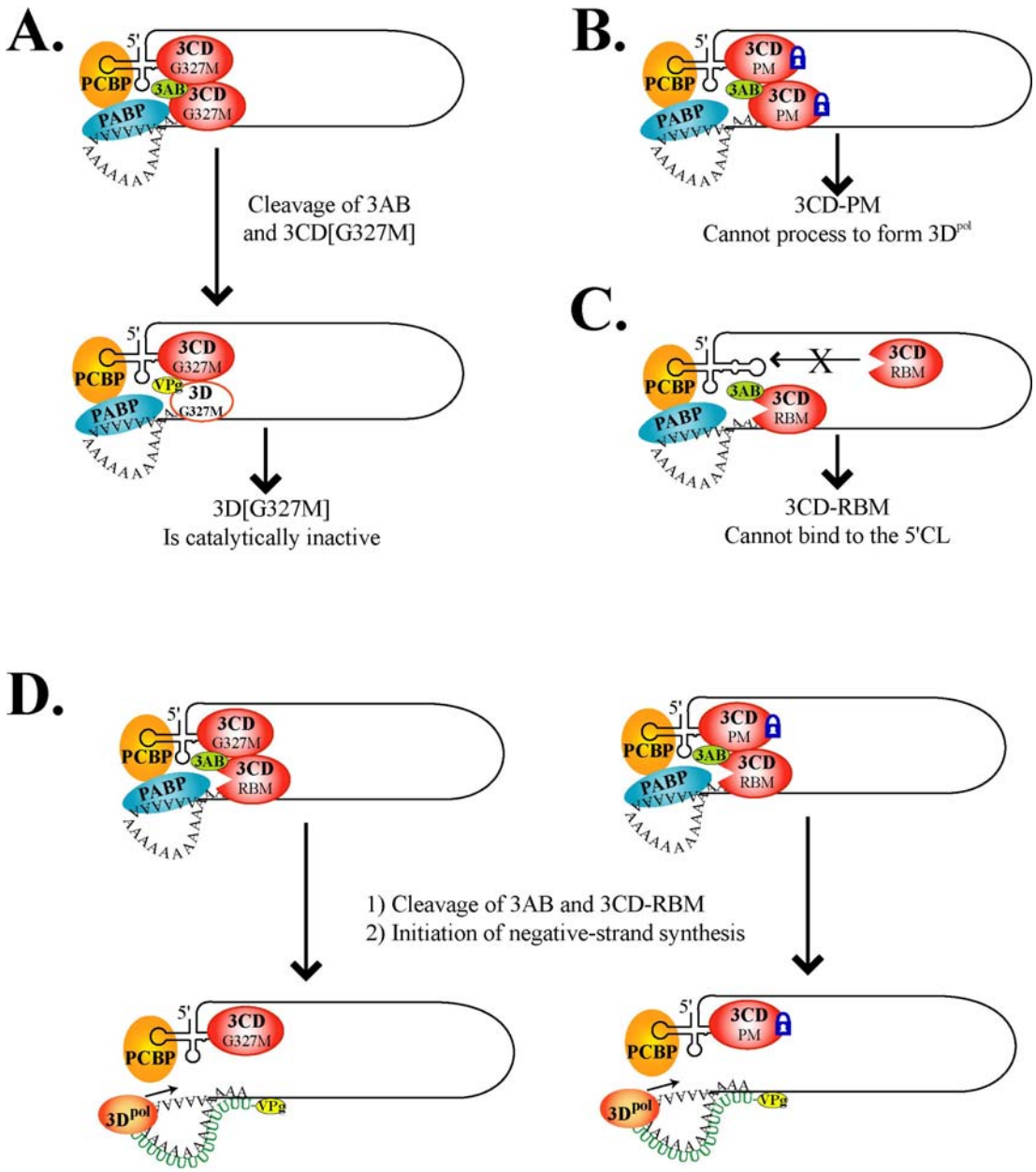

Figure 5-6. Schematic of *trans* complementation using two functionally distinct mutations in $3CD^{pro}$. A) In the presence of only 3CD[G327M], replication complexes could form and process, however, the $3D^{pol}$ generated is catalytically inactive and RNA replication is blocked. B) In the presence of processing mutant $3CD^{pro}$ (3CD[PM]), replication complexes could form, however, 3CD has no polymerase activity before it is processed. Since 3CD[PM] cannot process, negative-strand synthesis is blocked. C) In the presence of RNA binding mutant $3CD^{pro}$ (3CD[RBM]), the essential RNP complex at the 5'CL cannot be formed, and as a result, negative-strand synthesis is blocked. D) If a 3CD[RBM] is co-expressed with either 3CD[G327M] or 3CD[PM], the polymerase deficient precursor could bind the 5'CL and the RBM could provide the polymerase. This would allow initiation of negative-strand synthesis.

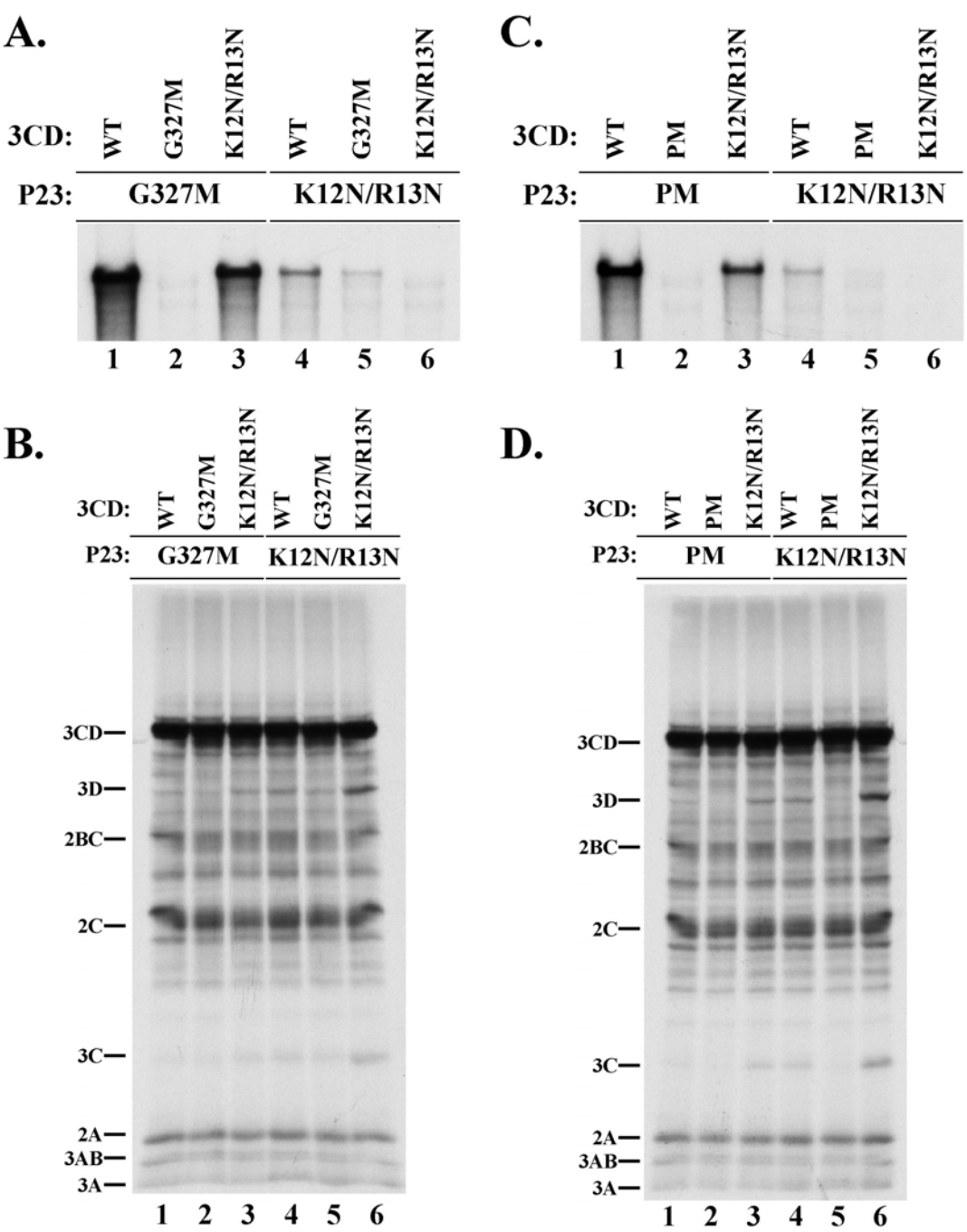

Figure 5-7. Two functionally distinct $3CD^{pro}$ mutants can complement each other in *trans*. A & C) Negative-strand synthesis was assayed using PIRCs isolated from HeLa S10 reactions as described in Chapter 2. Reactions contained P23 RNA with a mutated 3CD coding region (3D[G327M]/3CD[PM] or 3C[K12NR13N]) and a second complementing RNA expressing the indicated protein. All complementing RNAs contain the ΔGUA_3 mutation which inhibits negative-strand synthesis. Product RNA was analyzed by CH_3HgOH gel electrophoresis and autoradiography. B & D) A portion of the reactions described above was labeled with [^{35}S]methionine and analyzed by SDS-PAGE and autoradiography. Viral proteins are indicated at left.

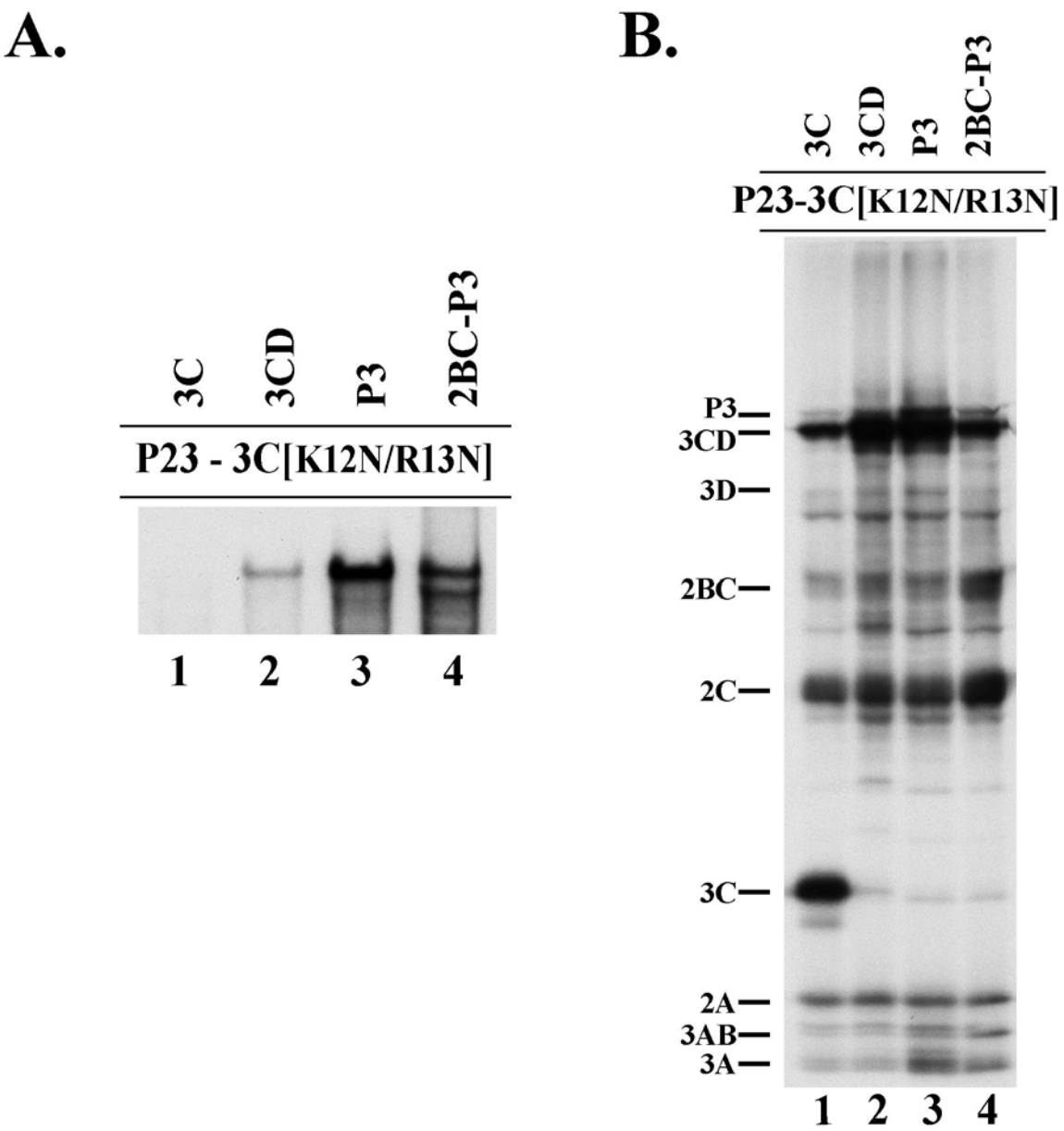

Figure 5-8. Complementation of a $3CD^{pro}$ RNA binding mutant is more efficient when P3 is provided in *trans*. A) Negative-strand synthesis was assayed using PIRCs isolated from HeLa S10 reactions as described in Chapter 2. Reactions contained P23[K12N/R13N] RNA and a second complementing RNA expressing 3C or 3C precursors of increasing size. All complementing RNAs contain the ΔGUA_3 mutation which inhibits negative-strand synthesis. Product RNA was analyzed by denaturing CH_3HgOH gel electrophoresis and autoradiography. B) A portion of the reactions described above was labeled with [^{35}S]methionine and these reactions were analyzed by SDS-PAGE and autoradiography. Viral proteins are indicated at left

CHAPTER 6
SUMMARY AND CONCLUSIONS

In this dissertation, I have presented and discussed the results from three distinct yet interconnected lines of investigation into the protein requirements for the initiation of poliovirus negative-strand RNA synthesis. Each of these studies has generated significant insight into how these key viral and cellular proteins function in PV replication complex assembly, and also to the broader understanding of the replication of related enteroviruses. Techniques developed to perform this work have already been applied to the study of other stages of the viral life cycle, including PV translation and *cre*(2C)-dependent VPg uridylylation, and will soon be adapted for characterization of Coxsackievirus B3 replication. Future work based on each of these lines of investigation will provide a more detailed understanding of the molecular mechanisms by which poliovirus, as well as other enteroviruses, regulate the critical steps of viral RNA replication.

The Role of PCBP in the Initiation of Poliovirus Negative-strand Synthesis

The first of the investigations presented herein probes the involvement of the multifunctional cellular protein PCBP in virus replication. To do so, our laboratory has developed and applied a novel protein-RNA tethering system to study of virus replication. Using this system we were able to confirm the activity of PCBP in supporting negative-strand synthesis and were further able to identify the functional domains within PCBP2. Morover, we were able to show that some, but not all members of the PCBP protein family can function in PV RNA replication. In future studies, these evolutionarily related, but functionally distinct isoforms can be used to direct more detailed mutagenic studies of the individual functional domains. This approach, in combination with the $(MS2)_2$ protein-RNA tethering system, can then be used to more precisely define the protein-protein interaction surfaces and binding partner critical to PCBP's ability to promote negative-strand synthesis.

The $(MS2)_2$ Protein-RNA Tethering System: Virus-Host Interaction

A defining characteristic of a virus is its ability to commandeer its host cell and subvert the cellular machinery for its own replication. The $(MS2)_2$ protein-RNA tethering system used in this study provides an ideal framework for additional studies on virus-host interactions critical to the understanding of virus replication and cellular protein functions therein. The specific integration of key host proteins into defined steps in the viral life cycle relieves the need of the viral genome to encode such proteins, but also functions as a post-entry determinant in cell tropism. For viruses like poliovirus which infect multiple distinct cell types, these cellular protein determinants could function as replicative rheostats, allowing the virus to tailor its replication to the cell type it has infected. These unique interactions between viral and cellular proteins are also very attractive antiviral drug targets, particularly given that cellular protein evolution is not subject to the same selective pressures as viral proteins.

The $(MS2)_2$ Protein-RNA Tethering System: Host Protein Function

An appealing extension to the $(MS2)_2$ protein-RNA tethering system, in addition to the generalized study of host protein involvement in the replication of other RNA viruses, is the potential to better understand the normal cellular role of these key proteins. Viral systems serve as microcosms for complex host cell processes, and have provided the foundation for much of our current understanding of cellular biology. DNA replication, mRNA splicing, innate immunity, endocytosis, oncogenesis, and apoptosis are among the many cellular processes initially characterized using viruses or virus-based approaches. Likewise, by understanding precisely how key cellular proteins are exploited during virus infection, we can better understand their role in cellular processes and in the global regulatory networks in which they often participate. This work would also extend to the role of these critical proteins in disease states, some of which may be directly related to virus infection. Dysregulation of PCBP regulated

mRNAs has been linked to liver cirrhosis, cervical cancer, and cardiomyopathy (123, 169, 191, 198). Interestingly, each of these conditions can also result from infection by a virus that utilizes PCBP during its replication: Hepatitis C Virus (HCV), Human Papillomavirus (HPV), and Coxsackievirus B (CVB), respectively. These all serve as examples of complex disease states where critical protein-protein and/or protein-RNA interactions could be initially examined in a simplified context, using a virus or virus-based system in combination with the $(MS2)_2$ tethered function system.

The Role of Viral Protein Precursors in the Initiation of PV Negative-strand Synthesis

Modeling Formation of the PV RNA Replication Complex

The second and third lines of investigation both deal with the critical role of distinct viral polyprotein precursors in the initiation of poliovirus negative-strand RNA synthesis. Firstly, we examine the molecular basis for the requirement of genomic translation in *cis* to promote efficient initiation of negative-strand synthesis. Using *trans* complementation assays, we showed that the activity of a protein precursor, rather than physical ribosome transit, was responsible for the observed *cis* enhancement of negative-strand synthesis. Further, we identified the critical *cis*-acting precursor as 2BC-P3 and generated a model of replication complex formation which accounts for this requirement. This model is able to account for the previously observed coupling between genomic translation and RNA replication observed in infected/transfected cells, as well as other previously reported protein complementation studies from our lab.

The last line of investigation also utilized *trans* complementation assays in combination with functionally defined mutants of the multifunctional viral precursor $3CD^{pro}$. Using this approach, we defined the functional polyprotein precursor of the active polymerase in the replication complex to be $3CD^{pro}$, however we showed that the preferred precursor utilized to

form the essential 5'CL RNP complex was P3. These experiments also validated the current model for initiation of negative-strand synthesis, which depicts two functionally discrete $3CD^{pro}$ polypeptides within the PV replication complex. This study allowed us to enrich our model of PV replication complex formation to include greater detail as to the source of protein precursors which form the critical 5'CL RNP complex, provide the VPg primer for RNA synthesis, and generate active $3D^{pol}$.

Close Coupling of the Viral Life-Cycle Ensures Viral Fitness

Both of these studies, in addition to defining critical components of the PV replication complex, also illustrate the tightly coupled nature of viral replication. In most cases, complementation in *trans* of a viral protein supports significantly lower levels of negative-strand RNA synthesis than would be observed if that protein was provided in *cis*. The evolutionary imperative to tightly couple the different stages of the viral life-cycle stems from the complexity inherent in coordinating a very intricate sequence of events in the context of the chaotic milieu of a host cell, in the face of extensive innate anti-viral defenses. This task is only complicated further by the high mutation rates exhibited by RNA viruses and the need to counter-balance the increased speed of viral evolution with extensive genomic quality control. However, by doing this, a virus ensures replication of complete genomes encoding fully functional proteins to the exclusion of incomplete or defective genomes, preventing the wasteful use of valuable cellular resources. Poliovirus, like other small RNA viruses, maximizes protein function using limited genomic sequence space by encoding a single large polyprotein and utilizing each unique precursor within the protein processing cascade. It now also appears that polyprotein processing also contains within it the intrinsic ability to tightly couple *cis* translation of PV RNA and subsequent replication complex formation. This coupling functions as a critical replication checkpoint, a penultimate guarantee that the PV template RNA about to be replicated encodes a

functional set of essential replication proteins, ensuring efficient RNA replication and evolutionary maintenance of viral fitness.

LIST OF REFERENCES

1. 2005. Poliomyelitis outbreak escalates in the Sudan. Wkly.Epidemiol.Rec. **80**:2-3.

2. 2005. Poliomyelitis outbreak spreads across Yemen; case confirmed in Indonesia. Wkly.Epidemiol.Rec. **80**:157-158.

3. 2009. Resurgence of wild poliovirus types 1 and 3 in 15 African countries, January 2008-March 2009. Wkly.Epidemiol.Rec. **84**:133-140.

4. 2009. Wild poliovirus type 1 and type 3 importations--15 countries, Africa, 2008-2009. MMWR Morb.Mortal.Wkly.Rep. **58**:357-362.

5. **Ackermann, W. W., A. Rabson, and H. Kurtz**. 1954. Growth characteristics of poliomyelitis virus in HeLa cell cultures; lack of parallelism in cellular injury and virus increase. J.Exp.Med. **100**:437-450.

6. **Adams, D. J., D. J. Beveridge, W. L. van der, H. Mangs, P. J. Leedman, and B. J. Morris**. 2003. HADHB, HuR, and CP1 bind to the distal 3'-untranslated region of human renin mRNA and differentially modulate renin expression. J.Biol.Chem. **278**:44894-44903.

7. **Agol, V. I., G. A. Belov, K. Bienz, D. Egger, M. S. Kolesnikova, N. T. Raikhlin, L. I. Romanova, E. A. Smirnova, and E. A. Tolskaya**. 1998. Two types of death of poliovirus-infected cells: caspase involvement in the apoptosis but not cytopathic effect. Virology **252**:343-353.

8. **Aldabe, R., A. Barco, and L. Carrasco**. 1996. Membrane permeabilization by poliovirus proteins 2B and 2BC. J.Biol.Chem. **271**:23134-23137.

9. **Aldabe, R. and L. Carrasco**. 1995. Induction of membrane proliferation by poliovirus proteins 2C and 2BC. Biochem.Biophys.Res.Commun. **206**:64-76.

10. **Ambros, V. and D. Baltimore**. 1978. Protein is linked to the 5' end of poliovirus RNA by a phosphodiester linkage to tyrosine. J.Biol.Chem. **253**:5263-5266.

11. **Ambros, V. and D. Baltimore**. 1980. Purification and properties of a HeLa cell enzyme able to remove the 5'-terminal protein from poliovirus RNA. J.Biol.Chem. **255**:6739-6744.

12. **Andino, R., G. E. Rieckhof, P. L. Achacoso, and D. Baltimore**. 1993. Poliovirus RNA synthesis utilizes an RNP complex formed around the 5'-end of viral RNA. EMBO J. **12**:3587-3598.

13. **Andino, R., G. E. Rieckhof, and D. Baltimore**. 1990. A functional ribonucleoprotein complex forms around the 5' end of poliovirus RNA. Cell **63**:369-380.

14. **Andino, R., G. E. Rieckhof, D. Trono, and D. Baltimore**. 1990. Substitutions in the protease (3Cpro) gene of poliovirus can suppress a mutation in the 5' noncoding region. J.Virol. **64**:607-612.

15. **Arnold, E., M. Luo, G. Vriend, M. G. Rossmann, A. C. Palmenberg, G. D. Parks, M. J. Nicklin, and E. Wimmer**. 1987. Implications of the picornavirus capsid structure for polyprotein processing. Proc.Natl.Acad.Sci.U.S.A **84**:21-25.

16. **Autret, A., S. Martin-Latil, L. Mousson, A. Wirotius, F. Petit, D. Arnoult, F. Colbere-Garapin, J. Estaquier, and B. Blondel**. 2007. Poliovirus induces Bax-dependent cell death mediated by c-Jun NH2-terminal kinase. J.Virol. **81**:7504-7516.

17. **Baltera, R. F., Jr. and D. R. Tershak**. 1989. Guanidine-resistant mutants of poliovirus have distinct mutations in peptide 2C. J.Virol. **63**:4441-4444.

18. **Banerjee, R., A. Echeverri, and A. Dasgupta**. 1997. Poliovirus-encoded 2C polypeptide specifically binds to the 3'-terminal sequences of viral negative-strand RNA. J.Virol. **71**:9570-9578.

19. **Banerjee, R., W. Tsai, W. Kim, and A. Dasgupta**. 2001. Interaction of poliovirus-encoded 2C/2BC polypeptides with the 3' terminus negative-strand cloverleaf requires an intact stem-loop b. Virology **280**:41-51.

20. **Barco, A. and L. Carrasco**. 1995. A human virus protein, poliovirus protein 2BC, induces membrane proliferation and blocks the exocytic pathway in the yeast Saccharomyces cerevisiae. EMBO J. **14**:3349-3364.

21. **Barton, D. J., E. P. Black, and J. B. Flanegan**. 1995. Complete replication of poliovirus in vitro: preinitiation RNA replication complexes require soluble cellular factors for the synthesis of VPg-linked RNA. J.Virol. **69**:5516-5527.

22. **Barton, D. J. and J. B. Flanegan**. 1993. Coupled translation and replication of poliovirus RNA in vitro: synthesis of functional 3D polymerase and infectious virus. J.Virol. **67**:822-831.

23. **Barton, D. J. and J. B. Flanegan**. 1997. Synchronous replication of poliovirus RNA: initiation of negative-strand RNA synthesis requires the guanidine-inhibited activity of protein 2C. J.Virol. **71**:8482-8489.

24. **Barton, D. J., B. J. Morasco, and J. B. Flanegan**. 1996. Assays for poliovirus polymerase, 3D(Pol), and authentic RNA replication in HeLa S10 extracts. Methods Enzymol. **275**:35-57.

25. **Barton, D. J., B. J. Morasco, L. E. Smerage, and J. B. Flanegan**. 2002. Poliovirus RNA Replication and Genetic Complementation in Cell-Free Reactions, p. 461-469. *In* B. L. Semler and E. Wimmer (eds.), Molecular Biology of Picornaviruses. ASM Press, Washington, D.C.

26. **Barton, D. J., B. J. O'Donnell, and J. B. Flanegan**. 2001. 5' cloverleaf in poliovirus RNA is a cis-acting replication element required for negative-strand synthesis. EMBO J. **20**:1439-1448.

27. **Basavappa, R., R. Syed, O. Flore, J. P. Icenogle, D. J. Filman, and J. M. Hogle**. 1994. Role and mechanism of the maturation cleavage of VP0 in poliovirus assembly: structure of the empty capsid assembly intermediate at 2.9 A resolution. Protein Sci. **3**:1651-1669.

28. **Bedard, K. M., S. Daijogo, and B. L. Semler**. 2007. A nucleo-cytoplasmic SR protein functions in viral IRES-mediated translation initiation. EMBO J. **26**:459-467.

29. **Bedard, K. M., B. L. Walter, and B. L. Semler**. 2004. Multimerization of poly(rC) binding protein 2 is required for translation initiation mediated by a viral IRES. RNA. **10**:1266-1276.

30. **Belov, G. A., A. G. Evstafieva, Y. P. Rubtsov, O. V. Mikitas, A. B. Vartapetian, and V. I. Agol**. 2000. Early alteration of nucleocytoplasmic traffic induced by some RNA viruses. Virology **275**:244-248.

31. **Belov, G. A., P. V. Lidsky, O. V. Mikitas, D. Egger, K. A. Lukyanov, K. Bienz, and V. I. Agol**. 2004. Bidirectional increase in permeability of nuclear envelope upon poliovirus infection and accompanying alterations of nuclear pores. J.Virol. **78**:10166-10177.

32. **Bergamini, G., T. Preiss, and M. W. Hentze**. 2000. Picornavirus IRESes and the poly(A) tail jointly promote cap-independent translation in a mammalian cell-free system. RNA. **6**:1781-1790.

33. **Bergmann, E. M., S. C. Mosimann, M. M. Chernaia, B. A. Malcolm, and M. N. James**. 1997. The refined crystal structure of the 3C gene product from hepatitis A virus: specific proteinase activity and RNA recognition. J.Virol. **71**:2436-2448.

34. **Bienz, K., D. Egger, and L. Pasamontes**. 1987. Association of polioviral proteins of the P2 genomic region with the viral replication complex and virus-induced membrane synthesis as visualized by electron microscopic immunocytochemistry and autoradiography. Virology **160**:220-226.

35. **Bienz, K., D. Egger, Y. Rasser, and W. Bossart**. 1983. Intracellular distribution of poliovirus proteins and the induction of virus-specific cytoplasmic structures. Virology **131**:39-48.

36. **Blair, W. S., T. B. Parsley, H. P. Bogerd, J. S. Towner, B. L. Semler, and B. R. Cullen**. 1998. Utilization of a mammalian cell-based RNA binding assay to characterize the RNA binding properties of picornavirus 3C proteinases. RNA. **4**:215-225.

37. **Blom, N., J. Hansen, D. Blaas, and S. Brunak**. 1996. Cleavage site analysis in picornaviral polyproteins: discovering cellular targets by neural networks. Protein Sci. **5**:2203-2216.

38. **Blyn, L. B., J. S. Towner, B. L. Semler, and E. Ehrenfeld**. 1997. Requirement of poly(rC) binding protein 2 for translation of poliovirus RNA. J.Virol. **71**:6243-6246.

39. **Brandenburg, B., L. Y. Lee, M. Lakadamyali, M. J. Rust, X. Zhuang, and J. M. Hogle**. 2007. Imaging Poliovirus Entry in Live Cells. PLoS.Biol. **5**:e183.

40. **Brunner, J. E., J. H. Nguyen, H. H. Roehl, T. V. Ho, K. M. Swiderek, and B. L. Semler**. 2005. Functional interaction of heterogeneous nuclear ribonucleoprotein C with poliovirus RNA synthesis initiation complexes. J.Virol. **79**:3254-3266.

41. **Bubeck, D., D. J. Filman, N. Cheng, A. C. Steven, J. M. Hogle, and D. M. Belnap**. 2005. The structure of the poliovirus 135S cell entry intermediate at 10-angstrom resolution reveals the location of an externalized polypeptide that binds to membranes. J.Virol. **79**:7745-7755.

42. **Bubeck, D., D. J. Filman, and J. M. Hogle**. 2005. Cryo-electron microscopy reconstruction of a poliovirus-receptor-membrane complex. Nat.Struct.Mol.Biol. **12**:615-618.

43. **Caliguiri, L. A. and R. W. Compans**. 1973. The formation of poliovirus particles in association with the RNA replication complexes. J.Gen.Virol. **21**:99-108.

44. **Caliguiri, L. A. and I. Tamm**. 1969. Membranous structures associated with translation and transcription of poliovirus RNA. Science **166**:885-886.

45. **Caliguiri, L. A. and I. Tamm**. 1970. Characterization of poliovirus-specific structures associated with cytoplasmic membranes. Virology **42**:112-122.

46. **Cao, X. and E. Wimmer**. 1995. Intragenomic complementation of a 3AB mutant in dicistronic polioviruses. Virology **209**:315-326.

47. **Carey, J., P. T. Lowary, and O. C. Uhlenbeck**. 1983. Interaction of R17 coat protein with synthetic variants of its ribonucleic acid binding site. Biochemistry **22**:4723-4730.

48. **Chkheidze, A. N. and S. A. Liebhaber**. 2003. A novel set of nuclear localization signals determine distributions of the alphaCP RNA-binding proteins. Mol.Cell Biol. **23**:8405-8415.

49. **Chkheidze, A. N., D. L. Lyakhov, A. V. Makeyev, J. Morales, J. Kong, and S. A. Liebhaber**. 1999. Assembly of the alpha-globin mRNA stability complex reflects binary interaction between the pyrimidine-rich 3' untranslated region determinant and poly(C) binding protein αCP. Mol.Cell Biol. **19**:4572-4581.

50. **Cho, M. W., N. Teterina, D. Egger, K. Bienz, and E. Ehrenfeld**. 1994. Membrane rearrangement and vesicle induction by recombinant poliovirus 2C and 2BC in human cells. Virology **202**:129-145.

51. **Choe, S. S. and K. Kirkegaard**. 2004. Intracellular topology and epitope shielding of poliovirus 3A protein. J.Virol. **78**:5973-5982.

52. **Choi, W. S., R. Pal-Ghosh, and C. D. Morrow**. 1991. Expression of human immunodeficiency virus type 1 (HIV-1) gag, pol, and env proteins from chimeric HIV-1-poliovirus minireplicons. J.Virol. **65**:2875-2883.

53. **Claridge, J. K., S. J. Headey, J. Y. Chow, M. Schwalbe, P. J. Edwards, C. M. Jeffries, H. Venugopal, J. Trewhella, and S. M. Pascal**. 2009. A picornaviral loop-to-loop replication complex. J.Struct.Biol. **166**:251-262.

54. **Clark, M. E., T. Hammerle, E. Wimmer, and A. Dasgupta**. 1991. Poliovirus proteinase 3C converts an active form of transcription factor IIIC to an inactive form: a mechanism for inhibition of host cell polymerase III transcription by poliovirus. EMBO J. **10**:2941-2947.

55. **Clark, M. E., P. M. Lieberman, A. J. Berk, and A. Dasgupta**. 1993. Direct cleavage of human TATA-binding protein by poliovirus protease 3C in vivo and in vitro. Mol.Cell Biol. **13**:1232-1237.

56. **Coller, J. and R. Parker**. 2004. Eukaryotic mRNA decapping. Annu.Rev.Biochem. **73**:861-890.

57. **Coller, J. and M. Wickens**. 2002. Tethered function assays using 3' untranslated regions. Methods **26**:142-150.

58. **Coller, J. M., N. K. Gray, and M. P. Wickens**. 1998. mRNA stabilization by poly(A) binding protein is independent of poly(A) and requires translation. Genes Dev. **12**:3226-3235.

59. **Collett, M. S., J. Neyts, and J. F. Modlin**. 2008. A case for developing antiviral drugs against polio. Antiviral Res. **79**:179-187.

60. **Collier, B., L. Goobar-Larsson, M. Sokolowski, and S. Schwartz**. 1998. Translational inhibition in vitro of human papillomavirus type 16 L2 mRNA mediated through interaction with heterogenous ribonucleoprotein K and poly(rC)-binding proteins 1 and 2. J.Biol.Chem. **273**:22648-22656.

61. **Collis, P. S., B. J. O'Donnell, D. J. Barton, J. A. Rogers, and J. B. Flanegan**. 1992. Replication of poliovirus RNA and subgenomic RNA transcripts in transfected cells. J.Virol. **66**:6480-6488.

62. **Cornell, C. T., J. E. Brunner, and B. L. Semler**. 2004. Differential rescue of poliovirus RNA replication functions by genetically modified RNA polymerase precursors. J.Virol. **78**:13007-13018.

63. **Coyne, C. B., K. S. Kim, and J. M. Bergelson**. 2007. Poliovirus entry into human brain microvascular cells requires receptor-induced activation of SHP-2. EMBO J. **26**:4016-4028.

64. **Czyzyk-Krzeska, M. F. and A. C. Bendixen**. 1999. Identification of the poly(C) binding protein in the complex associated with the 3' untranslated region of erythropoietin messenger RNA. Blood **93**:2111-2120.

65. **Dejgaard, K. and H. Leffers**. 1996. Characterisation of the nucleic-acid-binding activity of KH domains. Different properties of different domains. Eur.J.Biochem. **241**:425-431.

66. **Dildine, S. L. and B. L. Semler**. 1992. Conservation of RNA-protein interactions among picornaviruses. J.Virol. **66**:4364-4376.

67. **Du, Z., J. K. Lee, S. Fenn, R. Tjhen, R. M. Stroud, and T. L. James**. 2007. X-ray crystallographic and NMR studies of protein-protein and protein-nucleic acid interactions involving the KH domains from human poly(C)-binding protein-2. RNA. **13**:1043-1051.

68. **Du, Z., J. K. Lee, R. Tjhen, S. Li, H. Pan, R. M. Stroud, and T. L. James**. 2005. Crystal structure of the first KH domain of human poly(C)-binding protein-2 in complex with a C-rich strand of human telomeric DNA at 1.7 A. J.Biol.Chem. **280**:38823-38830.

69. **Dutta, A.** 2008. Epidemiology of poliomyelitis--options and update. Vaccine **26**:5767-5773.

70. **Egger, D. and K. Bienz**. 2005. Intracellular location and translocation of silent and active poliovirus replication complexes. J.Gen.Virol. **86**:707-718.

71. **Egger, D., N. Teterina, E. Ehrenfeld, and K. Bienz**. 2000. Formation of the poliovirus replication complex requires coupled viral translation, vesicle production, and viral RNA synthesis. J.Virol. **74**:6570-6580.

72. **Etchison, D., S. C. Milburn, I. Edery, N. Sonenberg, and J. W. Hershey**. 1982. Inhibition of HeLa cell protein synthesis following poliovirus infection correlates with the proteolysis of a 220,000-dalton polypeptide associated with eucaryotic initiation factor 3 and a cap binding protein complex. J.Biol.Chem. **257**:14806-14810.

73. **Flanegan, J. B. and D. Baltimore**. 1979. Poliovirus polyuridylic acid polymerase and RNA replicase have the same viral polypeptide. J.Virol. **29**:352-360.

74. **Flanegan, J. B. and T. A. Van Dyke**. 1979. Isolation of a soluble and template-dependent poliovirus RNA polymerase that copies virion RNA in vitro. J.Virol. **32**:155-161.

75. **Fricks, C. E. and J. M. Hogle**. 1990. Cell-induced conformational change in poliovirus: externalization of the amino terminus of VP1 is responsible for liposome binding. J.Virol. **64**:1934-1945.

76. **Funke, B., B. Zuleger, R. Benavente, T. Schuster, M. Goller, J. Stevenin, and I. Horak**. 1996. The mouse poly(C)-binding protein exists in multiple isoforms and interacts with several RNA-binding proteins. Nucleic Acids Res. **24**:3821-3828.

77. **Gamarnik, A. V. and R. Andino**. 1997. Two functional complexes formed by KH domain containing proteins with the 5' noncoding region of poliovirus RNA. RNA. **3**:882-892.

78. **Gamarnik, A. V. and R. Andino**. 1998. Switch from translation to RNA replication in a positive-stranded RNA virus. Genes Dev. **12**:2293-2304.

79. **Gamarnik, A. V. and R. Andino**. 2000. Interactions of viral protein 3CD and poly(rC) binding protein with the 5' untranslated region of the poliovirus genome. J.Virol. **74**:2219-2226.

80. **Gibson, T. J., J. D. Thompson, and J. Heringa**. 1993. The KH domain occurs in a diverse set of RNA-binding proteins that include the antiterminator NusA and is probably involved in binding to nucleic acid. FEBS Lett. **324**:361-366.

81. **Gordon, C. and S. Toze**. 2003. Influence of groundwater characteristics on the survival of enteric viruses. J.Appl.Microbiol. **95**:536-544.

82. **Gradi, A., Y. V. Svitkin, H. Imataka, and N. Sonenberg**. 1998. Proteolysis of human eukaryotic translation initiation factor eIF4GII, but not eIF4GI, coincides with the shutoff of host protein synthesis after poliovirus infection. Proc.Natl.Acad.Sci.U.S.A **95**:11089-11094.

83. **Graff, J., J. Cha, L. B. Blyn, and E. Ehrenfeld**. 1998. Interaction of poly(rC) binding protein 2 with the 5' noncoding region of hepatitis A virus RNA and its effects on translation. J.Virol. **72**:9668-9675.

84. **Gustin, K. E. and P. Sarnow**. 2001. Effects of poliovirus infection on nucleo-cytoplasmic trafficking and nuclear pore complex composition. EMBO J. **20**:240-249.

85. **Hagino-Yamagishi, K. and A. Nomoto**. 1989. In vitro construction of poliovirus defective interfering particles. J.Virol. **63**:5386-5392.

86. **Hansen, J. L., A. M. Long, and S. C. Schultz**. 1997. Structure of the RNA-dependent RNA polymerase of poliovirus. Structure. **5**:1109-1122.

87. **Harber, J., G. Bernhardt, H. H. Lu, J. Y. Sgro, and E. Wimmer**. 1995. Canyon rim residues, including antigenic determinants, modulate serotype-specific binding of polioviruses to mutants of the poliovirus receptor. Virology **214**:559-570.

88. **Harris, K. S., S. R. Reddigari, M. J. Nicklin, T. Hammerle, and E. Wimmer**. 1992. Purification and characterization of poliovirus polypeptide 3CD, a proteinase and a precursor for RNA polymerase. J.Virol. **66**:7481-7489.

89. **Harris, K. S., W. Xiang, L. Alexander, W. S. Lane, A. V. Paul, and E. Wimmer**. 1994. Interaction of poliovirus polypeptide 3CDpro with the 5' and 3' termini of the poliovirus genome. Identification of viral and cellular cofactors needed for efficient binding. J.Biol.Chem. **269**:27004-27014.

90. **Hellen, C. U. and P. Sarnow**. 2001. Internal ribosome entry sites in eukaryotic mRNA molecules. Genes Dev. **15**:1593-1612.

91. **Hellen, C. U. and E. Wimmer**. 1992. Maturation of poliovirus capsid proteins. Virology **187**:391-397.

92. **Herold, J. and R. Andino**. 2000. Poliovirus requires a precise 5' end for efficient positive-strand RNA synthesis. J.Virol. **74**:6394-6400.

93. **Herold, J. and R. Andino**. 2001. Poliovirus RNA replication requires genome circularization through a protein-protein bridge. Mol.Cell **7**:581-591.

94. **Hindiyeh, M., Q. H. Li, R. Basavappa, J. M. Hogle, and M. Chow**. 1999. Poliovirus mutants at histidine 195 of VP2 do not cleave VP0 into VP2 and VP4. J.Virol. **73**:9072-9079.

95. **Hobson, S. D., E. S. Rosenblum, O. C. Richards, K. Richmond, K. Kirkegaard, and S. C. Schultz**. 2001. Oligomeric structures of poliovirus polymerase are important for function. EMBO J. **20**:1153-1163.

96. **Hook, B., D. Bernstein, B. Zhang, and M. Wickens**. 2005. RNA-protein interactions in the yeast three-hybrid system: affinity, sensitivity, and enhanced library screening. RNA. **11**:227-233.

97. **Hyypia, T., T. Hovi, N. J. Knowles, and G. Stanway**. 1997. Classification of enteroviruses based on molecular and biological properties. J.Gen.Virol. **78 (Pt 1)**:1-11.

98. **Jablonski, S. A., M. Luo, and C. D. Morrow**. 1991. Enzymatic activity of poliovirus RNA polymerase mutants with single amino acid changes in the conserved YGDD amino acid motif. J.Virol. **65**:4565-4572.

99. **Jackson, R. J. and A. Kaminski**. 1995. Internal initiation of translation in eukaryotes: the picornavirus paradigm and beyond. RNA. **1**:985-1000.

100. **Jacobson, S. J., D. A. Konings, and P. Sarnow**. 1993. Biochemical and genetic evidence for a pseudoknot structure at the 3' terminus of the poliovirus RNA genome and its role in viral RNA amplification. J.Virol. **67**:2961-2971.

101. **Joachims, M., P. C. Van Breugel, and R. E. Lloyd**. 1999. Cleavage of poly(A)-binding protein by enterovirus proteases concurrent with inhibition of translation in vitro. J.Virol. **73**:718-727.

102. **Johannes, G., M. S. Carter, M. B. Eisen, P. O. Brown, and P. Sarnow**. 1999. Identification of eukaryotic mRNAs that are translated at reduced cap binding complex eIF4F concentrations using a cDNA microarray. Proc.Natl.Acad.Sci.U.S.A **96**:13118-13123.

103. **Johansen, L. K. and C. D. Morrow**. 2000. Inherent instability of poliovirus genomes containing two internal ribosome entry site (IRES) elements supports a role for the IRES in encapsidation. J.Virol. **74**:8335-8342.

104. **Jurgens, C. and J. B. Flanegan**. 2003. Initiation of poliovirus negative-strand RNA synthesis requires precursor forms of p2 proteins. J.Virol. **77**:1075-1083.

105. **Jurgens, C. K., D. J. Barton, N. Sharma, B. J. Morasco, S. A. Ogram, and J. B. Flanegan**. 2006. 2Apro is a multifunctional protein that regulates the stability, translation and replication of poliovirus RNA. Virology **345**:346-357.

106. **Kaplan, G. and V. R. Racaniello**. 1988. Construction and characterization of poliovirus subgenomic replicons. J.Virol. **62**:1687-1696.

107. **Kempf, B. J. and D. J. Barton**. 2008. Poly(rC) binding proteins and the 5' cloverleaf of uncapped poliovirus mRNA function during de novo assembly of polysomes. J.Virol. **82**:5835-5846.

108. **Kiledjian, M., C. T. DeMaria, G. Brewer, and K. Novick**. 1997. Identification of AUF1 (heterogeneous nuclear ribonucleoprotein D) as a component of the alpha-globin mRNA stability complex. Mol.Cell Biol. **17**:4870-4876.

109. **Kiledjian, M., X. Wang, and S. A. Liebhaber**. 1995. Identification of two KH domain proteins in the alpha-globin mRNP stability complex. EMBO J. **14**:4357-4364.

110. **Kim, J. H., B. Hahm, Y. K. Kim, M. Choi, and S. K. Jang**. 2000. Protein-protein interaction among hnRNPs shuttling between nucleus and cytoplasm. J.Mol.Biol. **298**:395-405.

111. **Koike, S., I. Ise, and A. Nomoto**. 1991. Functional domains of the poliovirus receptor. Proc.Natl.Acad.Sci.U.S.A **88**:4104-4108.

112. **Kong, J., X. Ji, and S. A. Liebhaber**. 2003. The KH-domain protein alpha CP has a direct role in mRNA stabilization independent of its cognate binding site. Mol.Cell Biol. **23**:1125-1134.

113. **Krausslich, H. G., M. J. Nicklin, C. K. Lee, and E. Wimmer**. 1988. Polyprotein processing in picornavirus replication. Biochimie **70**:119-130.

114. **Krug, M., P. L. de Haseth, and O. C. Uhlenbeck**. 1982. Enzymatic synthesis of a 21-nucleotide coat protein binding fragment of R17 ribonucleic acid. Biochemistry **21**:4713-4720.

115. **Kuge, S., I. Saito, and A. Nomoto**. 1986. Primary structure of poliovirus defective-interfering particle genomes and possible generation mechanisms of the particles. J.Mol.Biol. **192**:473-487.

116. **Kuyumcu-Martinez, N. M., M. E. Van Eden, P. Younan, and R. E. Lloyd**. 2004. Cleavage of poly(A)-binding protein by poliovirus 3C protease inhibits host cell translation: a novel mechanism for host translation shutoff. Mol.Cell Biol. **24**:1779-1790.

117. **Lama, J. and L. Carrasco**. 1996. Screening for membrane-permeabilizing mutants of the poliovirus protein 3AB. J.Gen.Virol. **77 (Pt 9)**:2109-2119.

118. **Laury-Kleintop, L. D., M. Tresini, and O. Hammond**. 2005. Compartmentalization of hnRNP-K during cell cycle progression and its interaction with calponin in the cytoplasm. J.Cell Biochem. **95**:1042-1056.

119. **Lawson, M. A. and B. L. Semler**. 1992. Alternate poliovirus nonstructural protein processing cascades generated by primary sites of 3C proteinase cleavage. Virology **191**:309-320.

120. **Lee, Y. F., A. Nomoto, B. M. Detjen, and E. Wimmer**. 1977. A protein covalently linked to poliovirus genome RNA. Proc.Natl.Acad.Sci.U.S.A **74**:59-63.

121. **Leffers, H., K. Dejgaard, and J. E. Celis**. 1995. Characterisation of two major cellular poly(rC)-binding human proteins, each containing three K-homologous (KH) domains. Eur.J.Biochem. **230**:447-453.

122. **Li, J. P. and D. Baltimore**. 1988. Isolation of poliovirus 2C mutants defective in viral RNA synthesis. J.Virol. **62**:4016-4021.

123. **Lindquist, J. N., W. F. Marzluff, and B. Stefanovic**. 2000. Fibrogenesis. III. Posttranscriptional regulation of type I collagen. Am.J.Physiol Gastrointest.Liver Physiol **279**:G471-G476.

124. **Liu, Y., D. Franco, A. V. Paul, and E. Wimmer**. 2007. Tyrosine 3 of poliovirus terminal peptide VPg(3B) has an essential function in RNA replication in the context of its precursor protein, 3AB. J.Virol. **81**:5669-5684.

125. **Lloyd, R. E., M. J. Grubman, and E. Ehrenfeld**. 1988. Relationship of p220 cleavage during picornavirus infection to 2A proteinase sequencing. J.Virol. **62**:4216-4223.

126. **Lyons, T., K. E. Murray, A. W. Roberts, and D. J. Barton**. 2001. Poliovirus 5'-Terminal Cloverleaf RNA Is Required in cis for VPg Uridylylation and the Initiation of Negative-Strand RNA Synthesis. J.Virol. **75**:10696-10708.

127. **Makeyev, A. V., A. N. Chkheidze, and S. A. Liebhaber**. 1999. A set of highly conserved RNA-binding proteins, alphaCP-1 and alphaCP-2, implicated in mRNA stabilization, are coexpressed from an intronless gene and its intron-containing paralog. J.Biol.Chem. **274**:24849-24857.

128. **Makeyev, A. V. and S. A. Liebhaber**. 2000. Identification of two novel mammalian genes establishes a subfamily of KH-domain RNA-binding proteins. Genomics **67**:301-316.

129. **Makeyev, A. V. and S. A. Liebhaber**. 2002. The poly(C)-binding proteins: a multiplicity of functions and a search for mechanisms. RNA. **8**:265-278.

130. **Marcotte, L. L., A. B. Wass, D. W. Gohara, H. B. Pathak, J. J. Arnold, D. J. Filman, C. E. Cameron, and J. M. Hogle**. 2007. Crystal structure of poliovirus 3CD protein: virally encoded protease and precursor to the RNA-dependent RNA polymerase. J.Virol. **81**:3583-3596.

131. **Martinez-Salas, E., A. Pacheco, P. Serrano, and N. Fernandez**. 2008. New insights into internal ribosome entry site elements relevant for viral gene expression. J.Gen.Virol. **89**:611-626.

132. **Matthews, D. A., W. W. Smith, R. A. Ferre, B. Condon, G. Budahazi, W. Sisson, J. E. Villafranca, C. A. Janson, H. E. McElroy, C. L. Gribskov, and .** 1994. Structure of human rhinovirus 3C protease reveals a trypsin-like polypeptide fold, RNA-binding site, and means for cleaving precursor polyprotein. Cell **77**:761-771.

133. **Matunis, M. J., W. M. Michael, and G. Dreyfuss**. 1992. Characterization and primary structure of the poly(C)-binding heterogeneous nuclear ribonucleoprotein complex K protein. Mol.Cell Biol. **12**:164-171.

134. **Mendelsohn, C. L., E. Wimmer, and V. R. Racaniello**. 1989. Cellular receptor for poliovirus: molecular cloning, nucleotide sequence, and expression of a new member of the immunoglobulin superfamily. Cell **56**:855-865.

135. **Michael, W. M., P. S. Eder, and G. Dreyfuss**. 1997. The K nuclear shuttling domain: a novel signal for nuclear import and nuclear export in the hnRNP K protein. EMBO J. **16**:3587-3598.

136. **Michel, Y. M., A. M. Borman, S. Paulous, and K. M. Kean**. 2001. Eukaryotic initiation factor 4G-poly(A) binding protein interaction is required for poly(A) tail-mediated stimulation of picornavirus internal ribosome entry segment-driven translation but not for x-mediated stimulation of hepatitis c virus translation. Mol.Cell Biol. **21**:4097-4109.

137. **Min, J. W., G. Haegeman, M. Ysebaert, and W. Fiers**. 1972. Nucleotide sequence of the gene coding for the bacteriophage MS2 coat protein. Nature **237**:82-88.

138. **Mirmomeni, M. H., P. J. Hughes, and G. Stanway**. 1997. An RNA tertiary structure in the 3' untranslated region of enteroviruses is necessary for efficient replication. J.Virol. **71**:2363-2370.

139. **Molla, A., A. V. Paul, M. Schmid, S. K. Jang, and E. Wimmer**. 1993. Studies on dicistronic polioviruses implicate viral proteinase 2Apro in RNA replication. Virology **196**:739-747.

140. **Molla, A., A. V. Paul, and E. Wimmer**. 1991. Cell-free, de novo synthesis of poliovirus. Science **254**:1647-1651.

141. **Morasco, B. J., N. Sharma, J. Parilla, and J. B. Flanegan**. 2003. Poliovirus cre(2C)-dependent synthesis of VPgpUpU is required for positive- but not negative-strand RNA synthesis. J.Virol. **77**:5136-5144.

142. **Mosimann, S. C., M. M. Cherney, S. Sia, S. Plotch, and M. N. James**. 1997. Refined X-ray crystallographic structure of the poliovirus 3C gene product. J.Mol.Biol. **273**:1032-1047.

143. **Murray, K. E. and D. J. Barton**. 2003. Poliovirus CRE-dependent VPg uridylylation is required for positive-strand RNA synthesis but not for negative-strand RNA synthesis. J.Virol. **77**:4739-4750.

144. **Murray, K. E., A. W. Roberts, and D. J. Barton**. 2001. Poly(rC) binding proteins mediate poliovirus mRNA stability. RNA. **7**:1126-1141.

145. **Netherton, C., K. Moffat, E. Brooks, and T. Wileman**. 2007. A guide to viral inclusions, membrane rearrangements, factories, and viroplasm produced during virus replication. Adv.Virus Res. **70**:101-182.

146. **Neu-Yilik, G. and A. E. Kulozik**. 2008. NMD: multitasking between mRNA surveillance and modulation of gene expression. Adv.Genet. **62**:185-243.

147. **Nishimura, K., K. Ueda, E. Guwanan, S. Sakakibara, E. Do, E. Osaki, K. Yada, T. Okuno, and K. Yamanishi**. 2004. A posttranscriptional regulator of Kaposi's sarcoma-associated herpesvirus interacts with RNA-binding protein PCBP1 and controls gene expression through the IRES. Virology **325**:364-378.

148. **Nomoto, A., A. Jacobson, Y. F. Lee, J. Dunn, and E. Wimmer**. 1979. Defective interfering particles of poliovirus: mapping of the deletion and evidence that the deletions in the genomes of DI(1), (2) and (3) are located in the same region. J.Mol.Biol. **128**:179-196.

149. **Nomoto, A., N. Kitamura, F. Golini, and E. Wimmer**. 1977. The 5'-terminal structures of poliovirion RNA and poliovirus mRNA differ only in the genome-linked protein VPg. Proc.Natl.Acad.Sci.U.S.A **74**:5345-5349.

150. **Novak, J. E. and K. Kirkegaard**. 1991. Improved method for detecting poliovirus negative strands used to demonstrate specificity of positive-strand encapsidation and the ratio of positive to negative strands in infected cells. J.Virol. **65**:3384-3387.

151. **Novak, J. E. and K. Kirkegaard**. 1994. Coupling between genome translation and replication in an RNA virus. Genes Dev. **8**:1726-1737.

152. **Nugent, C. I., K. L. Johnson, P. Sarnow, and K. Kirkegaard**. 1999. Functional coupling between replication and packaging of poliovirus replicon RNA. Journal of Virology **73**:427-435.

153. **O'Reilly, E. K. and C. C. Kao**. 1998. Analysis of RNA-dependent RNA polymerase structure and function as guided by known polymerase structures and computer predictions of secondary structure. Virology **252**:287-303.

154. **Ostareck, D. H., A. Ostareck-Lederer, M. Wilm, B. J. Thiele, M. Mann, and M. W. Hentze**. 1997. mRNA silencing in erythroid differentiation: hnRNP K and hnRNP E1 regulate 15-lipoxygenase translation from the 3' end. Cell **89**:597-606.

155. **Pallansch, M. A., O. M. Kew, B. L. Semler, D. R. Omilianowski, C. W. Anderson, E. Wimmer, and R. R. Rueckert**. 1984. Protein processing map of poliovirus. J.Virol. **49**:873-880.

156. **Palmenberg, A. C.** 1990. Proteolytic processing of picornaviral polyprotein. Annu.Rev.Microbiol. **44**:603-623.

157. **Parsley, T. B., C. T. Cornell, and B. L. Semler**. 1999. Modulation of the RNA binding and protein processing activities of poliovirus polypeptide 3CD by the viral RNA polymerase domain. J.Biol.Chem. **274**:12867-12876.

158. **Parsley, T. B., J. S. Towner, L. B. Blyn, E. Ehrenfeld, and B. L. Semler**. 1997. Poly (rC) binding protein 2 forms a ternary complex with the 5'-terminal sequences of poliovirus RNA and the viral 3CD proteinase. RNA. **3**:1124-1134.

159. **Pathak, H. B., H. S. Oh, I. G. Goodfellow, J. J. Arnold, and C. E. Cameron**. 2008. Picornavirus genome replication: roles of precursor proteins and rate-limiting steps in oriI-dependent VPg uridylylation. J.Biol.Chem. **283**:30677-30688.

160. **Paul, A. V., J. Mugavero, A. Molla, and E. Wimmer**. 1998. Internal ribosomal entry site scanning of the poliovirus polyprotein: implications for proteolytic processing. Virology **250**:241-253.

161. **Paul, A. V., J. Yin, J. Mugavero, E. Rieder, Y. Liu, and E. Wimmer**. 2003. A "Slide-back" mechanism for the Initiation of protein-primed RNA synthesis by the RNA polymerase of poliovirus. J.Biol.Chem.

162. **Paulding, W. R. and M. F. Czyzyk-Krzeska**. 1999. Regulation of tyrosine hydroxylase mRNA stability by protein-binding, pyrimidine-rich sequence in the 3'-untranslated region. J.Biol.Chem. **274**:2532-2538.

163. **Peabody, D. S. and F. Lim**. 1996. Complementation of RNA binding site mutations in MS2 coat protein heterodimers. Nucleic Acids Res. **24**:2352-2359.

164. **Pelletier, J. and N. Sonenberg**. 1988. Internal initiation of translation of eukaryotic mRNA directed by a sequence derived from poliovirus RNA. Nature **334**:320-325.

165. **Perera, R., S. Daijogo, B. L. Walter, J. H. C. Nguyen, and B. L. Semler**. 2007. Cellular protein modification by poliovirus: The two faces of Poly(rC)-binding protein. Journal of Virology **81**:8919-8932.

166. **Perez Bercoff R. and M. Gander**. 1978. In vitro translation of mengovirus RNA deprived of the terminally-linked (capping?) protein. FEBS Lett. **96**:306-312.

167. **Pfister, T., D. Egger, and K. Bienz**. 1995. Poliovirus subviral particles associated with progeny RNA in the replication complex. J.Gen.Virol. **76 (Pt 1)**:63-71.

168. **Pilipenko, E. V., S. V. Maslova, A. N. Sinyakov, and V. I. Agol**. 1992. Towards identification of cis-acting elements involved in the replication of enterovirus and rhinovirus RNAs: a proposal for the existence of tRNA-like terminal structures. Nucleic Acids Res. **20**:1739-1745.

169. **Pillai, M. R., P. Chacko, L. A. Kesari, P. G. Jayaprakash, H. N. Jayaram, and A. C. Antony**. 2003. Expression of folate receptors and heterogeneous nuclear ribonucleoprotein E1 in women with human papillomavirus mediated transformation of cervical tissue to cancer. J.Clin.Pathol. **56**:569-574.

170. **Pincus, S. E. and E. Wimmer**. 1986. Production of guanidine-resistant and -dependent poliovirus mutants from cloned cDNA: mutations in polypeptide 2C are directly responsible for altered guanidine sensitivity. J.Virol. **60**:793-796.

171. **Racaniello, V. R.** 2006. One hundred years of poliovirus pathogenesis. Virology **344**:9-16.

172. **Racaniello, V. R. and D. Baltimore**. 1981. Cloned poliovirus complementary DNA is infectious in mammalian cells. Science **214**:916-919.

173. **Racaniello, V. R. and D. Baltimore**. 1981. Molecular cloning of poliovirus cDNA and determination of the complete nucleotide sequence of the viral genome. Proc.Natl.Acad.Sci.U.S.A **78**:4887-4891.

174. **Reynolds, T.** 2007. Polio: an end in sight? BMJ **335**:852-854.

175. **Richards, O. C. and E. Ehrenfeld**. 1990. Poliovirus RNA replication. Curr.Top.Microbiol.Immunol. **161**:89-119.

176. **Rieder, E., A. V. Paul, D. W. Kim, J. H. van Boom, and E. Wimmer**. 2000. Genetic and biochemical studies of poliovirus cis-acting replication element cre in relation to VPg uridylylation. J.Virol. **74**:10371-10380.

177. **Roberts, L.** 2009. Polio eradication. Looking for a little luck. Science **323**:702-705.

178. **Roehl, H. H. and B. L. Semler**. 1995. Poliovirus infection enhances the formation of two ribonucleoprotein complexes at the 3' end of viral negative-strand RNA. J.Virol. **69**:2954-2961.

179. **Rothberg, P. G., T. J. Harris, A. Nomoto, and E. Wimmer**. 1978. The genome-linked protein of picornaviruses, V. O^4-(5'-uridylyl)tyrosine is the bond between the genome-linked protein and the RNA of poliovirus. Proc.Natl.Acad.Sci.U.S.A. **75**:4868-4872.

180. **Rothstein, M. A., O. C. Richards, C. Amin, and E. Ehrenfeld**. 1988. Enzymatic activity of poliovirus RNA polymerase synthesized in Escherichia coli from viral cDNA. Virology **164**:301-308.

181. **Rubinstein, S. J., T. Hammerle, E. Wimmer, and A. Dasgupta**. 1992. Infection of HeLa cells with poliovirus results in modification of a complex that binds to the rRNA promoter. J.Virol. **66**:3062-3068.

182. **Sarnow, P.** 1989. Role of 3'-end sequences in infectivity of poliovirus transcripts made in vitro. J.Virol. **63**:467-470.

183. **Sharma, N., B. J. O'Donnell, and J. B. Flanegan**. 2005. 3'-Terminal sequence in poliovirus negative-strand templates is the primary cis-acting element required for VPgpUpU-primed positive-strand initiation. J.Virol. **79**:3565-3577.

184. **Shen, Y., M. Igo, P. Yalamanchili, A. J. Berk, and A. Dasgupta**. 1996. DNA binding domain and subunit interactions of transcription factor IIIC revealed by dissection with poliovirus 3C protease. Mol.Cell Biol. **16**:4163-4171.

185. **Silvera, D., A. V. Gamarnik, and R. Andino**. 1999. The N-terminal K homology domain of the poly(rC)-binding protein is a major determinant for binding to the poliovirus 5'-untranslated region and acts as an inhibitor of viral translation. J.Biol.Chem. **274**:38163-38170.

186. **Silvestri, L. S., J. M. Parilla, B. J. Morasco, S. A. Ogram, and J. B. Flanegan**. 2006. Relationship between poliovirus negative-strand RNA synthesis and the length of the 3' poly(A) tail. Virology **345**:509-519.

187. **Simoes, E. A. and P. Sarnow**. 1991. An RNA hairpin at the extreme 5' end of the poliovirus RNA genome modulates viral translation in human cells. J.Virol. **65**:913-921.

188. **Siomi, H., M. J. Matunis, W. M. Michael, and G. Dreyfuss**. 1993. The pre-mRNA binding K protein contains a novel evolutionarily conserved motif. Nucleic Acids Res. **21**:1193-1198.

189. **Spangberg, K. and S. Schwartz**. 1999. Poly(C)-binding protein interacts with the hepatitis C virus 5' untranslated region. J.Gen.Virol. **80 (Pt 6)**:1371-1376.

190. **Spector, D. H. and D. Baltimore**. 1974. Requirement of 3'-terminal poly(adenylic acid) for the infectivity of poliovirus RNA. Proc.Natl.Acad.Sci.U.S.A **71**:2983-2987.

191. **Stefanovic, B., C. Hellerbrand, M. Holcik, M. Briendl, S. Aliebhaber, and D. A. Brenner**. 1997. Posttranscriptional regulation of collagen alpha1(I) mRNA in hepatic stellate cells. Mol.Cell Biol. **17**:5201-5209.

192. **Svitkin, Y. V., M. Costa-Mattioli, B. Herdy, S. Perreault, and N. Sonenberg**. 2007. Stimulation of picornavirus replication by the poly(A) tail in a cell-free extract is largely independent of the poly(A) binding protein (PABP). RNA.

193. **Svitkin, Y. V., H. Imataka, K. Khaleghpour, A. Kahvejian, H. D. Liebig, and N. Sonenberg**. 2001. Poly(A)-binding protein interaction with elF4G stimulates picornavirus IRES-dependent translation. RNA. **7**:1743-1752.

194. **Syverton, J. T., W. F. SCHERER, and P. M. ELWOOD**. 1954. Studies on the propagation in vitro of poliomyelitis viruses. V. The application of strain HeLa human epithelial cells for isolation and typing. J.Lab Clin.Med. **43**:286-302.

195. **Taylor, M. P., T. B. Burgon, K. Kirkegaard, and W. T. Jackson**. 2009. Role of microtubules in extracellular release of poliovirus. J.Virol.

196. **Teterina, N. L., D. Egger, K. Bienz, D. M. Brown, B. L. Semler, and E. Ehrenfeld**. 2001. Requirements for assembly of poliovirus replication complexes and negative-strand RNA synthesis. J.Virol. **75**:3841-3850.

197. **Teterina, N. L., W. D. Zhou, M. W. Cho, and E. Ehrenfeld**. 1995. Inefficient complementation activity of poliovirus 2C and 3D proteins for rescue of lethal mutations. J.Virol. **69**:4245-4254.

198. **Thiele, B. J., A. Doller, T. Kahne, R. Pregla, R. Hetzer, and V. Regitz-Zagrosek**. 2004. RNA-binding proteins heterogeneous nuclear ribonucleoprotein A1, E1, and K are involved in post-transcriptional control of collagen I and III synthesis. Circ.Res. **95**:1058-1066.

199. **Thompson, A. A. and O. B. Peersen**. 2004. Structural basis for proteolysis-dependent activation of the poliovirus RNA-dependent RNA polymerase. EMBO J. **23**:3462-3471.

200. **Tingting, P., F. Caiyun, Y. Zhigang, Y. Pengyuan, and Y. Zhenghong**. 2006. Subproteomic analysis of the cellular proteins associated with the 3' untranslated region of the hepatitis C virus genome in human liver cells. Biochem.Biophys.Res.Commun. **347**:683-691.

201. **Todd, S., J. S. Towner, D. M. Brown, and B. L. Semler**. 1997. Replication-competent picornaviruses with complete genomic RNA 3' noncoding region deletions. J.Virol. **71**:8868-8874.

202. **Tolskaya, E. A., L. I. Romanova, M. S. Kolesnikova, A. P. Gmyl, A. E. Gorbalenya, and V. I. Agol**. 1994. Genetic studies on the poliovirus 2C protein, an NTPase. A plausible mechanism of guanidine effect on the 2C function and evidence for the importance of 2C oligomerization. J.Mol.Biol. **236**:1310-1323.

203. **Tolskaya, E. A., L. I. Romanova, M. S. Kolesnikova, T. A. Ivannikova, E. A. Smirnova, N. T. Raikhlin, and V. I. Agol**. 1995. Apoptosis-inducing and apoptosis-preventing functions of poliovirus. J.Virol. **69**:1181-1189.

204. **Towner, J. S., M. M. Mazanet, and B. L. Semler**. 1998. Rescue of defective poliovirus RNA replication by 3AB-containing precursor polyproteins. J.Virol. **72**:7191-7200.

205. **Toyoda, H., D. Franco, K. Fujita, A. V. Paul, and E. Wimmer**. 2007. Replication of poliovirus requires binding of the poly(rC) binding protein to the cloverleaf as well as to the adjacent C-rich spacer sequence between the cloverleaf and the internal ribosomal entry site. J.Virol. **81**:10017-10028.

206. **Toyoda, H., M. J. Nicklin, M. G. Murray, C. W. Anderson, J. J. Dunn, F. W. Studier, and E. Wimmer**. 1986. A second virus-encoded proteinase involved in proteolytic processing of poliovirus polyprotein. Cell **45**:761-770.

207. **Verheyden, B., S. Lauwers, and B. Rombaut**. 2003. Quantitative RT-PCR ELISA to determine the amount and ratio of positive- and negative strand viral RNA synthesis and the effect of guanidine in poliovirus infected cells. J.Pharm.Biomed.Anal. **33**:303-308.

208. **Waggoner, S. A. and S. A. Liebhaber**. 2003. Regulation of alpha-globin mRNA stability. Exp.Biol.Med.(Maywood.) **228**:387-395.

209. **Walter, B. L., T. B. Parsley, E. Ehrenfeld, and B. L. Semler**. 2002. Distinct poly(rC) binding protein KH domain determinants for poliovirus translation initiation and viral RNA replication. J.Virol. **76**:12008-12022.

210. **Wang, Z., N. Day, P. Trifillis, and M. Kiledjian**. 1999. An mRNA stability complex functions with poly(A)-binding protein to stabilize mRNA in vitro. Mol.Cell Biol. **19**:4552-4560.

211. **Weiss, I. M. and S. A. Liebhaber**. 1994. Erythroid cell-specific determinants of alpha-globin mRNA stability. Mol.Cell Biol. **14**:8123-8132.

212. **Wells, S. E., P. E. Hillner, R. D. Vale, and A. B. Sachs**. 1998. Circularization of mRNA by eukaryotic translation initiation factors. Mol.Cell **2**:135-140.

213. **Xiang, W., K. S. Harris, L. Alexander, and E. Wimmer**. 1995. Interaction between the 5'-terminal cloverleaf and 3AB/3CDpro of poliovirus is essential for RNA replication. J.Virol. **69**:3658-3667.

214. **Yalamanchili, P., R. Banerjee, and A. Dasgupta**. 1997. Poliovirus-encoded protease 2APro cleaves the TATA-binding protein but does not inhibit host cell RNA polymerase II transcription in vitro. J.Virol. **71**:6881-6886.

215. **Yalamanchili, P., U. Datta, and A. Dasgupta**. 1997. Inhibition of host cell transcription by poliovirus: cleavage of transcription factor CREB by poliovirus-encoded protease 3Cpro. J.Virol. **71**:1220-1226.

216. **Yalamanchili, P., K. Weidman, and A. Dasgupta**. 1997. Cleavage of transcriptional activator Oct-1 by poliovirus encoded protease 3Cpro. Virology **239**:176-185.

217. **Yeap, B. B., D. C. Voon, J. P. Vivian, R. K. McCulloch, A. M. Thomson, K. M. Giles, M. F. Czyzyk-Krzeska, H. Furneaux, M. C. Wilce, J. A. Wilce, and P. J. Leedman**. 2002. Novel binding of HuR and poly(C)-binding protein to a conserved UC-rich motif within the 3'-untranslated region of the androgen receptor messenger RNA. J.Biol.Chem. **277**:27183-27192.

218. **Yogo, Y. and E. Wimmer**. 1972. Polyadenylic acid at the 3'-terminus of poliovirus RNA. Proc.Natl.Acad.Sci.U.S.A **69**:1877-1882.

219. **Zell, R. and A. Stelzner**. 1997. Application of genome sequence information to the classification of bovine enteroviruses: the importance of 5'- and 3'-nontranslated regions. Virus Res. **51**:213-229.

220. **Zuker, M.** 1989. On finding all suboptimal foldings of an RNA molecule. Science **244**:48-52.

221. **Zuker, M., D. H. Mathews, and D. H. Turner**. 1999. Algorithms and Thermodynamics for RNA Secondary Structure Prediction: A Practical Guide, *In* J. Barciszewski and B. F. C. Clark (eds.), RNA Biochemistry and Biotechnology. Kluwer Academic Publishers.

BIOGRAPHICAL SKETCH

Allyn Russell Spear was born in Milwaukee, Wisconsin in August of 1981 to Neal and Marlyn Spear. He grew up in Wauwatosa, Wisconsin and graduated from Wauwatosa East High School in June 1999. Following this, Allyn attended the University of Wisconsin-La Crosse, and graduated in May 2003 with bachelor's degrees in both microbiology and chemistry with an ACS certification. While at the University of Wisconsin-La Crosse, Allyn had the opportunity to train under the direction of Dr. Michael A. Hoffman, performing research on the role of the matrix protein in the assembly and budding of human parainfluenzavirus type-3. In August 2003, Allyn began the Interdisciplinary Program in Biomedical Sciences at the University of Florida. In the Spring of 2004, he had the opportunity to begin doctoral research in the laboratory of Dr. James Bert Flanegan, studying the biochemistry and molecular biology of poliovirus replication. Under Dr. Flanegan's direction, Allyn completed all required coursework and dissertation research in the Summer of 2009.